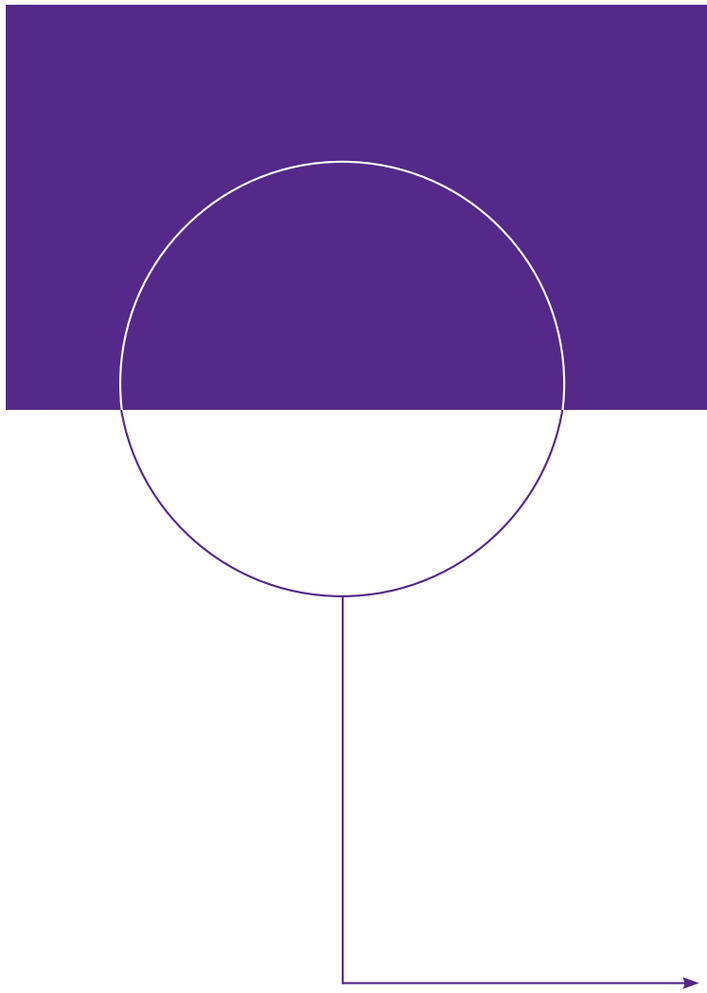

Master's thesis

2019

Ena Cemalovic

NTNU
Norwegian University of
Science and Technology
Faculty of Medicine and Health Sciences
Department of Clinical and Molecular Medicine

Master's thesis

Ena Cemalovic

TLR9 Trafficking and Signaling

June 2019

NTNU
Norwegian University of
Science and Technology

NTNU
Norwegian University of
Science and Technology

NTNU

Norwegian University of
Science and Technology

TLR9 Trafficking and Signaling

Ena Cemalovic

MSc Molecular Medicine
Submission date: June 2019
Supervisor: Nadra J. Nilsen
Co-supervisor: Alexander Gidon

Norwegian University of Science and Technology
Department of Clinical and Molecular Medicine

ABSTRACT

Toll-like Receptor 9 (TLR9) is an endosomal receptor found highly expressed in B cells and plasmacytoid dendritic cells (pDCs). It is activated by unmethylated CpG DNA and synthetic CpG oligodeoxyribonucleotides (ODNs) to produce pro-inflammatory cytokines (TNFα, IL-12) and type I interferons (IFNs). It senses viral and bacterial pathogens and activates adaptive immune responses. Dysregulation of TLR9 signaling can lead to progression and regression of various cancers and autoimmune diseases. Thus, modulation of TLR9 activity is an attractive target for immunotherapy. Due to scarcity of pDCs in the blood and a lack of a suitable model for studying of TLR9, knowledge about this receptor is lacking. The goal of this project was to characterize two experimental model cell lines (THP-1 TLR9 mCherry and CAL-1 TLR9 mCherry) for *in vitro* studies of TLR9, use them to study TLR9 expression, trafficking and signaling in pDC-like cells and investigate the role of Rab11a and Rab39a in these processes. Both cell lines express doxycycline-inducible TLR9 mCherry. The results showed that IL-4, GM-CSF-differentiated THP-1 TLR9 mCherry cells resemble immature dendritic cells in their ability to induce IFNβ1 and TNFα in response to CpG ODNs. Undifferentiated CAL-1 TLR9 mCherry cells potently induced IFNβ1 in response to CpG ODNs, validating their pDC-like properties. In IL-4, GM-CSF-differentiated THP-1 TLR9 mCherry cells TLR9 was primarily found in LAMP1-positive vesicles (late endosomes/lysosomes) before and after stimulation, indicating that TLR9 may reside and interact with its ligands in late endosomes. In CAL-1 TLR9 mCherry cells, the majority of TLR9 colocalized with late endosomes/lysosomes before and after stimulation with CpG ODN 2216, a CpG ligand thought to signal from early endosomes. Stimulation of TLR9 with CpG ODN 2006, a CpG ligand thought to signal from late endosomes, in CAL-1 TLR9 mCherry cells led to a decrease in TLR9-LAMP1 colocalization, indicating that TLR9 may be signaling and interacting with this ligand from other endosomal compartments. Rab11a regulates TLR4-induced IRF3 activation and IFNβ production, but its role in TLR9 signaling is unknown. Rab39a has been identified as a potential regulator of TLR9 signaling, but its exact role is still unclear. The results showed that both Rab11a and Rab39a may potentially play a role in TLR9-induced IFNβ1 signaling in IL-4, GM-CSF-differentiated THP-1 TLR9 mCherry cells. However, further experiments are required to validate these findings. In conclusion, the ability to study TLR9 expression, subcellular localization and response upon ligand stimulation, makes both THP-1 TLR9 mCherry and CAL-1 TLR9 mCherry cells promising experimental models for studying TLR9 signaling and trafficking *in vitro*.

ACKNOWLEDGEMENTS

This project was done as a part of the master's program in Molecular Medicine. The experiments were conducted at the Center for Molecular Inflammation Research (CEMIR), at the Faculty of Medicine and Health Sciences, Norwegian University of Science and Technology (NTNU).

I would first like to thank my main supervisor Dr. Nadra J. Nilsen for giving me a lot of freedom to explore topics I am interested in, but also steering me in the right direction whenever she thought I needed it, and for providing such invaluable support and assistance at all times, despite her very busy schedule. I would also like to thank my co-supervisor Dr. Alexandre Gidon for teaching me a lot about confocal microscopy in such a short period of time and providing assistance with the manuscript. I also wish to express my thanks to my former supervisor, Dr. Lene M. Grøvdal for introducing me to such a complicated, yet fascinating field of research and helping me conduct new experiments in the laboratory.

I would also like to thank everyone in the laboratory for always being willing to lend a helping hand, be it with experiments or on how to survive Trondheim winters. Last but not least, I would like to express my immense gratitude to my family and friends for always providing me with unfailing support, constant encouragement and love.

Table of Contents

List of Figures

List of Tables

List of Abbreviations

Ago2 – protein argonaute 2
Akt – protein kinase B
AP-1 – activator protein-1
AP-2 – adaptor protein complex 2
AP-3 – adaptor protein complex 3
BAD-LAMP – LAMP5, lysosomal associated membrane protein family member 5
BSA – bovine serum albumin
CD – cluster of differentiation
CD40L – cluster of differentiation 40 ligand
cDNA – complementary DNA
CDS – cytosolic DNA sensor
CLR – C-type lectin receptor
COPII – coat protein complex II
CXCR3 – CXC chemokine receptor
DAMP – danger-associated molecular pattern
DC – dendritic cell
DMEM – Dulbecco's Modified Eagle Medium
DNA – deoxyribonucleic acid
dNTP – deoxyribonucleotide triphosphate
DOTAP - Dioleoyl-3-trimethylammonium propane
Dox - doxycycline
DTT - dithiothreitol
EDTA - Ethylenediaminetetraacetic acid
EE – early endosome
EEA1 – early endosome antigen 1
EHD1 – EH domain-containing protein 1
ER – endoplasmic reticulum
ERC – endocytic recycling compartment
FCS – fetal calf serum
GAP – GTPase-accelerating protein/GTPase-activating protein
GAPDH - Glyceraldehyde 3-phosphate dehydrogenase
GDF – GDI displacement factor
GDI – GTP dissociation inhibitor
GDP – guanosine diphosphate
GEF – guanine nucleotide exchange factor
GFP – green fluorescent protein
GM-CSF – granulocyte-macrophage colony-stimulating factor
GM130 – Golgi matrix protein
gp96 – endoplasmin/heat shock protein 90kDa beta member 1 (HSP90B1)
GTP – guanosine triphosphate
HEK293 – human embryonic kidney cell
HLA-DR – human leukocyte antigen DR

HMGB1 – high mobility group box 1 protein
HRP – horse radish peroxidase
IFN - interferon
IKK – IκB kinase
IL - interleukin
IL-1R – interleukin 1 receptor
ILV – intraluminal vesicles
IRAK – interleukine-1 receptor associated kinase
IRF – interferon regulatory factor
ISG – interferon stimulated genes
IκB – inhibitor of NF-κB
JACoP – Just Another Colocalization Plugin
LAMP – lysosomal associated membrane protein
LDS – lithium dodecyl sulfate
LE – late endosome
LRR – leucin rich repeat
LRRNT – leucin rich repeat, N-terminus
MAPK – mitogen-activated protein kinase
MICAL-L1 – MICAL-like protein 1
MOPS - 3-(N-morpholino) propanesulfonic acid
mRNA – messenger RNA
mtDNA – mitochondrial DNA
mTOR – mammalian target of rapamycin
mTORC1 – mammalian target of rapamycin complex 1
MVB – multivesicular bodies
MyD88 – myeloid differentiation primary response 88
NEMO - NF-κB – essential modulator
NF-κB - **nuclear factor kappa-light-chain-enhancer of activated B cells**
NK – natural killer cells
NLR – NOD-like receptor
ODN - **oligodeoxyribonucleotides**
Opti-MEM – reduced serum medium, minimal essential medium
p-p38 – phosphorylated p38
PAMP – pathogen-associated molecular patterns
PBS – phosphate buffered saline
pDC – plasmacytoid dendritic cell
PFA - parafromaldehyde
PI(3,4)P2 – Phosphatidylinositol 3,4-bisphosphate
PI(3,5)P2 - Phosphatidylinositol 3,5-bisphosphate
PI3Kγ – phosphoinositide 3-kinase γ
PI3P - **Phosphatidylinositol 3-phosphate**
PMA – phorbol 12-myristate-13-acetate
PRAT4A – protein associated with Toll-like receptor 4
PRR – pathogen recognition receptor

pSTAT1 – phosphorylated STAT1
pTBK1 – phosphorylated TBK1
RE – recycling endosome
REP – Rab escort protein
Rh – recombinant human
RIPA – radioimmunoprecipitation assay
RISC – RNA-induced silencing complex
RLR – RIG-I-like receptor
RNA – ribonucleic acid
RPMI 1640 medium - Roswell Park Memorial Institute 1640 medium
RT – reverse transcription/reverse transcriptase
RT-qPCR – quantitative reverse transcription polymerase chain reaction
rtTA - reverse tetracycline-controlled transactivator
SDS – sodium dodecyl sulfate
siRNA – small interfering RNA
Snx – sorting nexin
STAT1 - Signal transducer and activator of transcription 1
TAB - TGF- β Activated Kinase
TAK1 - Mitogen-activated protein kinase kinase kinase 7
TBK1 – TANK-binding kinase 1
TBP – TATA-binding protein
TBS – Tris-buffered saline
TBS-T – Tris-buffered saline with Tween 20
Tet - tetracycline
tetO – tetracycline operator
TIR – Toll-interleukin receptor
TIRAP – TIR domain-containing adaptor protein
TLR – Toll-like receptor
$TLR9_C$ – cleaved TLR9 (C-terminal fragment)
$TLR9_{FL}$ – full length TLR9
$TLR9_N$ – cleaved TLR9 (N-terminal fragment)
$TLR9_S$ – short TLR9
TNFα – tumor necrosis factor α
TRAF -TNF receptor-associated factor
TRIF - TIR-domain-containing adapter-inducing interferon-β
tTA - tetracycline transactivator
Unc93B1 – Unc93-homolog B1
UV - ultraviolet
VAMP3 – vesicle-associated membrane protein 3

1 INTRODUCTION

1.1 Immune responses

The immune system is a complex network of cells, tissues, organs and molecules that constantly orchestrate immune responses which will recognize and eliminate pathogens and toxins that have breached the epithelial surfaces. Two types of immune responses, innate and adaptive, work closely together to accomplish their main goal of eliminating the foreign invader. The innate immune system includes physical and chemical barriers, the complement system, monocytes, macrophages, granulocytes, dendritic cells (DCs) and natural killer (NK) cells. These can provide early defense against many common pathogens through recognition of various conserved structures found in pathogens. The onset of response is rather quick (usually within minutes), but it has limited potency. Innate immunity tries to eliminate the pathogen, but if it is unsuccessful, its goal is to contain the infection until adaptive immune responses can be generated. Adaptive immunity includes both humoral responses, mediated by B cells and antibodies, and cell-mediated responses mediated by cytotoxic and helper T cells. It recognizes highly specific antigens and takes several days to weeks to generate such specific responses. Unlike innate immunity, adaptive immunity can generate immunological memory and mount strong and fast responses upon re-exposure to a certain pathogen.

Generation of the immune response starts when cells of the innate immune system, such as immature DCs or macrophages encounter a pathogen and ingest it. These cells express signaling pattern recognition receptors (PRRs). These are germline-encoded host receptors that recognize small molecular motifs conserved in pathogens known as pathogen-associated molecular patterns (PAMPs), as well as endogenous stress signals known as damage-associated molecular patterns (DAMPs). Upon stimulation by PAMPs/DAMPs, PRRs initiate signaling cascades that ultimately result in high production of cytokines and chemokines, upregulation of co-stimulatory molecules, and activation of antigen presenting cells, all of which will influence subsequent innate and adaptive immune responses[1,2]. Signaling PRRs are divided into five receptor families: Toll-like receptors (TLRs), RIG-1 like receptors (RLRs), C-type lectin receptors (CLRs), nucleotide oligomerization receptors (NLRs) and cytosolic dsDNA sensors (CDSs). TLRs have been the most extensively studied family, however, much about their signaling and trafficking pathways still remains unknown.

1.2 Toll-like Receptors

PRRs, such as Toll-like Receptors (TLRs) are highly expressed on innate immune cells such as macrophages and DCs, where they can sense components associated with infection, cellular stress or damage and initiate adequate signaling cascades that will lead to cytokine responses. Ten members of TLR family have been identified so far in humans. TLR1, 2, 5, 6 and 10 are expressed on the plasma membrane where they sense microbial components found in extracellular space[1,3]. TLR3, 7, 8 and 9 are found on various endosomal membranes where they recognize nucleic acids[1,4,5]. TLR4 can be found on the plasma membrane as well as the endosomes[6]. Proper subcellular localization of TLRs and their ligands is required for maintenance of appropriate immune responses. This is best demonstrated through mislocalization of endosomal TLRs, such TLR9, which when found on the plasma membrane becomes over-activated and results in fatal inflammatory disease[7]. In addition, mislocalization of endogenous stress signals into endosomes, such as self-nucleic acids, can potentially lead to hyperactivation of endosomal TLRs.

All ten members of TLR family are type I transmembrane glycoproteins composed of a cytoplasmic and an extracellular domain. The extracellular domain contains leucine-rich repeats (LRRs) which recognize a specific ligand[1,2]. The cytoplasmic domain is homologous to the interleukin-1 receptor (IL-1R) signaling domain and it is therefore known as the Toll/Interleukin-1 receptor (TIR) domain[2]. LRR-mediated recognition of a specific ligand will induce homodimerization of TLRs through TIR domains (except for TLR2 which heterodimerizes with TLR1 and TLR6 to recognize tri- and diacetylated lipopeptides, respectively), which in turn will recruit one of two main adaptor proteins, MyD88 or TRIF. Most TLRs signal through MyD88, with TLR2, 3 and 4 being the exceptions. TLR2 heterodimers use TIRAP (TIR domain-containing adaptor protein) to recruit MyD88, and TLR3 signals only through TRIF. After interacting with its ligand at the plasma membrane, TLR4 homodimerizes and uses TIRAP to recruit MyD88 and initiate signaling[6]. Then, TLR4 gets internalized into endosomes from where it uses TRAM to recruit TRIF, which subsequently induces the production of type I interferons (IFNs)[6]. Kagan et al. have also shown that in addition to signaling only through MyD88, TLR9 can also use TIRAP to recruit MyD88 in response to natural (viral) ligands[8]. A summary of TLR ligands, their sub-cellular localization, the adaptor proteins used to initiate their signaling cascades and their end product is shown in Table 1.

Toll-like receptor		Ligands[9]	Localization	Adaptor proteins[1]	End product[10]
TLR2	TLR1:TLR2	triacyl lipopeptides	Plasma membrane	TIRAP/MyD88	Pro-inflammatory cytokines
	TLR2:TLR6	diacyl lipopeptides			
TLR3		dsRNA	Endosome	TRIF	Pro-inflammatory cytokines, type I IFNs
TLR4		lipopolysaccharide	Plasma membrane, endosome	TRAM/TRIF, TIRAP/MyD88	Pro-inflammatory cytokines
TLR5		flagellin	Plasma membrane	MyD88	Pro-inflammatory cytokines
TLR7		ssRNA, base analogs	Endosome	MyD88	Pro-inflammatory cytokines, type I IFNs
TLR8		ssRNA	Endosome	MyD88	Pro-inflammatory cytokines, type I IFNs
TLR9		unmethylated CpG DNA	Endosome	TIRAP/MyD88	Pro-inflammatory cytokines, type I IFNs
TLR10		Unknown	Plasma membrane	Unknown	Anti-inflammatory cytokines, but a possible pro-inflammatory role has been noted

Table 1.1 Overview of TLRs, their best-known ligands and sub-cellular localization, adaptor proteins used to initiate signaling pathways, and the type of cytokines they typically induce.

1.3 TLR9

TLR9 is a 1032 amino acid (aa) endosomal receptor. It is highly expressed in human B cells and plasmacytoid dendritic cells (pDCs), but can also be expressed in myeloid dendritic cells, macrophages and NK cells[11]. TLR9 senses unmethylated CpG DNA and induces secretion of pro-inflammatory cytokines and type I interferons (IFNs). TLR9 has recently gained popularity as a therapeutic target as it appears to be involved in a number of autoimmune diseases and cancer. In autoimmune diseases like Sjögren's syndrome or systemic lupus erythematosus, TLR9 becomes activated by "self" DNA and results in the production of cytokines that lead to the inflammatory disease phenotype[12]. In cancer, TLR9 seems to have both tumor-progressing and tumor-regressing properties, depending on the cancer type. For example, loss of TLR9 appears to be correlated with worse outcomes in certain types of breast cancer. At the same time, upregulation of TLR9 in non-small cell lung cancer and ovarian cancer seems to contribute to increased cell proliferation and metastasis[13].

1.3.1 TLR9 isoforms

Human cells express five different isoforms of the protein (TLR9-A, TLR9-B, TLR9-C, TLR9-D, TLR9-E) generated by alternative splicing of TLR9 transcript[14]. All protein variants contain the 975 aa common region, with TLR9-A being the canonical protein sequence[14]. TLR9-B and TLR9-E are the truncated variants lacking 42 and 15 aa, respectively, whereas TLR9-C and TLR9-D consist of additional 23 and 15 aa, respectively[14]. They all associate with different organelles - TLR9-A, -C, -E and D• localize to the endoplasmic reticulum (ER), while TLR9-B is found in the mitochondria[14].

1.3.2 TLR9 ligands

To mount an immune response, TLR9 has to be activated by unmethylated CpG DNA or synthetic oligodeoxyribonucleotides (ODNs). Synthetic ODNs are short ssDNA molecules that contain CpG motifs (a hexamer with a central unmethylated CpG surrounded by two purines and two pyrimidines), a phosphodiester and/or phosphorothioate backbone and poly G tails at the 3' and 5' ends. CpG ODNs are classified into three different subclasses based on their structure. Class A CpG ODNs have a backbone made of both phosphodiester and phosphorothioate[15]. CpG motif is attached to the phosphodiester part of the backbone, while modified poly-G 3' and 5' ends are found on the phosphorothioate part of the backbone[15,16]. This class of CpG ODNs strongly induces IFNα in pDCs, but results in the weak induction of pro-inflammatory cytokines. It is thought that Class A CpG ODNs tend to spontaneously form nanoparticle-like structures which get taken up slowly and allow longer "self-priming" of pDCs through induction of small amounts of spontaneously released type I IFN[11,17]. Class B CpG ODNs have one or more CpG motifs attached to a phosphorothioate backbone. They potently activate B cells to produce pro-inflammatory cytokines[11,17]. Class C CpG ODNs have features of both above-mentioned classes, containing a single CpG motif associated with a phosphorothioate backbone, and can strongly activate B cells and induce IFN-α in pDCs.

In addition to the common inducers of TLR9 responses, this receptor can also be activated by double-stranded and single-stranded DNA without CpG motifs and by endogenous DNA delivered to endosomes at high enough concentration[11,18].

• TLR9-D lacks a cleavage site, and has an opposing orientation in the ER, with its ectodomain projecting into the cytosol

1.3.3 TLR9 structure

TLR9 is thought to have a horseshoe-shaped solenoid structure[19] (Figure 1.1[20]). Each solenoid turn appears to contain one LRR (for a total of 26LRRs), and the ectodomain ends are thought to be capped by cysteine-rich C- and N-termini[19,20]. For signaling to begin, TLR9 needs to homodimerize. Dimerization occurs upon ligand binding – CpG DNA acts as a "molecular bridge" between two TLR9 molecules by simultaneously allowing interactions of the CpG motif with LRRNT-LRR10 region in the N-terminus of one TLR9 protomer, and interactions between the backbone and LRR20-22 region in the C-terminus of the other protomer[19]. DNA-binding regions are also rich in histidine residues, which result in increased affinity of TLR9-CpG DNA under acidic conditions[19]. TLR9 also has a long insertion loop (Z-loop) located between LRR14 and 15[19]. Binding of both stimulatory and inhibitory DNA sequences is independent of the insertion loop, but the loop is still necessary for ligand-dependent dimerization of TLR9[19]. In addition to CpG motif, a cytosine nucleotide at the second position from the 5' end (5'-xCx) can enhance TLR9 dimerization and activation, suggesting that TLR9 binds its ligands at two different places[20,21]. Upon dimerization, two TLR9 protomers close tightly, not leaving any space for DNA to pass through. This leaves us with the assumption that two separate DNA molecules must independently bind TLR9 dimers, or that a single DNA molecule must have its CpG motif and 5'-xCx spaced at least 10-mer apart in order to bind both binding sites[20].

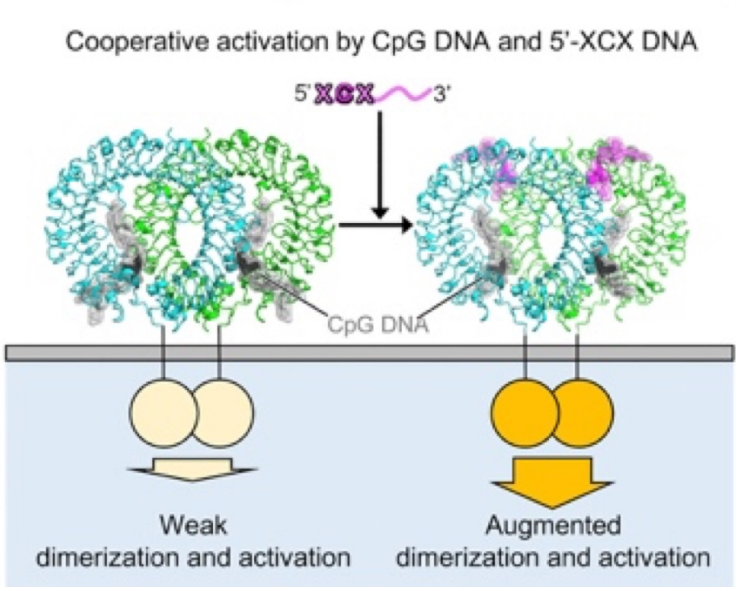

Figure 1.1[20] Structure and activation mechanisms of TLR9. TLR9 dimers bind their ligands at two different sites – the CpG motif and 5'-xCx. Binding of CpG DNA to 5'-xCx enhances TLR9 dimerization and activation

1.3.4 TLR9 signaling

For TLR9 to be able to signal, its ectodomain has to be proteolytically cleaved[22-24]. Studies have shown that proteolytic processing of TLR9 is a two-step process involving cathepsin-mediated cleavage of the ectodomain and trimming of the receptor N-terminus[23,25]. Only cleaved TLR9 ($TLR9_C$) can recruit MyD88[26]. Following the cleavage, N-terminus fragment of the ectodomain ($TLR9_N$) remains associated with $TLR9_C$, as without it, $TLR9_C$ is not able to sense CpG DNA[26]. When TLR9 cleavage has been accomplished, TLR9 is ready to signal. TLR9 stimulation can have two different outcomes: secretion of pro-inflammatory cytokines that results mostly from activation of NF-κB pathway, and secretion of type I IFNs resulting from activation of IRF signaling cascade (Figure 1.2[27]). The signaling events leading to the production of pro-inflammatory cytokines and type I IFN are thought to happen in different endosomal compartments. However, whether these pathways are activated simultaneously or sequentially has not yet been shown.

1.3.4.1 TLR9-induced production of pro-inflammatory cytokines

Ligand binding to TLR9 induces association of its TIR domains which will then recruit MyD88[28]. In addition to the TIR domain, MyD88 also has an N-terminal death domain through which it recruits IRAK4, which then in turn phosphorylates IRAK1 and IRAK2[29,30]. This activates TRAF6, an E3 ubiquitin ligase, which will form K63-linked polyubiquitin chains on NEMO and itself, where TRAF6, NEMO, TAB2, TAB1, TAK1 multiprotein complex will be formed[31-33]. TAK1 will get phosphorylated, and subsequently phosphorylate NEMO-recruited IKKβ and modulate its activity[33]. IKK complex-mediated phosphorylation of IκB will lead to its poly-ubiquitination and degradation by proteasomes, and translocation of NF-κB to the nucleus[29]. Further, TAK1 will activate the MAPK signaling pathway which will result in translocation of AP-1 to the nucleus[1,2,34,35]. Activation of NF-κB and AP-1 will lead to synthesis of TNFα, IL-6 and IL-12 (Figure 1.2[27]).

Secretion of pro-inflammatory cytokines is augmented by IRF1 and IRF5[36,37]. MyD88 can directly activate IRF1 to enhance TLR9-induced production of IL-12[38]. In pDCs, MyD88 activates IRF-5 which then cooperates with NF-κB p50 to induce IL-6 expression[39].

1.3.4.2 TLR9-induced production of type I IFN

TLR9-induced production of type I IFNs requires activation of multiple IRF proteins, such as IRF1, IRF3, IRF5 and IRF7 (Figure 1.2[27]). Upon ligand binding TLR9 will dimerize

and recruit MyD88 in TIRAP-dependent manner[40]. MyD88 will then recruit IRAK4, which will interact with TRAF6, TRAF3 and IRAK1 to form the myddosome[40-43]. Once the complex has been formed, MyD88 is able to associate and interact with different IRFs. IRF1 and IRF5 induce IFNβ production in response to TLR9 ligands in myeloid DCs and pDCs, respectively[38,39]. Upon activation of IRF3 by phosphorylated TBK1, IRF3 translocates to the nucleus and induces production of IFNβ. Secreted IFNβ can then bind to IFNAR which will lead to the activation of interferon stimulated genes (ISGs) and IRF7, which will result in increased production of IFNα. IRF7 can also be directly activated by MyD88 to produce IFNα[44]. IKKα phosphorylates IRF7, which then dissociates from the complex and translocates to the nucleus to induce secretion of type I IFN, which then act as positive regulators of their own pathway[44,45]. In addition, in pDCs, osteopontin, a highly negatively charged matricellular protein, can further enhance IRF7-mediate IFNα production by stabilizing interactions between MyD88 and IRF7[46].

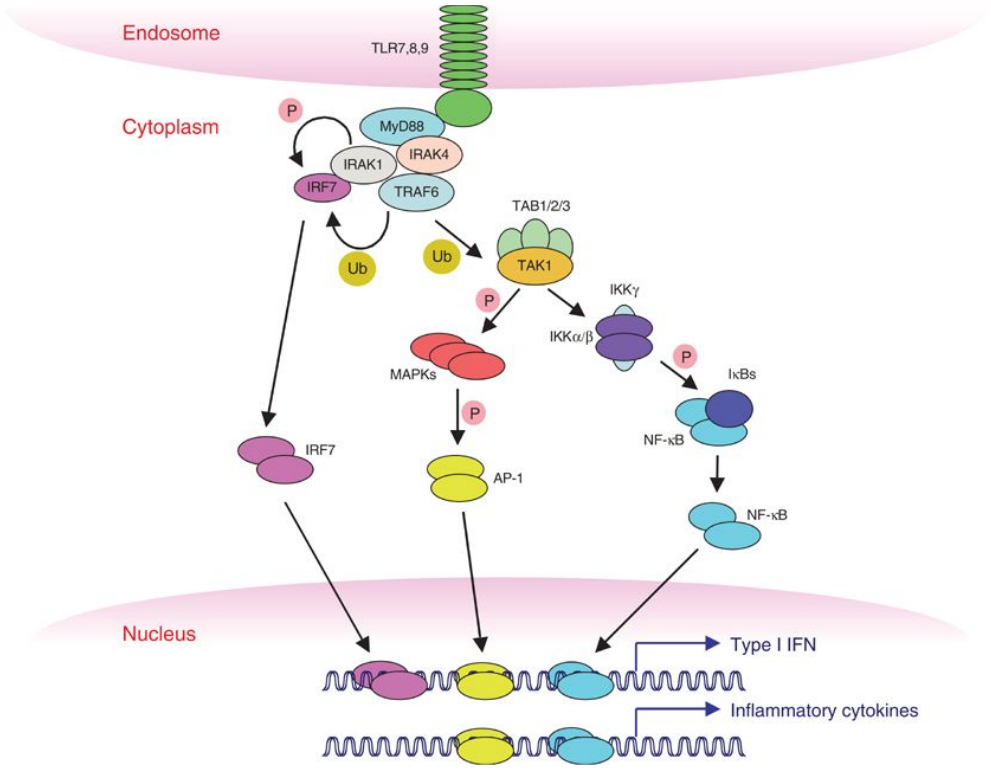

Figure 1.2[27] TLR9 induces production of type I IFNs and pro-inflammatory cytokines. Ligand binding to TLR9 results in recruitment of MyD88. Myd88 interacts with IRAKs and IRFs. Activated IRAKs activate TRAF6 which facilitates formation of K63 polyubiquitin chains where TAB1/2, TAK1 and NEMO will be recruited. IKK complex phosphorylates IκB, which in turn causes release of NFκB and its translocation to the nucleus to induce production of pro-inflammatory cytokines. TAK1 also phosphorylates and activates MAPK pathway that will induce translocation of AP-1 into the nucleus and augment production of pro-inflammatory cytokines. Activation of IRFs (IRF1, IRF3, IRF5, IRF7) will results in their nuclear translocation and induction of type I IFNs.

1.4 Endosomal network

TLR9 is an endosomal receptor that is synthesized in the endoplasmic reticulum (ER). From there it traffics to different endosomes where it encounters its ligands and induces cytokine response. TLR9 ligands are found in the extracellular space, but in order to be recognized by the receptor, they need to be internalized through endocytosis. To understand how TLR9 and CpG DNA traffic to different endosomes and eventually interact, it is first necessary to understand the endosomal network.

Endocytosis is a highly regulated process that enables cells to sample the extracellular environment for nutrients and potential pathogens, and to ingest them. Upon internalization, newly formed, cargo-containing endocytic vesicles will begin to move away from the plasma membrane. They will not fuse with each other, but instead mature at different rates, and eventually fuse with early endosomes (EEs)[47]. EEs are dynamic organelles that accept a large variety of internalized cargo, ranging from receptors and lipid membranes to extracellular fluids internalized through different internalization methods. Their membranes are rich in phosphoinositide phosphatidylinositol 3-phosphate (PI3P)[48] and also include Rab4, Rab5, Rab10, Rab14, Rab21 and Rab22 family proteins[49,50], which localize to distinct EE microdomains[51]. The EE lumen is acidic with a pH of 6.0-6.5 and this luminal acidification is maintained through the activity of V-ATPase proton pump[47,49].

At a certain point, that is still poorly characterized, EEs will stop fusing with endocytic vesicles, and will become sorting endosomes (SEs)[47]. SEs contain two regions – a tubular and a vacuolar region[47]. Tubular region of an SE has a large surface area that allows receptor-containing vesicles to bud off and get transported directly to the plasma membrane via fast recycling pathway[49,52,53]. This is done with the help of Rab4, Rab35, AP-1 and/or Snx17 and Snx27[52,53]. Other cargo is thought to be handled through the recycling endosomes (REs)[49] via the slow recycling pathway. REs are found in the perinuclear region of the cell called the endocytic recycling compartment (ERC)[49]. They have a tubular shape, and are rich in Rab11 and Rab8 family proteins, Rab22a, Arf6, EHD1 and MICAL-L1[49,54,55]. Once the cargo is in the REs, it will undergo process of budding and fission, and released vesicles will be delivered to the plasma membrane via the microtubule tracks[53].

Cargo found in the vacuolar region of SEs gets ubiquitinated and internalized into intraluminal vesicles (ILVs)[47], which will eventually bud off and become multivesicular bodies (MVBs)[56]. MVBs contain cargo that will be degraded by lysosomes, and for that to happen, MVBs that begin with EE-like characteristic must first acquire properties of late

endosomes (LEs). This involves the so-called Rab5-to-Rab7 conversion in which Rab5 becomes replaced by Rab7 as endosome matures, and changes in membrane lipid composition[49,56-60]. These lead to subsequent V-ATPase activity that acidifies the lumen and lowers the pH to 5.0-5.5[47], and gain of lysosomal hydrolases and highly glycosylated proteins (i.e. LAMP1)[47].

Once vesicles are fully transitioned to LEs and receptors recycled to the plasma membrane, transfer of LE content to lysosomes for degradation can occur. LE can directly fuse with lysosomes forming endolysosomes, or through kiss-and-run fusion[47,61]. Highly acidic lysosomal environment (pH < 4.5) will degrade the cargo, which will subsequently be transported out of the lysosomes. Lysosomes will then regenerate so they can be reused in future cargo break down[61].

1.5 Rab proteins

Immune cells consist of rich endosomal networks through which they internalize, and process pathogens and endogenous signals found in the extracellular space. Transport of endosomes within these cells must be highly regulated to ensure appropriate and accurate activation of immune responses. This is in part done by Rab proteins, small (21-25kDa) Ras-like GTPases that control signaling of PRRs, such as TLRs, by tightly controlling intracellular vesicle trafficking, budding and uncoating, recruitment of effector proteins, organelle biogenesis, and cargo degradation[47,62-67]. Rab proteins play these roles not only in the cells of the immune system, but also many other cells types.

Rab proteins can be expressed in the nucleus, plasma membrane, ER, Golgi, endosomes, lysosomes, mitochondria and centrioles[65]. During their lifetime they cycle between the cytosol and the membranes, and their activity is regulated by their nucleotide-bound state[62]. When bound to GDP, Rab proteins are inactive. Targeting and insertion of a Rab protein into the appropriate membrane is mediated by GDF (GDP dissociation inhibitor (GDI) dissociation factor)[62,68,69]. Once the Rab protein is located in the appropriate membrane, guanine nucleotide exchange factor (GEFs) will activate the Rab protein by replacing GDP with GTP, thus allowing Rab protein to interact with effector proteins. When Rab activity is no longer needed, GTPase accelerating proteins (GAPs) will catalyze hydrolysis of Rab-bound GTP to GDP, thus inactivating it again, and GDI will remove GDP-bound Rab from the membrane and sequester it in the cytosol[62,68-71].

All known Rabs contain conserved stretches of amino acids named F1-F5[62], and these help distinguish them from other Ras superfamily proteins. In addition to these, Rab proteins

also have conserved sequences named SF1-4 that allow classification of Rabs into several phylogenetic and functional groups[62,72]. All Rabs have a GTPase fold that is composed of a six-stranded β-sheets flanked by five α-helices[62]. The hypervariable region is composed of 35-40 aa and is located at the carboxyl terminus of the GTPase fold[62]. This region is responsible for targeting of Rab proteins to specific membranes[62,73]. Adjacent to the hypervariable region are the CAAX boxes to which geranylgeranyl tails are attached[62]. This modification allows Rab proteins to insert themselves into various membranes[62]. Prenylation of CAAX boxes increases their hydrophobicity, resulting in Rab escort proteins (REP) being necessary to deliver Rabs to appropriate membranes[65].

1.5.1 Rab proteins in TLR trafficking and signaling

In many cases, subcellular localization and trafficking of TLRs dictate cytokine responses induced by a given TLR. Rab proteins play an important role in TLR-induced responses by tightly controlling receptor trafficking and fine-tuning outcomes of TLR activation. Rab7b negatively regulates TLR4- and TLR9- induced signaling, by promoting lysosomal degradation of these receptors[74]. Rab8a is located on the micropinosome membrane. Upon stimulation of TLR3, 4 and 9 with their ligands, Rab8a recruits PI3Kγ which results in activation of Akt/mTOR signaling pathway[75]. Rab11a regulates TLR4 trafficking in and out of ERC as well as TLR4-induced IRF3 activation and IFNβ production[76]. In murine intestinal epithelial cells, Rab11a also contributes to maintenance of homeostatic distribution of TLR9 across the cell. Loss of Rab11a leads to accumulation of TLR9 inside intracellular vesicles and hyperactivation of the receptor, leading to an inflammatory bowel disease-like phenotype[77].

1.6 TLR9 and CpG DNA trafficking

In resting cells newly synthesized TLR9 can be found in the ER, but to interact with CpG DNA and induce immune response, it has to be transported to the endosomes through the endosomal network (Figure 1.3[78]). To leave the ER, TLR9 has to compete with TLR7 for binding of the chaperon protein Unc93B1 which will transport it to the Golgi[78]. Other chaperon proteins such as gp96 and PRAT4A have also been reported to act as chaperons for TLR9 as it exits the ER[22,78-80]. Once it reaches the Golgi, TLR9 is loaded into COPII vesicles by Unc93B1 and delivered to the plasma membrane, where AP-2 gets recruited to mediate TLR9 internalization in clathrin-dependent manner[81,82]. Upon internalization, TLR9 localizes to early endosomes[32]. Iwasaki et al. have shown that in murine bone marrow-derived pDCs

TLR9 then traffics to NF-κB signaling endosomes (characterized by VAMP3 and PI(3,5)P2 expression), from which it induces secretion of pro-inflammatory cytokines[83]. Phosphoinositide 3-phosphate 5-kinase generates phosphatidylinositol 3,4-bisphosphate (PI(3,4)P2) in NF-κB signaling endosomes and results in recruitment of AP-3[32,84]. AP-3 then interacts with TLR9 and induces trafficking of TLR9 into IRF signaling endosomes (characterized by VAMP3 and LAMP2 expression) from where they induce secretion of type I IFNs[83]. BAD-LAMP has also been shown to control TLR9 trafficking in human pDCs by directing the receptor into NF-κB signaling endosome[85]. AP-3 promotes BAD-LAMP access to late endosomes, thus further enhancing the secretion of pro-inflammatory cytokines[85].

CpG DNA present in the extracellular space is rapidly internalized in a clathrin-dependent, caveolin-independent manner[86]. CpG DNA shuttling through the endosomal network has to be tightly controlled for TLR9 to interact with it in appropriate endosomes. Internalized CpG DNA-containing vesicles are usually found near the nucleus. TLR9-containing vesicles are then trafficked to the CpG DNA-rich regions. Simultaneously, granulin, a cysteine-rich protein, shuttles CpG-containing vesicles to TLR9-rich vesicles and enhances interactions between CpG DNA and the C-terminus of TLR9[32,87]. In addition to granulin, HMGB1 also aids TLR9-mediated CpG DNA recognition. In bone-marrow derived DCs and monocytes it binds CpG DNA and enhance the release of pro-inflammatory cytokines by facilitating rapid interactions between TLR9 and CpG[88].

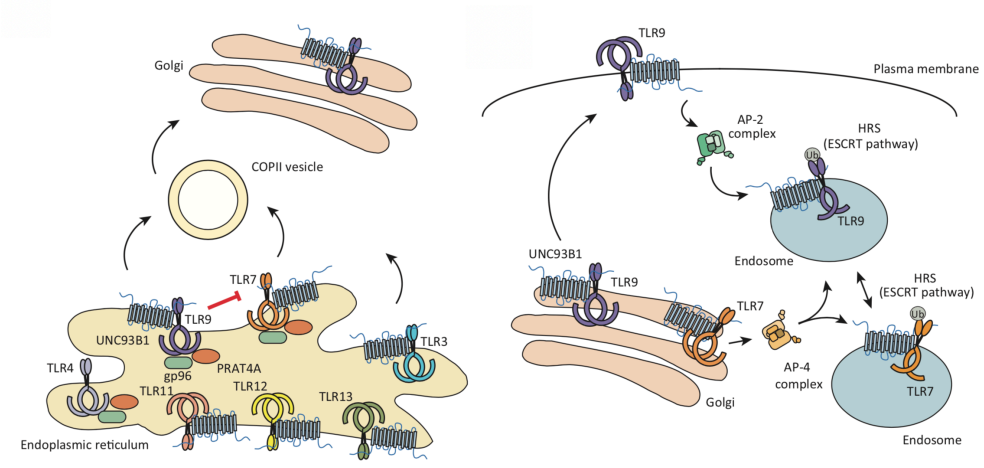

Figure 1.3[78] Current model for TLR9 trafficking. TLR9 is synthesized in the ER and remains there under resting conditions. For transport to endosomes, it competes with TLR7 for binding to Unc93B1. Unc93B1 facilitates loading of TLR9 into COPII vesicles, which transport the receptor to the Golgi. From the Golgi, Unc93B1 facilitates shuttling of TLR9 to the plasma membrane where TLR9 interacts with AP-2 complex. AP-2 complex mediate endocytosis of TLR9/Unc93B1.

2 AIMS

In addition to providing defense against many bacterial and viral pathogens, TLR9 also plays a role in anti- and pro-tumor immunity, as well as several autoimmune diseases. Therefore, modulation of TLR9 responses represents an attractive target for immunotherapy. TLR9 expression and signaling are largely studied in murine models which only partially mimic responses seen in the human immune system. In humans, TLR9 is highly expressed in pDCs, an immune cell type that specializes in antiviral responses and presents an important link between innate and adaptive immunity. pDCs are rare in peripheral blood and due to their fragility, they are very difficult to isolate, work with or modify genetically. This is why the goal of this project was to characterize experimental model cell lines (THP-1 TLR9 mCherry and CAL-1 TLR9 mCherry) that can be used for *in vitro* studies of TLR9. Undifferentiated THP-1 TLR9 mCherry cells share properties with human monocytes, while CAL-1 TLR9 mCherry cells resemble pDCs. Both cell lines were transfected with inducible TLR9 with an mCherry tag on the receptor's C-terminus. Expression of TLR9 in these cells is based on Tet-On system, which allows us to selectively turn on and off TLR9 expression by administration or withdrawal of doxycycline, respectively. This project further aimed to use these cell lines to study TLR9 expression, trafficking and signaling in pDC-like cells and investigate the role of Rab GTPases (Rab11a and Rab39a) in these processes. Rab11a is a key component of recycling endosomes. It was chosen for the study since it has been shown that it regulates trafficking and signaling of other TLRs (e.g. TLR4) and that it is also crucial for regulation of homeostatic TLR9 expression in murine intestinal epithelia. Rab39a associates with late endosomes/lysosomes and helps regulate endocytosis, and it has been identified as a potential regulator of TLR9 signaling (Grøvdal, Unpublished data). More specifically, the aims of the project were:

- Characterize THP-1 TLR9 mCherry and CAL-1 TLR9 mCherry cell lines with regard to TLR9 expression and signaling
- Determine cytokine responses induced with different CpG ligands in THP-1 TLR9 mCherry and CAL-1 TLR9 mCherry cells
- Study localization of TLR9 by confocal microscopy before and after stimulation with CpG ligands in THP-1 TLR9 mCherry and CAL-1 TLR9 mCherry cells
- Investigate signaling pathways down-stream of TLR9 activation
- Use siRNA-mediated gene silencing to study effects of Rab11a and Rab39a on TLR9 signaling in THP-1 TLR9 mCherry and CAL-1 TLR9 mCherry cells.

3 MATERIALS AND METHODS

3.1 Cell culture

All experiments in this project were done on THP-1 TLR9 mCherry and CAL-1 TLR9 mCherry cells, while Human embryonic kidney (HEK293) cells were used as positive and negative controls of TLR9 expression.

3.1.1 Reagents

6-well cell culture cluster (Costar, Cat. No: 3516), T25 Corning® cell culture flasks with vented caps (Sigma-Aldrich/Merck, Cat. No: 430639), T75 Corning® cell culture flasks with vented caps (Sigma-Aldrich/Merck, Cat. No: 430641), T175 Corning® cell culture flasks with vented caps (Sigma-Aldrich/Merck, Cat. No: 431080), Z2 Coulter counter (Beckman Coulter), Roswell Park Memorial Institute (RPMI)-1640 Medium (Gibco, Cat. No: A10491-01), RPMI-1640 (Sigma-Aldrich/Merck, Cat. No: R8758), Dulbecco's Modified Eagle Medium (DMEM) (Lonza/BioWhittaker, Cat. No: 12-604F), Fetal calf serum (FCS) (Gibco, Cat. No: 10270), L-glutamine (Sigma-Aldrich/Merck, Cat. No: G7513), Penicillin-Streptomycin solution (Sigma-Aldrich/Merck, Cat. No: P0781), puromycin (Sigma-Aldrich/Merck, Cat. No: 58-58-2), β-mercaptoethanol (Sigma-Aldrich/Merck, Cat. No: 60-24-2), Trypsin/EDTA (Lonza/BioWhittaker, Cat. No: BE17-161E), Phorbol 12-myristate 13-acetate (PMA) (Sigma-Aldrich/Merck, Cat. No: P8139), recombinant human GM-CSF (R&D Systems, Cat. No: 215-GM), recombinant human IL-3 (R&D Systems, Cat. No: 203-IL), recombinant human IL-4 (PEPRO TECH, Cat. No: 200-04), ionomycin (Sigma-Aldrich/Merck, Cat. No: I3909), Dulbecco's Phosphate Buffered Saline (PBS) (Sigma-Aldrich, Cat. No: D8537).

3.1.2 CAL-1 cell line

CAL-1 is a pDC-like cell line established in 2000 upon isolation of primary malignant cells in leukemic phase from a 76-year old male patient with blastic NK cell lymphoma[89]. CAL-1 cells have small and round morphology, resembling plasma cells and grow in suspension, usually in clusters. They have abundant mitochondria, large nucleolus and parallel arrays of rough ER[89]. They express pDC markers CD4, CD56, CD38, CD45RA and HLA-DR on their surface, as well as mRNA for TLR2, TLR4, TLR7 and TLR9[89]. Incubation with recombinant GM-CSF (100pg/ml) or recombinant IL-3 (10ng/ml) and soluble CD40L (0.5mg/ml) for 72h differentiates CAL-1 into mature dendritic-like cells. Differentiation of

CAL-1 downregulates CXCR3 and CXCR4, while simultaneously and weakly upregulating CD11c, CD13 and CD33[89]. They produce TNFα upon stimulation with CpG ODN 2216 (Class A CpG ODN), but IFNα levels are not always detectable[89]. They are cultured in RPMI-1640 (Sigma-Aldrich/Merck) with 10% FCS and 2mM L-glutamine at 37°C and 5% CO_2, and split every two days ensuring the concentration between 10 000 and 50 000 cells/ml.

CAL-1 TLR9 mCherry inducible cell line was made by Lene M. Grøvdal through lentiviral transfection using Gateway cloning. mCherry tag is located on the C-terminus of TLR9. CAL-1 TLR9 mCherry cells are selected after transduction by culturing cells in standard CAL-1 medium with 0.25µg/ml puromycin. Administration of doxycycline is required to induce TLR9 expression through Tet-On system (for more details see section 3.2).

3.1.3 THP-1 cell line

THP-1 is a monocytic-like cell line established from a 1-year old boy with acute monocytic leukemia[90]. These cells are characterized by the presence of a-naphthyl butyrate esterase (cytochemical marker for monocytes), phagocytic activity through Fc and C3b receptors and lysozyme production[90,91]. They are cultured in RPMI-1640 (Gibco) with 10% FCS, 2mM L-glutamine, 0.05mM β-mercaptoethanol, 100 units/ml penicillin, 0.1 mg/ml streptomycin at 5% CO_2 at 37°C. They double every 19-26h and are split every three days ensuring density between 200 000 and 600 000 cells/ml. When undifferentiated, these cells grow in suspension as large, round single cells[90].

It is not completely clear whether THP-1 cells have a fully functional TLR9 - several studies have shown a lack of responsiveness of THP-1 monocytes to CpG ODNs, thereby indicating a lack of the functional receptor, but at the same time other groups have shown that THP-1 cells express functional TLR9 that signals upon stimulation with bacterial DNA and CpG ODNs[92-97]. THP-1 TLR9 mNeon and THP-1 TLR9 mCherry cells were then made to bypass the uncertainty regarding expression of a functional endogenous TLR9 in THP-1.

THP-1 TLR9 mNeon cells were made by Kai S. Beckwith. They were used in the initial screen of cell lines to determine the most suitable cell line for the project, but due to the lack of TLR9 expression on western blot they were not used in further experiments. THP-1 TLR9 mCherry inducible cell line was made by Lene M. Grøvdal through lentiviral transfection using the Gateway cloning. mCherry tag is located on the C-terminus of TLR9. THP-1 TLR9 mCherry cells are selected after transduction by culturing cells in THP-1 medium with 0.25µg/ml puromycin. Administration of doxycycline is required to induce TLR9 expression through Tet-On system (for more details see section 3.2). Wild type THP-1

was only used in initial screen of cell lines to determine endogenous TLR9 expression in these cells.

3.1.3.1 Differentiation of THP-1 cells into macrophage-like cells

THP-1 cells can be differentiated into macrophage-like cells by incubation with phorbol 12-myristate 13-acetate (PMA). PMA differentiation results in upregulation of surface markers such as CD14 and CD11b[98]. In addition, this type of differentiation is terminal, resulting in proliferation arrest and increased adherence to culture plates. THP-1 cells are differentiated with different concentrations of PMA for 24-72h. Fully differentiated THP-1 macrophages must rest for at least 24h in PMA-free culture medium to decrease upregulated NF-kB activity[99]. In this project, THP-1 cells were differentiated with 40ng/ml PMA in standard THP-1 TLR9 mCherry medium for 72h. Cells were allowed to rest for 48h in PMA-free medium before stimulation.

3.1.3.2 Differentiation of THP-1 cells into dendritic-like cells

Incubation of THP-1 cells with recombinant human IL-4 (rhIL-4) (200ng/ml) and recombinant human GM-CSF (rhGM-CSF) (100ng/ml) for 5 days, with cytokine replenishment every 48h, results in cells adopting immature dendritic-cell like properties[100]. Immature dendritic-like THP-1 cells are characterized by expression of CD80, CD86, CD40, CD209 and CD120b, all of which are absent from cell surface of undifferentiated THP-1 cells[100]. They have poor T-cell stimulatory capability, but are able to rapidly and efficiently take up large molecules via receptor-mediated endocytosis[100]. When THP-1 cells are incubated with rhIL-4 (200ng/ml), rhGM-CSF (100ng/ml), TNFα (20ng/ml) and ionomycin (200ng/ml) for 24h in serum-free medium they differentiate into mature dendritic cells[100]. In addition to cell surface markers found on immature dendritic-like THP-1 cells, these cells also express de novo CD83, CD120a, CD206 and HLA-DR[100]. Endocytic activity of mature dendritic-like THP-1 cells is much lower than that of immature dendritic-like THP-1 cells[100]. Upregulation of RelB and RelA, a hallmark of differentiation and final maturation of human DCs, is seen in mature dendritic-like THP-1 cells, but not in THP-1 cells differentiated only with rhIL-4 and rhGM-CSF[100].

In this project, immature dendritic-like cells were generated by differentiating THP-1 TLR9 mCherry cells with rhIL-4 (200ng/ml) and rhGM-CSF (100ng/ml) for 5 days. Cells were seeded with cytokines in standard THP-1 TLR9 mCherry medium (or antibiotic-free THP-1 medium if siRNA transfection was done during differentiation). Cytokines were

replenished 48h after seeding, and removed on day 5, upon which further treatment was administered to the cells. As immature dendritic-like THP-1 cells are non-adherent, cells were centrifuged at 200xg for 5 min prior to medium change and during washing steps. Differentiation of THP-1 TLR9 mCherry cells into cells that morphologically resemble mature dendritic cells was done with rhIL-4 (200ng/ml), rhGM-CSF (100ng/ml) and ionomycin (200ng/ml) for 5 days. Cytokines and ionomycin were replenished 48h after seeding and removed on day 5. These cells were only used to determine signaling capability of THP-1 dendritic-like cells, and since IL-4, GM-CSF-differentiated cells proved to be stronger producers of IFNβ1 and TNFα, only immature dendritic-like THP-1 cells were used from this differentiation protocol.

3.1.4 HEK293 cell line

HEK293 cell line was created by Van der Eb's lab in 1970s by transformation of human embryonic kidney cells, isolated from a healthy aborted fetus, with sheared adenovirus 5 DNA[101]. Since embryonic kidneys are very heterogenous it is difficult to determine what type of a kidney cell HEK293 is, but due to the presence of neuron-typical mRNA and gene products, it is suspected that it may have a neuronal origin. HEK293 cells are a frequently used cell line in molecular biology due to high transfection efficiency and protein production, and ability to synthesize gene products artificially inserted into the cells[101]. However, due to its experimentally transformed origin and a lack of information about its origin prior to transformation, HEK293 use *in vitro* to study different cell types is very limited.

HEK293 cells are cultured in DMEM supplemented with 10% FCS, 2mM L-glutamine, 100 units/ml penicillin and 0.1 mg/ml streptomycin, at 37°C and 8% CO_2. Medium was replenished every two to three days, and cells were kept at the concentration between 100 000 and 300 000 cells/ml. During sub-culturing, 0.5 g/l trypsin was added to culture flasks to detach cells, upon which fresh culture medium was added to inhibit trypsin activity.

HEK293 TLR9 Apex is a cell line made by Lene M. Grøvdal for use in preliminary microscopy experiments. Apex, a 28kDa monomeric tag derived from ascorbate peroxidase, is located on the C-terminus of TLR9[102]. Apex tag can withstand strong cell fixation methods making it very useful in electron microscopy. This cell line was used as a positive control for TLR9 expression in initial western blot screening experiments. HEK293XL hTLR9-HA and HEK293XL hTLR8-HA are two cell lines obtained from InvivoGen that were made by stable transfection of HEK293XL cells containing a human antiapoptotic Bcl-XL gene with pUNO-

hTLR9-HA and pUNO-hTLR8-HA plasmids, respectively. In both cell lines the TLR was fused to the 3' end of the HA tag, a 3kDa tag derived from human influenza hemagglutinin. HEK293XL hTLR9-HA cell line was used as a positive control in initial screens to identify TLR9-expressing cell lines, while HEK293XL TLR8-HA as a negative control due to the lack of endogenous TLR9 in HEK293 cells.

3.2 Induction of TLR9 expression

3.2.1 Reagents

Doxycycline (Echelon Bioscience, Cat. No: B-0801)

3.2.2 Background

Tetracycline (Tet) technology is based on Tet-controlled genetic switches found in Gram-negative bacteria, such as *Escherichia coli*. Tet-Off and Tet-On gene expression systems allow turning target gene expression on and off with high precision. In a Tet-Off system, target gene expression is shut down upon removal of doxycycline or tetracycline from the culture medium. Tet-On system functions in the opposite way – administration of doxycycline only (Tet-On does not respond to tetracycline) turns on target gene expression (Figure 3.1[103]).

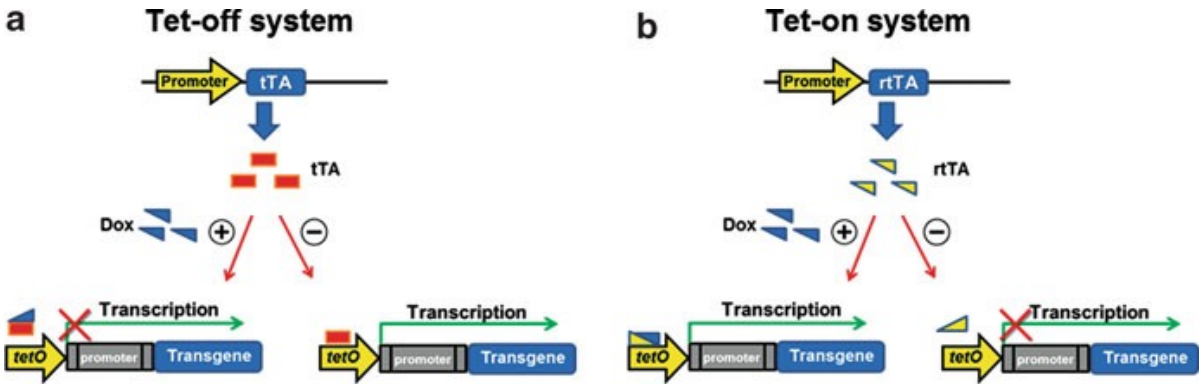

Figure 3.1[103] Tet-Off/Tet-On-mediated regulation of gene expression. **A)** Tet-Off system: when doxycycline (Dox) is not present, tet transactivators (tTAs) bind tet-operator (tetO) and drive gene expression. Presence of Dox prevents tTAs from binding tetO and inducing target gene expression. **B)** Tet-On system: when Dox is not present, reverse tTAs (rtTAs) cannot bind the tetO and induce gene expression. Presence of Dox leads to binding of rtTAs to the tetO and induction of target gene expression.

In *E.coli*, in the absence of Tet, Tet repressor (TetR) negatively regulates tetracycline resistance genes by binding tightly to the Tet operators (*tetO*) located in the *tetA* promoter[104].

This suppresses *tetA* expression. Administration of Tet leads to a conformational change and dissociation of TetR from *tetO*, resulting in de-repression of *tetA* and subsequent efflux of Tet[104].

There are two critical components of the Tet-Off/Tet-On gene expression system. The first one is the regulatory protein that is a fusion of TetR and the C-terminal of Herpes simplex virus VP16 activation domain[105,106]. The fusion is known as the tetracycline-controlled transactivator (tTA) as it converts TetR from a repressor to a transcriptional activator. The regulatory protein in the Tet-On system differs by 4 amino acids from the TetR and it is based on the reverse Tet repressor (rTetR)[106]. Both tTA and rtTA (reverse TA) are encoded by the pTet-Off and pTet-On regulator plasmids, respectively. These plasmids also contain an antibiotic-resistance gene which allows for selection of stably transfected cells.

The second component of the system is the response plasmid which contains the gene of interest. The gene of interest is expressed under the control of the tetracycline-response element (TRE) which contains *tetO* and a CMV promoter, that lacks the strong enhancer elements[106]. When Tet cell lines are created, they contain both regulatory and response plasmids, and in these cell lines the gene of interest is only expressed when tTA or rtTA bind TRE. This allows precise, dose-dependent control of gene expression that can be mediated by administration or removal of tetracycline or its less toxic derivatives. Summary of Tet-Off and Tet-On and the general principle are shown in Figure 3.1[103]. Tet-On system was used in this project to induce TLR9 expression in THP-1 TLR9 mCherry and CAL-1 TLR9 mCherry cells.

3.2.3 Procedure

1µg/ml doxycycline was used to induce TLR9 mCherry expression in THP-1 TLR9 mCherry cells while 0.5µg/ml was required for induction of TLR9 mCherry in CAL-1 TLR9 mCherry cells. Doxycycline was administered for 24-48h in both cell lines, depending on the method used for sample analysis. Exact induction times are specified in figure texts for each experiment.

3.3 Stimulation of cells with CpG ODN

3.3.1 Reagents

CpG ODN 2006 (Biomers, Cat. No: 00202305-1), CpG ODN 2006 (TIB MOLBIO, Cat.No: 1611821), CpG ODN 2006 (TIB MOLBIO, Cat. No: 1712649), CpG ODN 2216 (TIB

MOLBIO, Cat. No: 10668-3237), Dulbecco's Phosphate Buffered Saline (PBS) (Sigma-Aldrich, Cat. No: D8537).

3.3.2 Background

TLR9 signaling pathways are activated by foreign DNA or synthetic oligodeoxyribonucleotides (ODNs) containing unmethylated CpG sequences. There are three different subclasses of synthetic ODNs: A, B and C. CpG ODN 2216 and 2006 used in this project are Class A and B CpG ODNs, respectively. Class A CpG ODNs contain a single CpG motif attached to the phosphodiester backbone, and modified poly-G 3' and 5' ends attached to the phosphorothioate backbone[15,16]. Class B CpG ODNs contain a phosphorothioate backbone with a single or multiple CpG motifs attached to it, while Class C CpG ODNs have features of both above-mentioned classes[11,17].

3.3.3 Procedure

CpG ODN 2216 and 2006 were resuspended in sterile PBS for final concentration of 500μM. Prior to stimulation, cells were placed in fresh medium, then stimulated with CpG ODNs, concentrations ranging 1-10μM, for 1-5h, depending on the experimental setup, and kept at 37^{o}C, 5% CO_2 throughout the entire stimulation.

3.4 Transient gene silencing with siRNA

To study localization of TLR9 and how its localization regulates CpG-induced signaling, mediators of TLR9 signaling and trafficking pathway would have to be silenced. A large portion of the project focused on establishing and optimizing a protocol for siRNA gene silencing in THP-1 TLR9 mCherry and CAL-1 TLR9 mCherry cells. In addition, this transient gene silencing was also used to study effects of Rab39a and Rab11a on signaling ability of TLR9 in THP-1 TLR9 mCherry cells.

3.4.1 Reagents

6-well cell culture cluster (Costar, Cat. No: 3516), Opti-Mem® (Gibco, Cat. No: 11058-021), Dulbecco's Phosphate Buffered Saline (PBS) (Sigma-Aldrich, Cat. No: D8537), Lipofectamine® RNAiMAX (Invitrogen, Cat. No: 13778-150), Lipofectamine® 3000 (Invitreogen, Cat. No: L3000-015), DOTAP Liposomal Transfection Reagent (Roche, Cat. No: 11202375001), Viromer BLUE (LabLife Nordic AB, Cat. No: VB-01LB-00), Viromer

GREEN (LabLife Nordic AB, Cat. No: VG-01LB-00), QiAzol (Qiagen, Cat. No: 79306), Rab11a siRNA – 5 (Qiagen, Cat. No:SI00301553), Rab39a siRNA – 5 (Qiagen, Cat. No: SI02663276), Rab39a siRNA – 6 (Qiagen, Cat. No: SI02663283), Rab39a siRNA – 7 (Qiagen, Cat. No: SI04439918), Rab39a siRNA – 8 (Qiagen, Cat. No: SI04439925), Allstar Negative Control siRNA (Qiagen, Cat. No: S103650318).

3.4.2 Background

Small interfering RNAs (siRNAs) are 20-25 base pair-long, dsRNA molecules commonly used to transiently silence genes. Short-term gene silencing mimics single gene loss-of-function mutations and thus allows studying the roles of certain genes both *in vitro* and *in vivo*. siRNA is delivered to the cell via viral or non-viral routes. Viral delivery involves the use of lentivirus, retrovirus or adeno-associated virus to deliver siRNA into difficult-to-transfect cells[107]. It is suitable for *in vivo* studies and stable transfections, but as with use of any virus, the method carries a risk of stimulating antiviral responses in transfected cells. Non-viral routes include electroporation, cationic liposome- and polymer-based siRNA delivery. Electroporation relies on the electrical pulse to open up cell membranes and deliver the siRNA to the inside of the cell. While effective for difficult-to-transfect cells, electroporation often results in high cell mortality[107]. Cationic liposome-based method is relatively easy to perform and works with a variety of eukaryotic cells. Cationic liposomes are specially designed lipids that consist of one or two hydrocarbon chains and a positively charged group which interacts with the RNA phosphate backbone to form siRNA-liposome complexes. These complexes are taken up by the cell most likely via endocytosis. Once inside the cell, the siRNA will bind to the RNA induced silencing complex (RISC) and siRNA strands will become separated[107]. Antisense single-stranded siRNA will guide the complex to the target mRNA in the nucleus where complimentary mRNA will be cleaved by Ago2 found in the RISC[107]. Overall, regardless of the transfection method used, siRNA-mediated gene silencing always carries a risk of having an off-target effect, induction of immune response and cell death. In order to monitor for these effects, several controls can be used in an experimental setup: an untreated sample to determine normal gene expression, a mock-transfected control incubated only with the transfection reagent to monitor for effects of the transfection reagent on cell survival and immune responses, a positive control in which siRNA that gives a high knockdown efficiency is used, and a negative control in which a scrambled siRNA oligonucleotide that does not bind to any mRNA is used to monitor for any non-specific changes in gene expression.

In this project, several liposomal reagents were used to transfect THP-1 TLR9 mCherry and CAL-1 TLR9 mCherry cells with siRNA against Rab39a and Rab11a siRNA oligonucleotides. Allstar siRNA was used as a negative control as it does not bind to any mRNA sequence.

3.4.3 Principle

Both forward and reverse transfection methods were used in this project. In forward transfection, siRNA-liposome complexes were formed in sterile tubes, and added to cells previously seeded in culture plates. In reverse transfection the complexes were incubated in culture plates, and cells in suspension were added to them. All siRNA transfections were performed in 6-well culture plates in antibiotic-free medium to reduce cell death. Efficiency of siRNA-mediated knockdown was assessed by RT-qPCR. Every transfection method except Viromer BLUE- and Viromer GREEN-mediated siRNA transfection, was done in both THP-1 TLR9 mCherry and CAL-1 TLR9 mCherry cells.

3.4.3.1 siRNA transfection with Lipofectamine RNAiMAX

siRNA oligonucleotide and Lipofectamine RNAiMAX (8µl) were diluted in 240µl pre-heated Opti-MEM in separate sterile tubes. Diluted siRNA was added to pre-diluted Lipofectamine RNAiMAX and the complex was incubated at room temperature for 20 min (in a sterile tube for forward transfection, and in culture plates for reverse transfection). The complexes (480µl) were then added to cells (forward transfection) or cells were added to pre-complexed siRNA-liposomes in culture plates (reverse transfection), and cultured at 37ºC, 5% CO_2 (different incubation times with siRNA are specified in the experimental timeline in each figure). Final siRNA concentration ranged 16-20nM.

3.4.3.2 siRNA transfection with Lipofectamine 3000

siRNA oligonucleotide and Lipofectamine 3000 (7.5µl) were diluted in pre-heated Opti-Mem (125µl) in separate sterile tubes. Diluted siRNA was added to diluted Lipofectamine 3000 and the complex was incubated for 10-15 min at room temperature (in a sterile tube for forward transfection, and in culture plates for reverse transfection). The siRNA-Lipofectamine 3000 mixture (250µl) was added to cells (forward transfection) or cells were added to pre-complexed siRNA-liposomes in culture plates (reverse transfection), and cultured at 37ºC, 5% CO_2 (different incubation times are specified in the experimental timeline in each figure). Final siRNA concentration was 33nM.

3.4.3.3 siRNA transfection with DOTAP

siRNA was diluted in sterile PBS to a concentration of 0.1µg/µl in the final volume of 50µl. DOTAP (30µl) was mixed with PBS (70µl). Diluted siRNA was added to DOTAP diluted in PBS, gently mixed and the complexes were incubated at room temperature for 10-15 min. The mixture (150µl) was then added to cells and incubated for 3-20h (different incubation times are specified in the experimental timeline in each figure), after which fresh medium was added to cells. Final siRNA concentration ranged 160-178nM. Only forward transfection was performed with DOTAP.

3.4.3.4 siRNA transfection with Viromer BLUE and Viromer GREEN

siRNA was diluted to 11µM in Viromer BLUE buffer for the final volume of 20µl. 2µl droplet of Viromer BLUE reagent was placed onto the wall of a fresh tube, and 180µl of Viromer BLUE buffer was immediately added. 180µl of diluted Viromer BLUE reagent was added to pre-diluted siRNA, mixed and placed in culture plates. The mixture was incubated at room temperature for 15 min, after which cells were added to the plates and incubated for 48h at 37°C and 5% CO_2. Final siRNA concentration was 100nM. The same protocol applies to Viromer GREEN. Only reverse transfection was performed with Viromer BLUE and Viromer GREEN, and it was only done in CAL-1 TLR9 mCherry cells.

3.5 Western blot

Western blot was used to detect TLR9 in initial screening experiments and to study effects of different treatments (i.e. doxycycline induction, stimulation with CpG) on TLR9 protein expression. In addition, western blot was also used to study signaling pathways downstream of TLR9 by observing changes in expression of phospho-TBK1 (pTBK1), phospho-p38 (p-p38), phospho-STAT1 (pSTAT1), and total IκB.

3.5.1 Reagents

Radioimmunoprecipitation (RIPA) buffer (Sodium chloride (Merck, Cat. No:1.06404.1000), EDTA (Sigma, Cat. No: E6578-100G), Triton X-100 (Sigma, Cat. No: T8787-100ML), Trizma Base (Sigma, Cat. No:T1503), Hydrochloric acid (Merck, Cat. No: 1.00317.1000), cOmplete™ Mini, EDTA-Free Protease Inhibitor Cocktail (Roche, Cat. No: 11836170001), PhosSTOP Phosphatase Inhibitor tablets (Roche/Sigma, Cat. No: 04906837001)), TBS-T

(Tween-20 (Sigma, Cat. No: P1379-500ML), Sodium chloride (Merck, Cat. No: 1.06404.1000), Trizma Base (Sigma, Cat. No: T1503), Hydrochloride acid (Merck, Cat. No: 1.00317.1000)), Dithiothreitol (DTT) (Applied Chemistry, Cat. No:A3668.0050), NuPage™ LDS Sample Buffer (4x) (Invitrogen, Cat. No: NP0007), NuPage™ 4-12% Bis-Tris Protein Gels, 10-well (Invitrogen, Cat. No: NP0321Box), NuPage™ 4-12% Bis-Tris Protein Gels, 12-well (Invitrogen, Cat. No: NP0322Box), NuPage™ 4-12% Bis Tris Midi Protein Gels, 20-well (Invitrogen, Cat. No: WG1402BOX), NuPAGE™ MOPS SDS Running Buffer (20X) (Invitrogen, Cat. No: NP0001), SeeBlue® Plus2 Pertained Standard (Invitrogen, Cat. No: LC5925), MagicMark™ XP Western Protein Standard (Invitrogen, Cat. No: LC5602), Bovine Serum Albumin (Sigma, Cat. No: A7906-500g), iBlot™ 2 Transfer Stacks, nitrocellulose, mini (Invitrogen, Cat. No: IB23002), iBlot™ 2 Transfer Stacks, nitrocellulose, regular size (Invitrogen, Cat. No: IB23001), SuperSignalTM West Femto Maximum Sensitivity Substrate (Invitrogen, Cat. No: 34096). Antibodies used in this method can be found in Table 3.1.

Antibody	Primary/Secondary	Host species	Clonality	Supplier	Product number
RFP	Primary	mouse	monoclonal	Chromotek	6G6-100
TLR9 (D9M9H)	Primary	rabbit	monoclonal	Cell Signaling Technology	13647T
TLR9 (H-100)	Primary	rabbit	polyclonal	Santa Cruz Biotechnology	25468
TLR9 (N-15)	Primary	goat	polyclonal	Santa Cruz Biotechnology	sc13215
TLR9 (NBP2)	Primary	mouse	monoclonal	Novus Biologics	24729SS
TLR9 (NBP1)	Primary	rabbit	polyclonal	Novus Biologics	77254
HA	Primary	rabbit	monoclonal	Sigma	H6908-100UL
pSTAT1 (Ser727)	Primary	rabbit	polyclonal	Cell Signaling Technology	9177S
pTBK1/NAK (Ser172)	Primary	rabbit	monoclonal	Cell Signaling Technology	5483S
p-p38 MAPK (Thr180/Tyr182)	Primary	rabbit	monoclonal	Cell Signaling Technology	4511
IκBα	Primary	rabbit	polyclonal	Cell Signaling Technology	9242
β-tubulin	Primary	rabbit	polyclonal	Abcam	ab6046
GAPDH	Primary	mouse	monoclonal	Abcam	ab8245
Goat anti-mouse immunoglobulins HRP	Secondary	goat	polyclonal	Dako	P0447
Swine anti-rabbit immunoglobulins HRP	Secondary	swine	polyclonal	Dako	P0399
Rabbit anti-goat immunoglobulins HRP	Secondary	rabbit	polyclonal	Dako	P0449

Table 3.1 Primary and secondary antibodies used in western blot. Phosphorylated proteins are denoted with a prefix "p"

3.5.2 Background

Western blot is a semi-quantitative method used to detect and analyze proteins of interest in a given sample, such as cells or tissues. Samples are lysed with various lysis buffers (e.g. Radioimmunoprecipitation (RIPA) buffer, Triton X-100, Tris-HCl, etc.) to solubilize the membranes and separate proteins from non-soluble components of the cells. Choice of lysis buffer will depend on the location of the protein of interest. RIPA lysis buffer preserves membrane-bound proteins, and given that TLR9 is a transmembrane protein, RIPA was used as a lysis buffer in all experiments in this project (1% SDS, 4M urea was used as

lysis reagent only in experiments in which protein was extracted from organic phase in QiAzol lysate, for more details see sections 3.6.2.1.1 and 3.6.3). Once the samples are lysed, gel electrophoresis, blotting and protein detection are done.

Gel electrophoresis makes use of neutrally charged, thermo-stable and transparent polyacrylamide gels to separate samples. By adjusting the concentration of acrylamide and bis-acrylamide, it is possible to create both smaller and larger pores in the gel. In addition, bottom (resolving gel) and top (stacking gel) part of the gel can vary in polyacrylamide concentration – resolving gel ranges from 5-15%, whereas stacking gel is usually made of 5% polyacrylamide[108]. The percentage of the gel will vary with the size of the protein of interest with smaller proteins requiring higher polyacrylamide percentages. NuPage™ 4-12% Bis-Tris gels were used in this project to attempt to achieve good separation of proteins of similar size – post-translation modifications of TLR9 protein, presence of several isoforms of similar predicted sizes, and addition of a 29kDa mCherry tag could possibly make distinguishing different forms of TLR9 isoforms difficult on non-gradient gel.

Prior to loading onto the gel, samples are mixed with sodium dodecyl sulfate (SDS), an anionic detergent which breaks hydrogen bonds within proteins and denatures their secondary and tertiary structures and reducing agents that disrupt disulfide bonds between cysteine residues, such as β-mercaptoethanol or dithiothreitol (DTT). Sample preparation in this way results in depolymerization of proteins and subsequent heating of the depolymerized samples increases adherence of negative charge from SDS to the proteins, thus allowing electrophoretic mobility to be based on protein size, and not charge[108]. In addition, glycerol and bromophenol blue dye are added to samples – glycerol increases sample density and allows them to sink into the wells more easily and migrate faster through the gel towards the positive electrode, whereas the dye helps track the progress of electrophoresis. For electrophoresis to proceed, a running buffer that enables flow of electric current through the gel must also be supplied. In this project NuPAGE Bis-Tris gel electrophoresis system was used with MOPS (3-(N-mopholino) propane sulfonic acid) as a running buffer, given that all proteins of interest were relatively large (>30kDa). Bis-Tris ions are the common ions present in the gel and the running buffer provides Tris cations. Negatively charged chloride ions (Cl^-) are supplied in the gel buffer and they act as leading ions that have high mobility, and negatively charged MOPS ions acts as low mobility, trailing ions[108]. As appropriate voltage is supplied, SDS-bound depolymerized proteins will begin to migrate towards the anode in the lower chamber.

After the proteins have been separated on the gel, they are transferred onto nitrocellulose or polyvinylidene difluoride (PVDF) membranes. Nitrocellulose membranes have high protein-binding affinity and can immobilize proteins through hydrophobic interactions. They do not require pre-activation and are cheap and easy to use. However, small proteins (<20kDa) can be easily washed away from these membranes, so PVDF membranes are usually used for detection such proteins[108]. Prior to blotting, positively charged groups on the PVDF membranes must be activated by methanol, in order to be able to interact with negatively charged proteins. Transfer of proteins to a membrane can be done in semi-dry or wet conditions. Semi-dry transfer is less time-consuming, as electric current is directly applied to the gel and membrane. On the other hand, in wet transfer the gel and the membrane are placed between filter papers and sponges, creating a "sandwich", and then submerged into transfer buffer. Electrode plates that supply high intensity electric field are found parallel to the "sandwich" and will govern the protein transfer onto the membrane. Semi-dry transfer of proteins onto nitrocellulose membrane was used in this project as it is less time-consuming, and proteins of interest can successfully be transferred onto the membrane with adjustments in voltage and transfer time.

After the proteins have been transferred to the membrane, unreacted sites on the membrane are blocked with blocking agents (bovine serum albumin (BSA), non-fat dry milk, gelatin), and Tween-20, PBS and TBS are used as blocking buffers. The choice of the agent and buffer will depend on the protein of interest. While non-fat dry milk is the most cost-effective choice, it is not recommended for use with biotin-conjugated antibodies or when phosphorylated proteins are the target. In the same manner, when alkaline phosphatase-conjugated secondary antibodies are used, TBS buffer is preferred over PBS as PBS can interfere with normal function of alkaline phosphatase[108]. 5% BSA in TBS-T was used as a blocking agent for all western blots, as several phosphorylated proteins were studied as part of the project.

After blocking, the membrane is incubated in the primary antibody specific to the target protein. Both monoclonal and polyclonal antibodies can be used. Monoclonal antibodies tend to have lower background noise as they are specific for a single epitope, while polyclonal antibodies may have higher background noise, but they can recognize the target through several epitopes and thus often have higher affinity for the target. Membranes are rinsed in a washing buffer (PBS, TBST, etc.) before incubation with secondary antibody, to wash off unbound antibodies and minimize background noise. Species in which primary antibody was raised will determine the choice of an enzyme-conjugated secondary antibody.

To get the signal from the secondary antibody, a substrate that reacts with the enzyme conjugated to it must be added. Horse radish peroxidase (HRP) is an extensively used enzyme in this setting. When the substrate is present, HRP will oxidize it, and this will produce a detectable characteristic color change. Enhancers are also added to the substrate, thus increasing the signal intensity 1000-fold.

3.5.3 Procedure

For experiments in which western blot was used for analysis of protein expression, cells were seeded at a density ranging from 400 000 – 1 000 000 cells/well in 6-well plates (seeding cell density is specified in each experimental figure). Prior to lysis, culture medium was removed, and cells were quickly washed with cold PBS (suspension cells were centrifuged at 200-500xg for 5 min to remove culture medium and PBS). Cells were then lysed in 200µl RIPA (150mM NaCl, 10mM EDTA, 2% Triton X-100, 200mM Trizma Base, HCl pH to 7.5, PhosSTOP phosphatase inhibitor cOmplete mini protease inhibitor, ion-free water) and centrifuged at maximum speed, for 10 min at 4ºC. Cellular debris pelleted to the bottom of the tube and was discarded. Supernatant containing proteins released from lysed cells was mixed with 4X LDS sample buffer containing 10% 1M DTT. Final concentration of LDS sample buffer in the mixture was 1X. Samples were boiled at 95ºC for 10 min and loaded onto pre-made NuPAGE 4-12% Bis-Tris gels. SeeBlue® Pre-Stained Protein Standard and MagicMark™ XP Western Protein standard were used as molecular ladders. NuPAGE gel electrophoresis system was assembled according to manufacturer's recommendations. 1X MOPS was used as a running buffer. The gels were run at 100V for 30 min, then 150V for 105 min, unless otherwise specified in figure text. iBlot® 2 Gel Transfer Device was used to transfer the proteins onto nitrocellulose membranes. Blotting was done in three steps, first at 20V for 2 min, then 23V for 5 min and finally 25V for 3 min, unless otherwise specified in figure text. After blotting, membranes were quickly washed with TBS-T (0.1% Tween-20, 150mM NaCal, 50mM Trizma Base, HCl to pH 7.5, ion-free water) and blocked with 5% BSA in TBS-T for 30 min-2h. Membranes were incubated in primary antibodies diluted in 1% BSA in TBS-T overnight at 4ºC, with gentle shaking. β-tubulin and GAPDH were used as loading controls and membranes were only incubated with them for 2h at room temperature. Membranes were washed with TBS-T for 30 min-1h before incubation with a secondary antibody. HRP-conjugated secondary antibodies were diluted in 1% BSA in TBS-T according to manufacturers' recommendations. SuperSignal™ West Femto Maximum Sensitivity

Substrate was used as a substrate for HRP. Signal was detected on LI-COR Odyssey Fc Imager. Band quantitation was done using ImageStudio Lite.

3.6 RT-qPCR

In this project, RT-qPCR was used to detect TLR9-mediated changes in IFNβ1 and TNFα mRNA levels, before and after treatment of THP-1 TLR9 mCherry and CAL-1 TLR9 mCherry cells (i.e. doxycycline induction of TLR9 expression, stimulation with CpG ligands). In addition, it was also used to determine knockdown efficiency of Rab39a and Rab11a, and assess the ability of several different siRNA transfection reagents to facilitate gene silencing.

3.6.1 Reagents

QiAzol (Qiagen, Cat. No: 79306), Dulbecco's Phosphate Buffered Saline (PBS) (Sigma-Aldrich, Cat. No: D8537), Chloroform EMSURE® (Sigma-Aldrich/Merck, Cat. No: 67-66-3), RNeasy Mini Kit (Qiagen, Cat. No: 74106), Ethanol absolute (VWR Chemicals, Cat. No: VWRC20821.296), Ispropanol prima (Antibac AS, Cat. No: 600079), Guanidine hydrochloride (Sigma, Cat. No: G4504-100G), Water, nuclease-free (Thermo Scientific, Cat. No: 4346907), 5X Reaction mix (Thermo Scientific, Cat. No: R1362), Maxima enzyme mix (Thermo Scientific, Cat. No: K1642), PerfeCTa® qPCR FastMix® UNG, ROX (Quanta Bioscience, Cat. No: 84079), MicroAmp® 8-Tube Strip (Thermo Fisher, Cat. No: N8010580), MicroAmp® Fast 96-Well Reaction Plate (Thermo Fisher, Cat. No: 4346907), IFNβ1 TaqMan probe (Thermo Fisher, Cat. No: HS01077958_s1), IL-12B TaqMan probe (Thermo Fisher, Cat. No: HS01011518_m1), TNFα TaqMan probe (Thermo Fisher, Cat. No: HS00174128_m1), TBP TaqMan probe (Thermo Fisher, Cat. No:HS00427620_m1), Rab11a TaqMan probe (Thermo Fisher, Cat. No: HS00900539_m1), Rab39a TaqMan probe (Thermo Fisher, Cat. No: HS00380029_m1).

3.6.2 Background

Quantitative reverse transcription polymerase chain reaction (RT-qPCR) is used to detect and quantitatively analyze expression of a specific RNA in a sample. RNA is extracted from a sample, and through reverse transcription (RT) converted into complementary DNA (cDNA). qPCR is then used to measure the amount of DNA each cycle during a PCR. Reverse transcription can be done directly with qPCR (one-step RT-qPCR) or separately (two-step RT-qPCR). Two-step RT qPCR was used in all experiments in this project.

3.6.2.1 RNA extraction

Isolation and purification of RNA from a sample (tissue, blood, cells, etc.) is one of the most important steps in RT-qPCR, and if not done properly can affect all downstream processes. There are various ways of RNA isolation depending on the sample it comes from, but all of them aim for stabilization of the RNA molecule, inhibition of RNase activity, preservation of RNA structure, maximum yield and removal of compounds that can interfere with enzymatic activity during cDNA and qPCR.

QiAzol was used to lyse cells in this project. It contains guanidine thiocyanate which prevents RNA degradation by inhibition of RNases, and phenols which allow separation of RNA into aqueous supernatant when chloroform is added[109]. Phenol-chloroform mix is centrifuged and the solution separates into three layers: an organic phase which contains proteins, a middle phase with DNA, and an upper aqueous phase containing RNA. In RNA phenol-chloroform extraction, the pH must be acidic to separate RNA from DNA (Figure 3.2). At lower pH DNA becomes uncharged and migrates to the middle phase. RNA remains in the aqueous phase and is later transferred and mixed with 75% ethanol, which washes away salts that can interfere with reverse transcriptases and enhances RNA binding to the silica membrane found in RNeasy Mini spin columns[110]. In this project, RNasy Mini Kit was used to purify RNA, and buffers found in the kit are used to wash away any contaminants. RNA is eluted in RNase free water. UV spectroscopy is used to determine RNA concentration and purity. 260/280 and 260/230 absorbance ratios are used to asses purity of isolated RNA. 260/280 ratio of 2.0 indicates pure RNA. 260/230 ratio higher than 260/280 ratio also indicates pure RNA. Contaminants such phenols, guanidine or other reagents used in extraction protocol will usually result in lower 260/280 ratios.

3.6.2.1.1 Protein extraction from QiAzol lysate

Proteins found in the organic phase during phenol-chloroform RNA extraction can be isolated and analyzed by western blot (Figure 3.2). Absolute ethanol is added to the organic phase to wash away salts, and then isopropanol, which is less polar than ethanol, is used to precipitate proteins as pellets. Guanidine hydrochloride, a chaotropic agent is used to wash and denature proteins found in the pellet. Afterwards, the pellet is dissolved in urea and SDS, and prepared for western blot (detailed in Sections 3.5.2 and 3.5.3)

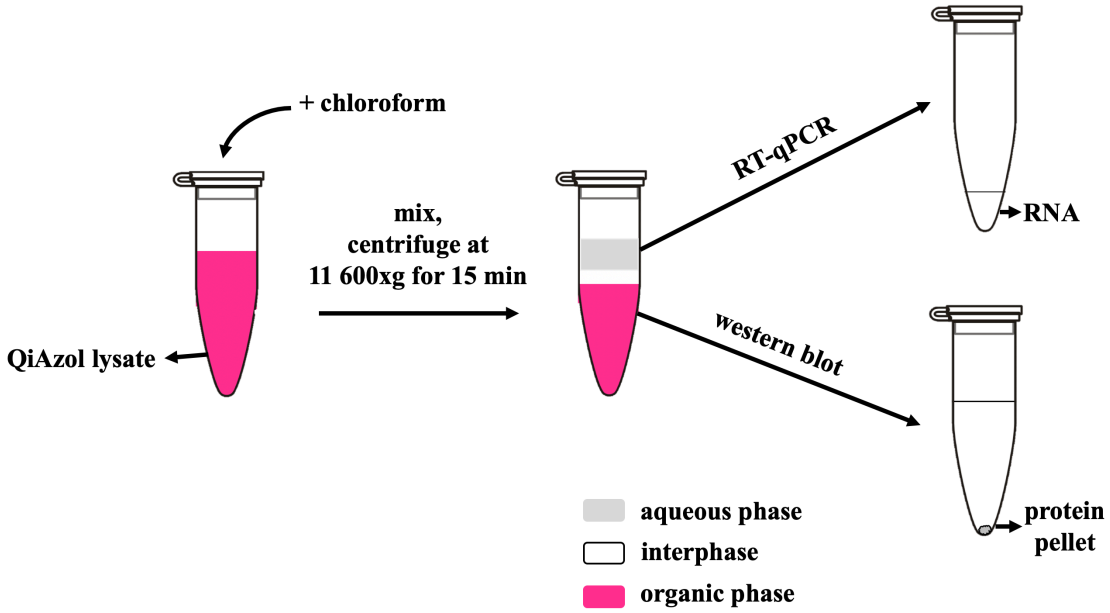

Figure 3.2 Both protein and RNA can be isolated from QiAzole cell lysate. Upon administration of chloroform, and centrifugation, phenol-chloroform mixture separates into three layers: aqueous phase containing RNA, interphase containing DNA and organic phase containing protein. RNA for RT-qPCR use is isolated from the aqueous phase and proteins for western blot are extracted from organic phase via isopropanol-precipitation.

3.6.2.2 cDNA synthesis

cDNA is synthesized from an RNA template by reverse transcriptases (RTs), enzymes commonly found in retroviruses that have RNA-dependent DNA polymerase activity. A short primer complementary to the 3' end of the RNA is added to the cDNA reaction mix which will then govern the reverse transcriptase-mediated cDNA synthesis. This method consists of three steps: primer annealing, DNA polymerization and enzyme deactivation. At the beginning of cDNA synthesis, a short primer and RNA template are mixed and heated to 65ºC for 5 min, and the cooled down at 4ºC for at least 1 min[111]. This allows the primer to anneal to the template, and it also ensures that RNA is single stranded. Then, reverse transcriptase, dNTPs, RNase inhibitors and buffers are added to the reaction mix. DNA polymerization is done at 25-60ºC, for 10-90 min, depending on the primer and enzyme used[111]. After cDNA has been synthesized, temperatures are increased to 70-85ºC for 5-15 min to inhibit the transcriptase[111].

3.6.2.3 qPCR

In qPCR, a thermostable DNA polymerase, a combination of temperature changes and a set of primers are used to amplify specific parts of the DNA template that correspond to the gene of interest sequence. At the beginning of the amplification cycle, temperature is increased to 95ºC. This will denature dsDNA into single strands. Primers specific for the sequence of gene of interest, are added to the reaction mix and will anneal to ssDNA when temperature is lowered to 50-60ºC. polymerase will synthesize a complementary DNA strand. The amount of short DNA sequence doubles every cycle, leading to an exponential amplification of target DNA. In this project, TaqMan hydrolysis probes were used to detect florescence signal. They contain a fluorophore linked to a quencher. When they are linked together, florescence cannot be detected. When TaqMan probe is added to qPCR mix, it will bind the sequence of interest on ssDNA, between forward and reverse primers. When DNA polymerase encounters the probe, it will degrade it and break the link between the fluorophore and the quencher. This will lead to an increase in fluorescence in the sample. The more of the gene of interest in the sample, the higher the fluorescence. C_T value (a cycle in which fluorescence observed from amplified gene of interest is above the background levels) can then be used to determine the amount of gene of interest in each sample[112]. C_T value is inversely proportional to the amount of gene of interest in the sample - the higher the C_T value, the less of the amplified gene of interest there is.

C_T value can be used to determine the absolute amount of DNA in a sample (by using a standard curve), or it can be used for determining the relative amount of DNA (by using a $\Delta\Delta C_T$ method). In this project, the goal was to determine the changes in gene expression upon stimulation, gene silencing, etc., so $\Delta\Delta C_T$ method was used. The following equations were used to calculate the fold change:

$$\Delta C_T = C_{T\ \text{gene of interest}} - C_{T\ \text{endogenous control}}$$

$$\Delta\Delta C_T = \Delta C_{T\ \text{sample 1}} - \Delta C_{T\ \text{calibrator}}$$

$$\text{Fold change} = 2^{-\Delta\Delta CT}$$

Housekeeping genes (e.g. TBP, GAPDH) that are not affected by treatment of cells and are equally expressed across experimental conditions are used as endogenous controls. Calibrator is an untreated sample (e.g. non-stimulated) that all other samples are compared to.

3.6.3 Procedure

Cells were seeded at a density of 400 000 cells/well in 6-well plates for all experiments in which RT-qPCR was used for quantification of protein expression. Prior to cell lysis with QiAzol, cells were washed quickly with cold PBS, three times (suspension cells were centrifuged at 200-500xg for 5 min after each wash to discard unnecessary PBS). Cell lysis was done on ice with 750µl of QiAzol. 150µl chloroform was added to each sample and vigorously mixed. Samples were centrifuged at 11 600xg for 15 min, after which 200µl of aqueous supernatant containing RNA was transferred to another tube and mixed with 200µl of 75% ethanol. The mixture was transferred to an RNeasy Mini spin column and extraction was done according to RNeasy Mini Kit protocol. Proteins were precipitated from the same QiAzol lysate by mixing the organic phase with 225µl of absolute ethanol and incubating for 2-3 min at room temperature. Samples were centrifuged at 2000xg for 5 min, and phenol phase was transferred to another tube and mixed with 1.125ml of isopropanol. Pelleted DNA was discarded as it was no longer needed. Samples were incubated for 10 min at room temperature and then centrifuged at 12 000xg for 10 min. Supernatant was discarded and protein pellet was washed three times for 20 min with 1.5ml of 0.3 guanidine hydrochloride in 96% ethanol. After each washing step, samples were centrifuged at 7500xg for 5 min and supernatant was discarded. 1.5ml of 96% ethanol was added to protein pellet. Samples were incubated at room temperature for 20 min, then centrifuged at 7500xg for 5 min. The pellet was air-dried for 5-10 min after discarding the supernatant and lysed in 200µl buffer containing 1% SDS and 4M urea. Western blot was run on precipitated proteins (See section 3.5.3. for further details on western blot procedure used in the project).

Isolated RNA was used for cDNA synthesis and qPCR. Purity of RNA was measured by NanoDrop™ 1000, and concentration was adjusted to 50µg/µl, or to the lowest concentration if concentrations were below 50µg/µl. cDNA was synthesized using Maxima First Strand cDNA synthesis kit. The following settings were used on the thermal cycler: 25°C for 10 min, 50°C for 30 min and 85°C for 5 min. Upon completion, cDNA was diluted 1:5 with RNase free water. TaqMan probes PerfeCTa qPCR FastMix were used to prepare 20µl qPCR mixes in a MicroAmp Fast Optical 96-well reaction plate. All samples were run in technical duplicates for qPCR, unless otherwise specified in figure text. StepOne Plus RT PCR cycler was used to run qPCR with the following settings: 50°C for 2 min, 95°C for 10 min (95°C for 15sec, 60°C for 60sec) x 40 cycles. TBP was used as endogenous control in all

experiments. C_T values were obtained from StepOne software and fold change was calculated using the $\Delta\Delta C_T$ method.

3.7 Confocal microscopy

In this project, confocal microscopy was used to determine expression of TLR9 mCherry and its localization in THP-1 TLR9 mCherry and CAL-1 TLR9 mCherry cells prior to and post stimulation with TLR9 ligands. Endosomal trafficking markers, EEA1 (early endosomes), LAMP1 (late endosomes/lys3osomes) and GM130 (*cis*-Golgi) were used to determine localization of the receptor at several times points.

3.7.1 Reagents

Dulbecco's Phosphate Buffered Saline (PBS) (Sigma-Aldrich, Cat. No: D8537), Paraformaldehyde (PFA) 16% (VWR Chemicals, Cat. No: 43368.9M), Pooled A+ serum from blood bank (St. Olav's Hospital). Saponin (Sigma-Aldrich/Merck, Cat. No: 47036), All antibodies used in this method are listed in Table 3.2.

Antibody	Dilution	Primary/ Secondary	Host species	Clonality	Supplier	Product number
RFP	1:1000	Primary	rat	monoclonal	Chromotek	5f8-100
TLR9 (D9M9H)	1:100	Primary	rabbit	monoclonal	Cell Signaling	13647T
TLR9 (H-100)	1:100	Primary	rabbit	polyclonal	Santa Cruz Biotechnology	sc-25468
LAMP1	1:100	Primary	mouse	monoclonal	Santa Cruz Biotechnology	sc-20011
EEA1	1:100	Primary	mouse	monoclonal	Santa Cruz Biotechnology	sc-53939
GM130	1:1000	Primary	rabbit	monoclonal	Abcam	ab52649
AlexaFluor 488 goat anti-rabbit IgG (H+L	1:1000	Secondary	goat	polyclonal	AlexaFluor	A11034
AlexaFluor 488 goat anti-mouse IgG (H+L)	1:1000	Secondary	goat	polyclonal	AlexaFluor	A28175
AlexaFluor 488 chicken anti-rabbit IgG (H+L)	1:1000	Secondary	chicken	polyclonal	AlexaFluor	A21441
AlexaFluor 488 donkey anti-rabbit IgG (H+L)	1:1000	Secondary	doneky	Polyclonal	AlexaFluor	A21206
AlexaFluor 647 goat anti-rat IgG (H+L)	1:1000	Secondary	goat	polyclonal	AlexaFluor	A-21247

Table 3.2 Primary and secondary antibodies used in immunostaining for confocal microscopy

3.7.2 Background

Confocal microscopy is an imaging method that allows for visualization and creation of two- and three-dimensional images of a sample. When the laser light is applied, dichromatic mirrors will bounce the laser light from the objective onto a second mirror (Figure 3.3[113]). When the laser light passes through an immunofluorescently-stained sample, not all of the sample will be illuminated at once (Figure 3.3[113]). Instead, the focus will be only on a specific spot of a specific depth within a sample and the fluorescent light will be emitted exactly at this spot. Out-of-focus signal coming from the above and below the focus point will be filtered and eliminated from the final image through a “pinhole” located between a sample and a detector. Even though only a small section of the sample is being imaged at a time,

confocal microscopes are able to quickly take numerous images which can then be used to make two- or three-dimensional constructs of the sample.

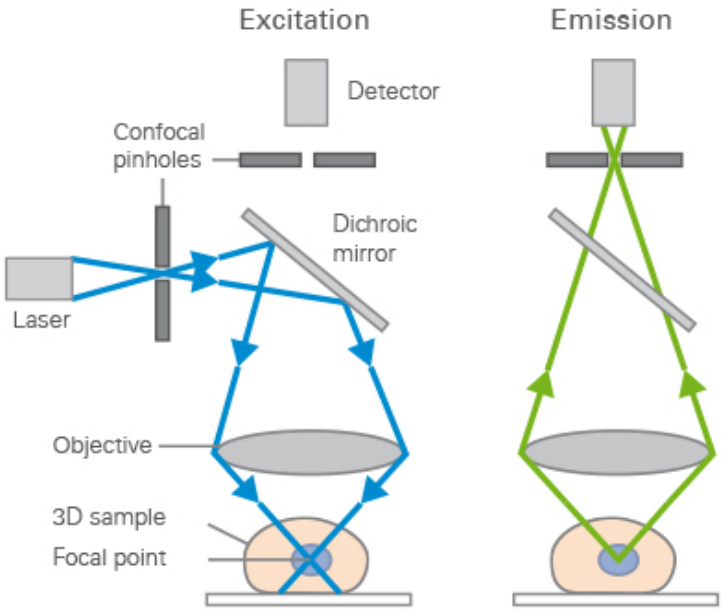

Figure 3.3[113] Principle behind confocal microscopy. Lasers provide excitation light. Dichromatic (dichroic) mirror bounces the laser light from the objective onto the second mirror, allowing the light to pass through the sample. Emitted light gets de-scanned by second mirror. The emitted light passes through the dichromatic mirror and through the pinhole. The pinhole eliminates "out-of-focus" signal. Light that goes through the pinhole is measured by the detector.

3.7.2.1 Immunoflourescence

For samples to be detected by a confocal microscope, they first need to be stained with antibodies specific for target molecule(s) through immunofluorescence, a method that relies on the use of antibodies conjugated to a fluorescent dye. The staining can be done directly or indirectly. Direct fluorescence takes advantage of primary antibodies that are already conjugated to a fluorophore, and it results in shorter staining time and reduced background noise that can be seen due to antibody cross-reactivity or non-specificity. On the other hand, indirect immunofluorescence requires the use of two antibodies – a primary antibody specific for the target molecule, and a fluorophore-conjugated secondary antibody that can recognize the primary antibody. It is a more time-consuming method, but it can result in higher signal intensity as multiple secondary antibodies can bind to a single primary antibody and thus amplify the signal.

Prior to staining with antibodies, samples must be fixed to allow preservation of the cells in their current state for as long as possible. Sample fixation is done with chemical crosslinkers such as formaldehyde or organic solvents like methanol or acetone. Each fixation

method can have a different effect on cellular morphology and the target epitopes – formaldehyde preserves cellular morphology quite well, but it also results in crosslinking of epitopes, thereby reducing antibody binding capacity, while organic solvents are good at preserving cell architecture, they have an extremely negative impact on many epitopes and largely diminish signal from fluorescent proteins such as GFP[114]. 4% paraformaldehyde (PFA) was chosen as a fixative agent in this project because even though PFA could potentially damage epitopes and lead to a decrease in antibody binding, methanol-acetone fixation would permeabilize membranes and could lead to precipitation of proteins out of the cytosol, and acetone treatment would largely diminish the fluorescence from mCherry tag. After fixation, NH_4Cl can be used to quench fluorescence coming from free or crosslinked aldehydes.

PFA fixation largely preserves cell membrane structure, meaning that if the target molecule is found on the inside of the cell, samples need to be permeabilized after fixation to allow antibodies to enter the cell interior. Triton X-100, a strong, nonionic detergent, is commonly used as a permeabilization agent as it can dissolve both the plasma membrane and interior membranes without affecting protein-protein interactions[115]. On the other hand, saponin, a milder detergent permeabilizes membranes by selectively removing cholesterol from the membrane[116]. This allows antibodies to access the inside of the cell without completely dissolving the membrane. Since TLR9 is a transmembrane protein, saponin was chosen as a permeabilization agent due to its mild nature and ability to permeabilize membrane while leaving it largely intact.

After permeabilization, blocking is done to prevent antibodies from binding to unspecific sites. BSA, nonfat dry milk or serum are commonly used as blocking agents. When serum is used, it is important that it does not come from the same species as the primary antibody, otherwise, secondary antibody will lose its specificity for binding sites on the primary antibody. In this project blocking was done with human A+ serum diluted in PBS with 0.1% saponin.

When blocking is done, samples are incubated with primary antibody specific for the target molecule. Cells can be incubated in multiple primary antibodies at the same time as long as they originate from different species. Primary antibodies are diluted in blocking solution and samples are incubated 1-2h at room temperature or overnight at 4^{o}C. Before incubating with secondary antibodies, samples are extensively washed with an isotonic buffer, such as PBS to remove all of primary antibody and reduce unspecific binding. Secondary antibodies are also diluted in blocking or washing buffer, and samples are incubated for 1h at

room temperature. All subsequent steps are done in dark to prevent bleaching of the fluorophores conjugated to secondary antibodies. After secondary antibodies are removed, samples are washed with and stored in PBS at 4°C, in a light tight container to avoid bleaching of the fluorophores.

3.7.3 Procedure

Cells were seeded at densities of 100 000 cells/well on 8-well cell culture slides and 100 000–600 000 cell/well in 24-well glass bottom plates. In experiments with PMA-differentiated cells, plates were coated with poly-L-lysine prior to seeding. Suspenion cells (IL-4, GM-CSF-differentiated THP-1 TLR9 mCherry cells and unidfferentiated CAL-1 TLR9 mCherry cells) were seeded without poly-L-lysine coating, and after each step, cells were centrifuged at 200-500xg, for 5 min to pellet the cells and remove unecessary supernatant.

After appropriate treatment of cells (specified in each figure text), they were washed three times, for 5 min with cold PBS. Fixation was done with 4% PFA, for 10 min at room temperature, after which samples were washed again three times, for 5 min with cold PBS. Cells were incubated with 50mM NH_4Cl for 10min at room temperature to quench flourescence (quenching of flourescence was done only for experiments shown in Figure 4.8.1, Figure 4.8.1.1, Figure 4.8.2, Figure 4.8.2.1), and then washed again three times for 5 min with cold PBS. Permeabilization of the cells was done with 0.1% saponin, 20% A+ in PBS for 30 min-1h at room temeprature. Samples were stained with primary antibodies in 0.1% saponin, 2% A+ in PBS at room temperature for 2h, or overnight at 4°C. Washing with cold PBS, three times for 5 min was done after removal of primary antibody. Samples were stained with AlexaFluor secondary antibodies diluted 1:1000 in 0.1% saponin, 2%A+ in PBS for 30 min-1h at room temperature. After removal of secondary antibodies, samples were washed with 0.1% saponin in PBS twice, for 5 min. Samples were stored in PBS at 4°C. Images were acquired using a 63x/1.40 objective on Leica SP8 STED 3x. Pearson's correlation coeffeicient was calculated in Fiji using Just Another Colocalization Plugin (JACoP).

4 RESULTS

The aim of this project was to study TLR9 signaling and trafficking, and gain insight into how TLR9 trafficking regulates signaling. TLR9 is highly expressed in pDCs, which in addition to being scarce in peripheral blood, are extremely fragile, making studying TLR9 very difficult. Therefore, THP-1 and CAL-1 expressing fluorescently tagged TLR9 were made to study TLR9 signaling and trafficking (Grøvdal, Unpublished data). HEK293 cells expressing tagged TLR9 and TLR8 were used as positive and negative controls, respectively.

4.1 Assessing TLR9 expression in THP-1, CAL-1 and HEK293 cell lines

In preliminary experiments, anti-TLR9 antibodies were screened to determine their specificity and ability to detect the protein in HEK293 TLR8HA and HEK293 TLR9HA cells by western blot. The results showed that two anti-TLR9 antibodies, D9M9H and NBP2, are suitable for studying of specifically recognized bands corresponding to TLR9 (Supplementary Figure 1). These antibodies were therefore used to determine whether TLR9 expression could be detected in CAL-1, CAL-1 TLR9 mCherry, THP-1, THP-1 TLR9 mCherry and THP-1 TLR9 mNeon cells (Figure 4.1). CAL-1 is a pDC-like cell line that has been shown to prominently express TLR9 mRNA, while CAL-1 TLR9 mCherry, in addition to endogenous TLR9, also expresses doxycycline-inducible TLR9 with a 28kDa mCherry tag at the protein's C-terminus[89]. THP-1 cells have been shown to induce cytokine responses upon stimulation with TLR9 ligands (bacterial DNA and CpG ODNs), but there is some controversy as to whether this cell line expresses functional TLR9 endogenously[92-97]. THP-1 TLR9 mCherry cell lines expresses doxycycline-inducible TLR9 mCherry, while THP-1 TLR9 mNeon was designed to express fluorescently-tagged TLR9 constitutively. HEK293XL cells containing anti-apoptotic Bcl-XL gene and expressing HA-tagged TLR9, and HEK293 cells expressing TLR9 tagged with a 27kDa Apex tag were used as positive controls for TLR9 expression. HEK293 TLR8HA and HEK293XL TLR8HA cells were used as negative controls as they lack endogenous TLR9, but express TLR8, a related endosomal TLR.

The results showed a band at 120kDa in HEK293 TLR9HA and at 150kDa in HEK293 TLR9 Apex cells (Figure 4.1A). Although TLR9 is a highly modified protein, its full length form ($TLR9_{FL}$) usually has a size of 120-150kDa, while cleaved TLR9 ($TLR9_C$) can be found at ≈80kDa[117]. The 120kDa band corresponds to $TLR9_{FL}$ (Figure 4.1A) and the 150kDa band is likely $TLR9_{FL}$ Apex which consists of $TLR9_{FL}$ (120kDa) and the Apex tag (27kDa) (Figure 4.1A). No bands corresponding to TLR9 were observed in negative controls,

indicating that anti-TLR9 (NBP2) antibody is specific for TLR9 in these cells (Figure 4.1A). Bands were also not observed in THP-1, CAL-1 or CAL-1 TLR9 mCherry cells. In the subsequent experiment cell number was increased, but no additional bands were observed (Figure 4.1B). These results indicate that resting THP-1, THP-1 TLR9 mCherry, THP-1 TLR9 mNeon, CAL-1 and CAL-1 TLR9 mCherry do not express TLR9 at high enough levels to be detected by western blot with the anti-TLR9 (NBP2) antibody, but a 150kDa band corresponding to $TLR9_{FL}$ Apex was readily detected in resting HEK293 cells overexpressing TLR9.

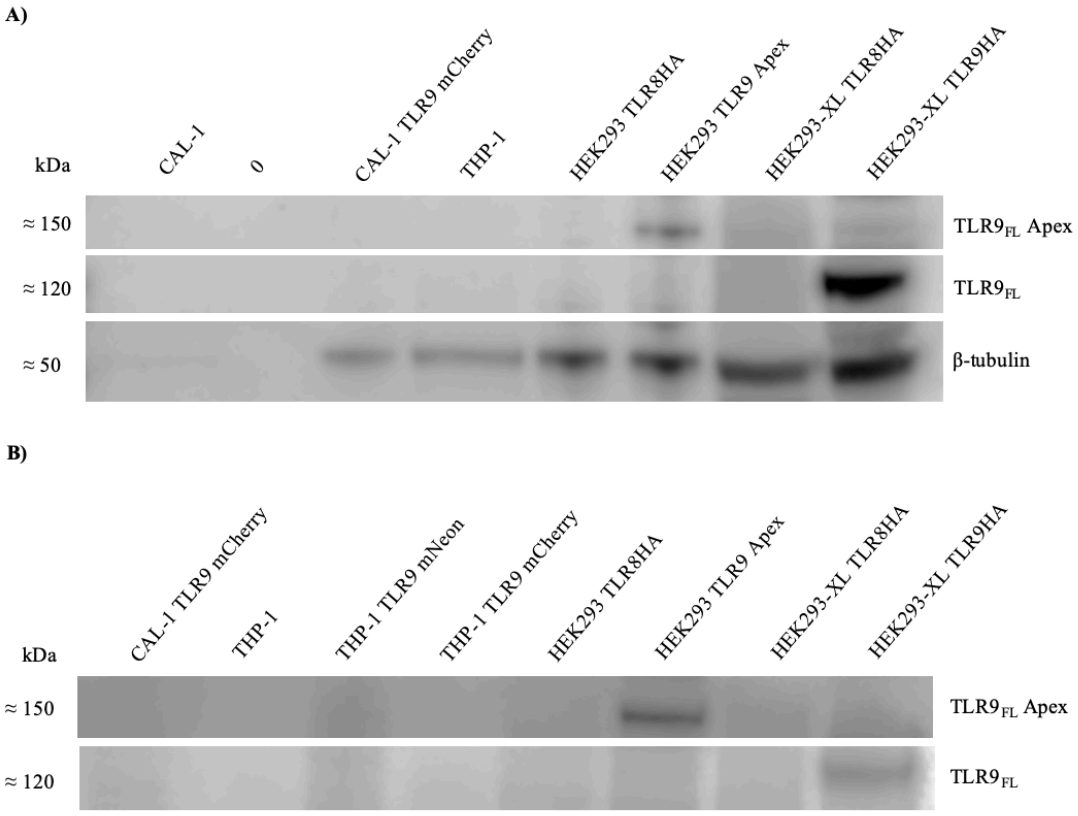

Figure 4.1 Identification of TLR9 expression in CAL-1, THP-1 and HEK293 cell lines by western blot. Cells were seeded in 6 well plates at a density of **A)** 500 000 cells/well and **B)** 10^6 cells/well and lysed in RIPA. Gel electrophoresis was done at 100V for 30 min, then 150V for 90 min. Proteins were transferred to a nitrocellulose membrane using iBlot 2 Gel Transfer Device program P0 (20V for 1 min, 23V for 4 min, 25V for 2 min). Membranes were blotted with anti-TLR9 (NBP2) antibody. β-tubulin was used as a loading control. $TLR9_{FL}$ – full length TLR9

4.2 Doxycycline induces TLR9 expression in THP-1 TLR9 mCherry and CAL-1 TLR9 mCherry cells

Results seen in the previous section (Figure 4.1) indicated that resting THP-1 TLR9 and CAL-1 TLR9 mCherry cells did not express TLR9 at high enough levels to be detected by

western blot. These two cell lines are based on the tetracycline technology which allows for selective and reversible switching on and off of target gene expression by administration or removal of tetracycline or its derivatives[118]. In the initial experiment (Figure 4.1), doxycycline (a tetracycline derivative) was not administered to THP-1 TLR9 mCherry and CAL-1 TLR9 mCherry cells prior to assessing TLR9 expression, so the following experiment aimed at determining whether TLR9 expression could be induced by administration of doxycycline and subsequently detected by western blot. To that end, undifferentiated THP-1 TLR9 mCherry and CAL-1 TLR9 mCherry cells were treated with increasing concentrations of doxycycline (0.1, 0.5 or 1µg/ml) for 2h, 24h or 48h (only 24h and 48h for CAL-1 TLR9 mCherry cells). Cells were then lysed and assayed for mCherry and TLR9 expression by western blot with both anti-mCherry (RFP) (Figure 4.2A, Figure 4.3A) or anti-TLR9 (D9M9H) (Figure 4.2B, Figure 4.3B) antibodies. Anti-mCherry antibody detects the mCherry tag, while anti-TLR9 (D9M9H) antibody detects TLR9 expression directly.

Lysates from THP-1 TLR9 mCherry cells stained with anti-mCherry antibody showed two bands (150kDa and 115kDa) after 24h induction with 1µg/ml of doxycycline (Figure 4.2A). The 150kDa band likely corresponds to full length TLR9 ($TLR9_{FL}$) mCherry which consists of $TLR9_{FL}$ (120kDa) and the mCherry tag (29kDa) (Figure 4.2A). The shorter band (115kDa) (Figure 4.2A) could correspond to cleaved TLR9 ($TLR9_C$) mCherry, which is normally produced upon TLR9 activation, or to deglycosylated $TLR9_{FL}$ mCherry[117]. However, deglycosylated $TLR9_{FL}$ has a size of approximately 80kDa[117]. When combined with the mCherry tag (29kDa) both of these forms of TLR9 could appear as a 115kDa band on western blot. Further, phosphorylated TLR9 and TLR9-B variant are predicted to be of the similar size, therefore as we cannot be certain which TLR9 form corresponds to this band, the 115kDa band seen on membranes blotted with anti-mCherry antibody will be referred to as short TLR9 ($TLR9_S$) throughout the rest of the manuscript.

On membranes with THP-1 TLR9 mCherry lysates blotted with anti-TLR9 (D9M9H) antibody, two bands (150kDa and 130kDa) were observed upon doxycycline (1µg/ml) administration for 24h (Figure 4.2B). As mentioned above, the 150kDa band is likely to correspond to $TLR9_{FL}$ mCherry. The 130kDa band appears only after doxycycline induction, indicating that it is TLR9-specific (Figure 4.2B). However, this band is not detected on membranes blotted with anti-mCherry antibody, suggesting that this form of TLR9 does not contain the mCherry tag, but is induced by presence of doxycycline. The 130kDa band corresponds to full length TLR9 without the mCherry tag and is therefore referred to as

$TLR9_{FL}$. No bands were detected in untreated samples on either blot, indicating that doxycycline administration is required for TLR9 expression in these cells.

Western blots of CAL-1 TLR9 mCherry cells showed two bands of 150kDa and 115kDa which were detected after 48h induction with 0.5µg/ml of doxycycline using the anti-mCherry antibody (Figure 4.3A). The 150kDa band is likely to correspond to $TLR9_{FL}$ mCherry in these cells, while the identity of the 115kDa short TLR9 ($TLR9_S$) band is unclear (Figure 4.2A). An additional 90kDa band was also detected in CAL-1 TLR9 mCherry cells after 48h induction with 1µg/ml of doxycycline (Figure 4.3A). This band is not detected in untreated samples or on membranes stained with anti-TLR9 antibody, indicating that this is possibly a form of an mCherry-tagged TLR9 (Figure 4.3). TLR9 size can vary due to post-translational modifications. While deglycosylated full length TLR9 is thought to have the size of 80kDa, Sinha et al. have shown that a fully deglycosylated TLR9 can be found at as low as 65kDa as well[24,117]. Therefore, this band could correspond to fully deglycosylated, full length TLR9 mCherry. Further, TLR9 has also been shown to have several cleavage sites, in addition to the main site located at 441-470aa, so this band could also possibly correspond to an alternatively cleaved, C-terminal fragment of TLR9 mCherry[10,11].

On membranes of CAL-1 TLR9 mCherry lysates blotted with anti-TLR9 antibody, two bands (150kDa and 130kDa) were detected after doxycycline (0.5µg/ml) induction for 48h (Figure 4.3B). Just as in THP-1 TLR9 mCherry cells, the 150kDa band corresponds to full length $TLR9_{FL}$ mCherry and 130kDa band is likely to correspond to full length TLR9 ($TLR9_{FL}$) without the mCherry tag, in CAL-1 TLR9 mCherry cells. No bands were detected in untreated sample with either antibody, indicating that doxycycline administration is required for TLR9 expression in these cells (Figure 4.3).

Overall the results in these experiments show that doxycycline administration is necessary for induction of TLR9 mCherry expression in both THP-1 TLR9 mCherry and CAL-1 TLR9 mCherry cells. In addition, the results also show that full length TLR9 can be detected by both anti-mCherry and anti-TLR9 antibodies, while smaller bands potentially corresponding to cleaved TLR9, can only be detected using anti-mCherry antibody.

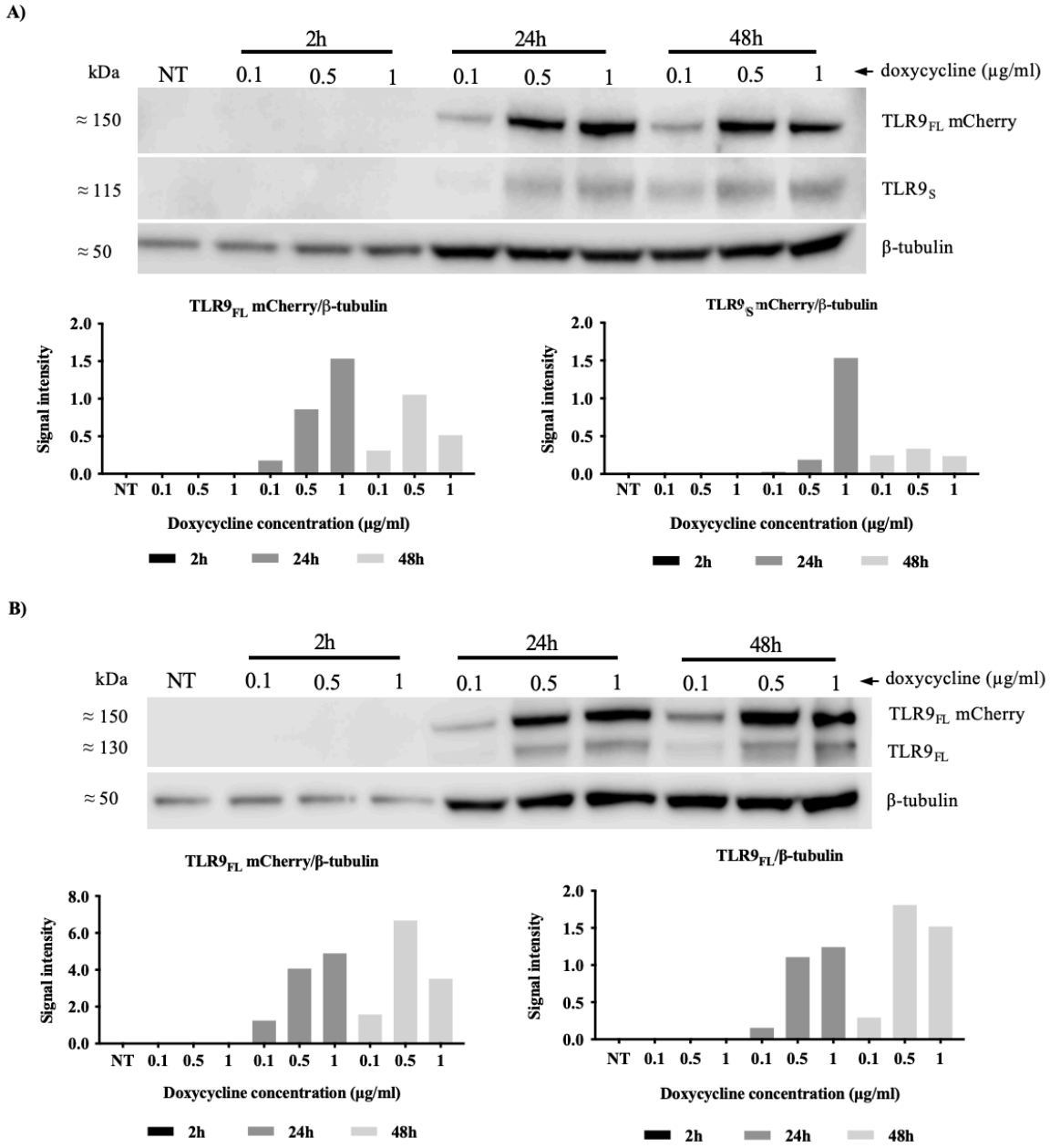

Figure 4.2 Doxycycline (1µg/ml) treatment of undifferentiated THP-1 TLR9 mCherry cells for 24h triggers a potent induction of full length TLR9 mCherry. THP-1 TLR9 mCherry cells were seeded in 6 well plates (10^6 cells/well) and treated with appropriate concentrations of doxycycline for 2h, 24h and 48h to induce TLR9 expression. Then cells were lysed and assayed by western blotting for **A)** mCherry (anti-RFP) or **B)** TLR9 (anti-TLR9 (D9M9H)). β-tubulin was used as a loading control. Results are representative of three independent experiments showing similar results. Bar diagrams show signal intensity of **A)** $TLR9_{FL}$ mCherry and $TLR9_S$ mCherry, and **B)** $TLR9_{FL}$ mCherry and $TLR9_{FL}$ normalized to β-tubulin.

NT- no doxycycline treatment; $TLR9_{FL}$- full length TLR9, $TLR9_{FL}$ mCherry - full length TLR9 mCherry, $TLR9_S$ mCherry– short TLR9 mCherry

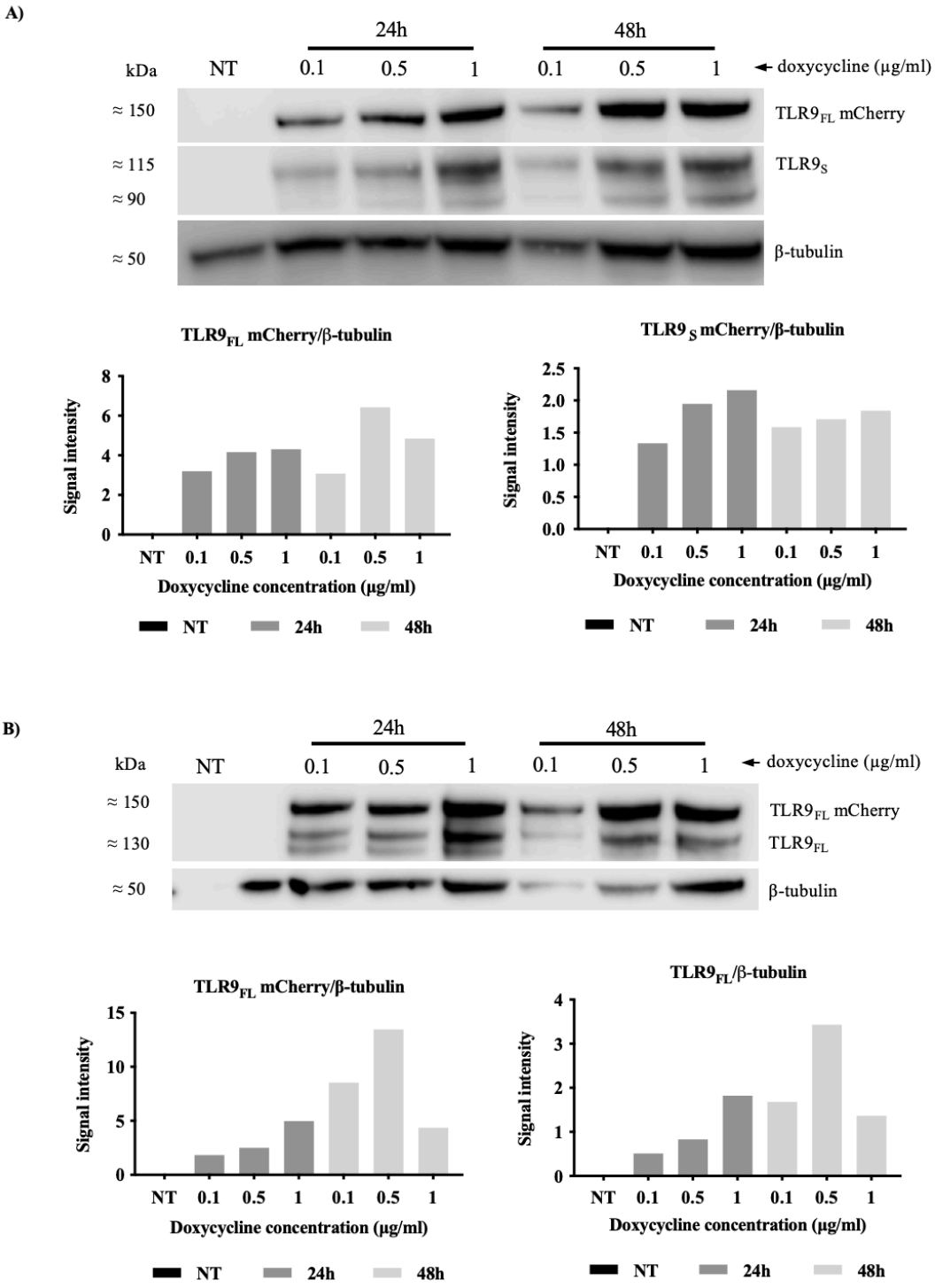

Figure 4.3 Doxycycline (0.5µg/ml) treatment of undifferentiated CAL-1 TLR9 mCherry cells for 48h strongly induces full length mCherry. CAL-1 TLR9 cells were seeded in 6-well plates (400 000 cells/well) and treated with appropriate concentrations of doxycycline for 24h and 48h to induce TLR9 expression. Cells were then lysed and assayed for **A)** mCherry (anti-RFP antibody) or **B)** TLR9 (anti-TLR9 antibody D9M9H). Blots were stained with anti- β-tubulin as a loading reference. Results are representative of three independent experiments showing similar results. Bar diagrams show signal intensity of **A)** $TLR9_{FL}$ mCherry and $TLR9_S$ mCherry, and **B)** $TLR9_{FL}$ mCherry and $TLR9_{FL}$ normalized to β-tubulin.

NT- no doxycycline treatment; $TLR9_{FL}$- full length TLR9, $TLR9_{FL}$ mCherry - full length TLR9 mCherry $TLR9_S$ mCherry– short TLR9 mCherry

4.3 TLR9 mCherry expression does not increase with CpG ODN 2006 stimulation

Upon stimulation with a ligand, TLR9 becomes proteolytically cleaved into two smaller fragments, a C-terminal fragment and an N-terminal fragment. The C-terminal fragment has a size of approximately 80kDa and it consists of the cytoplasmic and transmembrane domains and a part of the ectodomain[23]. It is required for TLR9-induced cytokine production, whereas the role of N-terminal fragment in regulation of TLR9 signaling is somewhat unclear[23,117,119]. To test whether stimulation of TLR9 would lead to an increased amount of cleaved receptor, THP-1 TLR9 mCherry cells were first differentiated with 40ng/ml of PMA for 72h, and TLR9 mCherry expression was induced with 1µg/ml of doxycycline for 48h. After removal of doxycycline, cells were stimulated with the synthetic TLR9 ligand CpG ODN 2006 (10µM) for up to 4h (Figure 4.4A). Cells were then lysed and assayed by western blot for mCherry or TLR9 expression using the anti-mCherry and anti-TLR9 antibody, respectively.

Western blots of lysates of THP-1 TLR9 mCherry cells stained with both antibodies show that there is a slight increase in both $TLR9_{FL}$ and $TLR9_{FL}$ mCherry expression after 3-4h of stimulation with CpG ODN 2006 (Figure 4.4B, C). $TLR9_S$ mCherry detected as a 115kDa (Figure 4.4B) could be the C-terminal cleavage product generated from TLR9. $TLR9_S$ mCherry expression did not change markedly during the 4h of stimulation.

Combined, these results indicate that TLR9 expression is markedly induced with doxycycline, but stimulation of these cells with TLR9 with CpG ODN 2006 does not induce further upregulation of the TLR9.

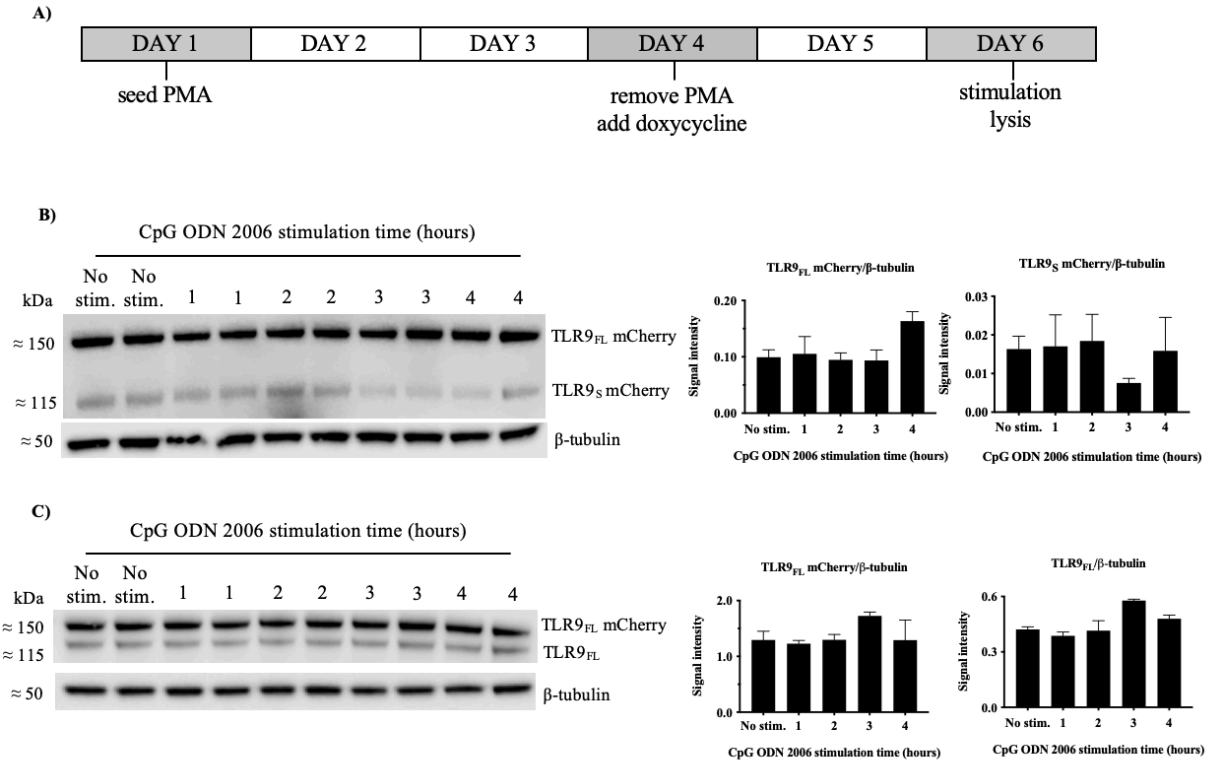

Figure 4.4 TLR9 expression does not markedly change with CpG ODN 2006 stimulation. A) THP-1 TLR9 mCherry cells (400 000 cells/well) were differentiated with PMA (40ng/ml) for 72h later. TLR9 expression was induced with doxycycline (1µg/ml) for 48h, after which cells were stimulated with 10µM CpG ODN 2006 for 1, 2, 3 and 4h. Cells were lysed and assayed for **B)** mCherry (anti-RFP antibody) and **C)** TLR9 (anti-TLR9 D9M9H antibody). Blots were stained with anti-β-tubulin as a loading reference. Western blots are a representative of two independent experiments run on the same membrane. Bar diagrams show signal intensity of **B)** $TLR9_{FL}$ mCherry and $TLR9_{S}$ mCherry, and **C)** $TLR9_{FL}$ mCherry and $TLR9_{FL}$ normalized to β-tubulin. Error bars represent standard deviation between two independent experiments.

$TLR9_{FL}$- full length TLR9, $TLR9_{FL}$ mCherry - full length TLR9 mCherry, $TLR9_{S}$ mCherry– short TLR9 mCherry

4.4 Doxycycline-induced TLR9 mCherry expression can be detected by confocal microscopy

Previous results showed that TLR9 mCherry expression could be induced by administration of doxycycline to both THP-1 TLR9 mCherry (1µg/ml for 24h) and CAL-1 TLR9 mCherry (0.5µg/ml for 48h) cells and detected by western. While western is useful for quantification of total TLR9 expression, confocal microscopy allows us to study trafficking and subcellular expression of the receptor. Confocal microscopy is more easily done with adherent cells, as attachment to the surface of a culture dish prevents them from freely floating in the suspension. This prevents loss of focus and loss of cells of interest from the observation filed during imaging. Both undifferentiated THP-1 TLR9 mCherry and CAL-1

TLR9 mCherry cells grow in suspension. Differentiation of CAL-1 TLR9 mCherry does not lead to generation of adherent cells (see section 4.7.2.2). On the other hand, THP-1 TLR9 mCherry cells can be differentiated with PMA into macrophage-like cells that firmly adhere to the surface of culture plates. So, to facilitate the detection of TLR9 mCherry expression by confocal microscopy, THP-1 TLR9 mCherry cells were differentiated with 40ng/ml of PMA for 72h, before TLR9 mCherry expression was induced with 1µg/ml of doxycycline for 48h (Figure 4.5A). Cells were subsequently fixed with 4% PFA and stained with anti-mCherry (RFP) or anti-TLR9 (D9M9H) antibodies.

The results showed that the mCherry signal was weak, but detectable after 48h doxycycline administration to PMA-differentiated THP-1 TLR9 mCherry cells (Figure 4.5B, C). Anti-mCherry (RFP) antibody- (Figure 4.5B) and anti-TLR9 (D9M9H) antibody-stained (Figure 4.5C) structures colocalized with mCherry signal, indicating that these two antibodies detected TLR9 mCherry. TLR9 mCherry staining was spread throughout the cytosol and appeared to be expressed in tubular ER-like structures (Figure 4.5B, C).

Overall the results in this experiment showed that both anti-mCherry (RFP) and anti-TLR9 (D9M9H) antibodies are specific for TLR9 and can be used to detect TLR9 expression by confocal microscopy after 48h doxycycline induction.

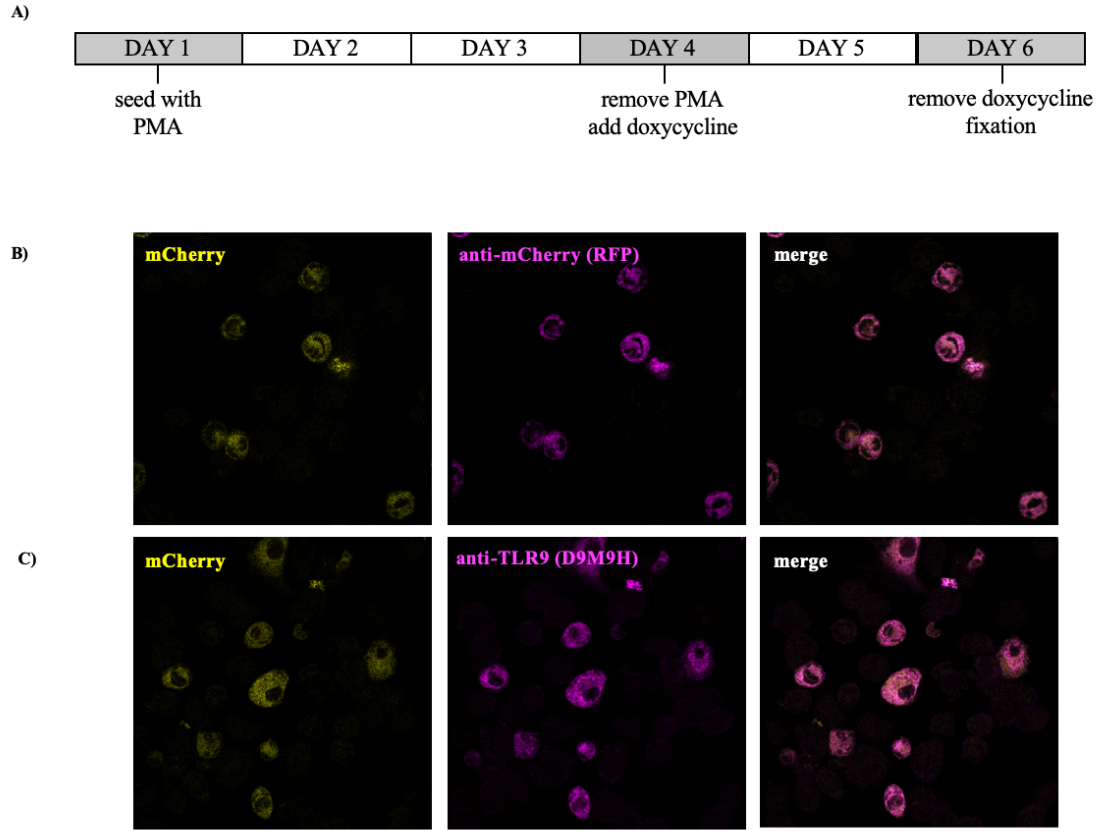

Figure 4.5 Anti-mCherry (RFP) and anti-TLR9 (D9M9H) antibodies colocalize with TLR9 mCherry. A) THP-1 TLR9 mCherry cells were seeded on poly-L-lysine-coated 8-well microscopy chamber (100 000 cells/well) and differentiated with PMA (40 ng/ml). Doxycycline (1µg/ml) was added for 48h after removal of PMA. Cells were fixed with 4% PFA and stained with **B)** anti-mCherry (RFP) and **C)** anti-TLR9 (D9M9H) antibodies. mCherry signal is obtained by exciting the tag at 560-580 nm. The experiment was done once.

4.5 $TLR9_{FL}$ mCherry is less stable than $TLR9_S$ mCherry after removal of doxycycline

In the previous section (Section 4.4) it was shown that TLR9 mCherry can be detected by confocal microscopy in PMA-differentiated THP-1 TLR9 mCherry cells. TLR9 is an endosomal receptor, so it was expected that its staining would predominantly be vesicular-like (small, dot-like structures spread around the cytosol). However, the results showed that the majority of TLR9 mCherry aggregated in ER-like structures (Figure 4.5B, C). This could be due to overexpression of newly synthesized TLR9 mCherry caused by administration of doxycycline. In the following experiment, we used western blot to determine stability of induced TLR9 and to deduce whether this issue could be remedied by doxycycline withdrawal and resting of cells in fresh medium for several hours prior to immunostaining. To that end, cells were differentiated with 40ng/ml of PMA for 72h before TLR9 mCherry

expression was induced with 1µg/ml of doxycycline for 48h (Figure 4.5A). After removal of doxycycline, cells were placed in fresh culture medium and harvested at time intervals for 0-3h (Figure 4.5B, C) and for 0-24h (Figure 4.5D, E). TLR9 expression was assessed with anti-mCherry (RFP) (Figure 4.5B, D) and anti-TLR9 (D9M9H) (Figure 4.5C, E) antibodies.

Western blots of THP-1 TLR9 Cherry stained with anti-mCherry antibody, showed two bands (150kDa and 115kDa) (Figure 4.5B, D). Expression of the 150kDa band corresponds to $TLR9_{FL}$ mCherry and appeared to be stable up to 3h after doxycycline removal (Figure 4.5B). 6h after doxycycline removal, expression of $TLR9_{FL}$ mCherry is reduced by approximately 50%, and continues to steadily decline (Figure 4.5D). After 24h, $TLR9_{FL}$ mCherry expression is reduced by approximately 90% of the expression seen right after doxycycline removal (Figure 4.5D). However, the $TLR9_{FL}$ mCherry protein levels were still high enough to be detected by western. The shorter, 115kDa, band detected on these membranes ($TLR9_S$ mCherry) was stable for the first 12h after removal of doxycycline (Figure 4.6B, D). There is a sudden reduction of $TLR9_S$ mCherry expression by approximately 80% 24h after doxycycline withdrawal (Figure 4.6D). According to the literature, cleaved TLR9 fragment is highly stable and it can remain present for up to 12h after the cleavage event, supporting the assumption that the shorter band seen on anti-mCherry antibody-blotted membranes could be cleaved TLR9 mCherry[25].

Lysates of THP-1 TLR9 mCherry cells stained with anti-TLR9 antibody showed two bands - a 150kDa and a 130kDa band (Figure 4.6C, E). As mentioned in previous section, 150kDa band is likely to correspond to $TLR9_{FL}$ mCherry, while 130kDa band corresponds to $TLR9_{FL}$. Both bands follow a similar pattern as the 150kDa band observed on the membranes stained with anti-mCherry antibody – $TLR9_{FL}$ mCherry and $TLR9_{FL}$ expression remains relatively stable for 3h (Figure 4.6C), and then sees a 50% reduction after 6h of doxycycline removal (Figure 4.6E). After 24h of doxycycline removal, 150kDa and 130kDa bands detected by anti-TLR9 antibody (Figure 4.6E) are much weaker than the 150kDa band detected by anti-mCherry antibody (Figure 4.6D).

Overall, these results indicate that without stimulation, $TLR9_{FL}$ mCherry has a half-life of 6h and that its expression is less stable than the expression of the shorter TLR9 band ($TLR9_S$ mCherry).

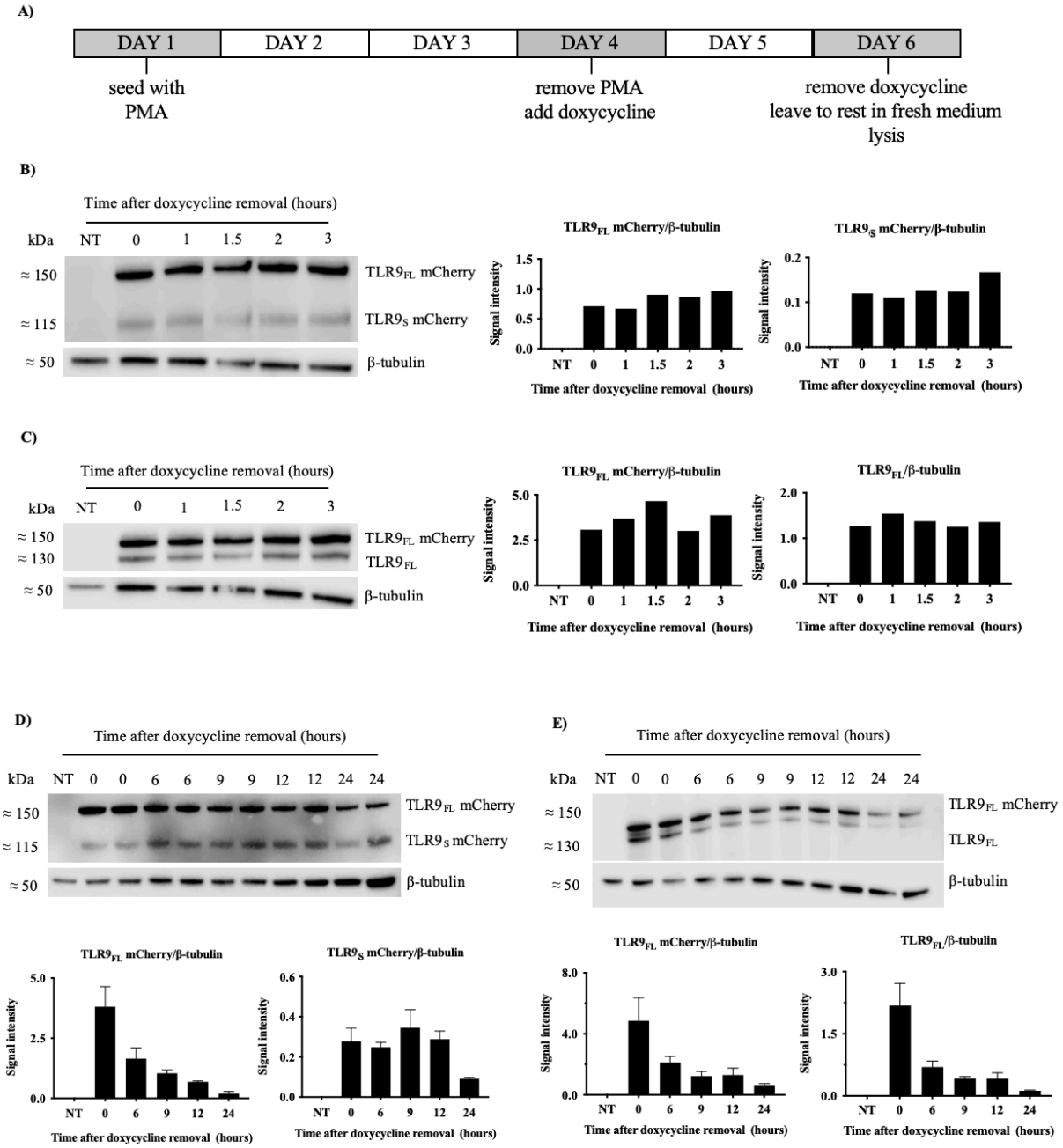

Figure 4.6 TLR9FL mCherry is less stable than TLR9S mCherry after doxycycline withdrawal. A) THP-1 TLR9 mCherry cells (400 000 cells/well) were differentiated with PMA (40ng/ml) for 72h. Doxycycline (1µg/ml) was added for 48h to induce TLR9 expression. After doxycycline removal cells were placed in fresh culture medium and harvested at time intervals **A, B)** 0-3h and **C, D)** 0-24h. Samples were then assayed for **B, D)** mCherry (anti-RFP antibody) and **C, E)** TLR9 (anti-TLR9 D9M9H antibody). Blots were stained with anti-β-tubulin as a loading reference. Western blots are a representative of two independent experiments showing similar results. Each time point (except NT sample) in western blots in **D)** and **E)** was run in two biological replicates within a single independent experiment. Bar diagrams show signal intensity of **B, D)** TLR9FL mCherry and TLR9S mCherry, and **C, E)** TLR9FL mCherry and TLR9FL normalized to β-tubulin. Error bars in **D)** and **E)** represent standard error for two biological replicates within a single experiment.

NT- no doxycycline treatment; TLR9FL- full length TLR9, TLR9FL mCherry - full length TLR9 mCherry TLR9S mCherry– short TLR9 mCherry

4.6 TLR9 colocalizes with LAMP1, but not with EEA1 and GM130 before and after stimulation with CpG ODN 2006

TLR9 localization and a type of ligand that activates it influence TLR9 signaling outcomes[78]. TLR9 that preferentially binds Class A CpG ODNs signals from early endosomes, while TLR9 that interacts with Class B CpG ODNs is found signaling from late endosomes[78,120]. In the following experiments the goal was to determine whether TLR9 colocalized with EEA1 (early endosome marker), GM130 (*cis*-Golgi marker) or LAMP1 (late endosome/lysosome marker) before or after stimulation with CpG ODN 2006, which is a Class B CpG ligand that is thought to induce secretion of pro-inflammatory cytokines from late endosomes[11,17]. Anti-mCherry (RFP) antibody, targeting the mCherry tag, was used to stain TLR9 in these experiments.

THP-1 TLR9 mCherry cells were differentiated with PMA (40ng/ml) for 72h, and TLR9 expression was subsequently induced with doxycycline (1µg/ml) for 48h. To visualize TLR9 under more relaxed conditions and prevent accumulation of ER-like structures likely caused by TLR9 overexpression (observed in 4.5B), cells were allowed to rest for 6h after doxycycline induction of TLR9. Cells were then stimulated with 10µM CpG ODN 2006 for 2h before being fixed with 4% PFA and stained with anti-mCherry and anti-EEA1 (Figure 4.7B, C), or anti-mCherry and anti-GM130 (Figure 4.7D, E).

Weak EEA1 staining was observed in both stimulated and unstimulated cells. No colocalization was observed between TLR9 and EEA1 (Figure 4.7B, C), indicating that TLR9 does not localize to early endosomes neither in unstimulated nor CpG-stimulated cells. Results also showed that TLR9 did not colocalize with the Golgi marker GM130 before or after stimulation (Figure 4.7D, E). 6-hour rest from doxycycline induction also appeared to be efficient in clearing up some of the newly synthesized TLR9. However, some of the cells still contained relatively large aggregates of TLR9-stained structures, suggesting that an even longer rest period may be beneficial for visualization of vesicular TLR9 staining (Figure 4.7B, C).

Confocal microscopy was also applied to study localization of TLR9 to late endosomes/lysosomes in THP-1 TLR9 Cherry cells. This was done by first differentiating THP-1 TLR9 mCherry cells with PMA for 72h, before TLR9 mCherry expression was induced with 1µg/ml of doxycycline for 48h. After removal of doxycycline, cells were allowed to rest in fresh culture medium for 12h prior to stimulation. Cells were subsequently stimulated with 10µM CpG ODN 2006 for 30, 60 and 120 minutes, before being fixed, and stained for mCherry and the late endosome/lysosome marker LAMP1 (Figure 4.8B, C, D, E).

It appeared that most of the newly synthesized TLR9 had regressed 12h after doxycycline withdrawal, and the receptor appeared to be more confined to vesicles (Figure 4.8B, C). The results also showed that TLR9 colocalized with LAMP1 before and after stimulation (Figure 4.8 B, C, D, E). The extent of colocalization appeared to be approximately the same under all conditions. Quantification of TLR9 and LAMP1 colocalization could not be done due to having too few TLR9 mCherry-positive cells. LAMP1 staining is normally characterized by small, dot-like structures spread throughout the cytosol, but in PMA-differentiated THP-1 TLR9 mCherry cells, LAMP1-stained structures appeared as unusually large aggregates in the cytosol (Figure 4.8B, D). It is possible that these large aggregates (Figure 4.8B, D) are a result of PMA-induced lysosomal clustering and mTORC1 activation[121].

Overall, TLR9 appeared to colocalize with LAMP1-positive late endosomes/ lysosomes before and after stimulation, but not with early endosomes or the Golgi. These results indicate that in PMA-differentiated cells TLR9 may reside in late endosomes/lysosomes before stimulation, and also interact with CpG ODN 2006 in these compartments to induce cytokine responses.

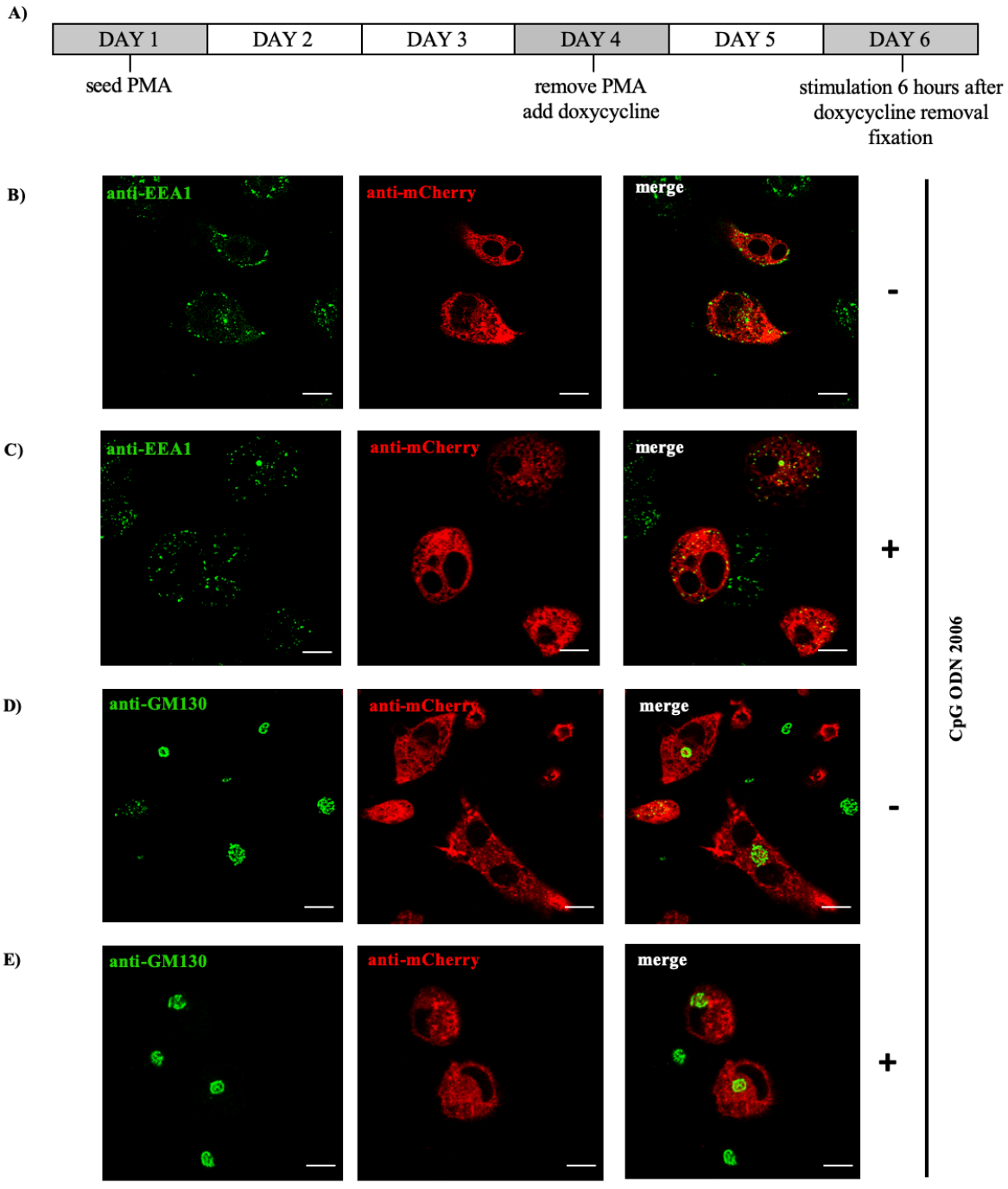

Figure 4.7 TLR9 does not colocalize with EEA1 or GM130 before or after CpG ODN 2006 stimulation. A) THP-1 TLR9 mCherry cells (100 000 cells/well) were differentiated on poly-L-lysine-coated 24-well glass bottom plates with PMA (40ng/ml) for 72h. After 72h, medium was changed and doxycycline (1µg/ml) was added for 48h to induce TLR9 expression. After doxycycline removal cells were left to rest for 6 hours in fresh medium before stimulation. Stimulation was done with **C, E)** 10µM CpG ODN 2006 for 2h. Cells were fixed and stained for TLR9 mCherry, **B, C)** EEA1 and **D, E)** GM130. Experiment was done once. Quantification of colocalization was not possible due to having too few TLR9-positive cells. Scale bars are 15µm.

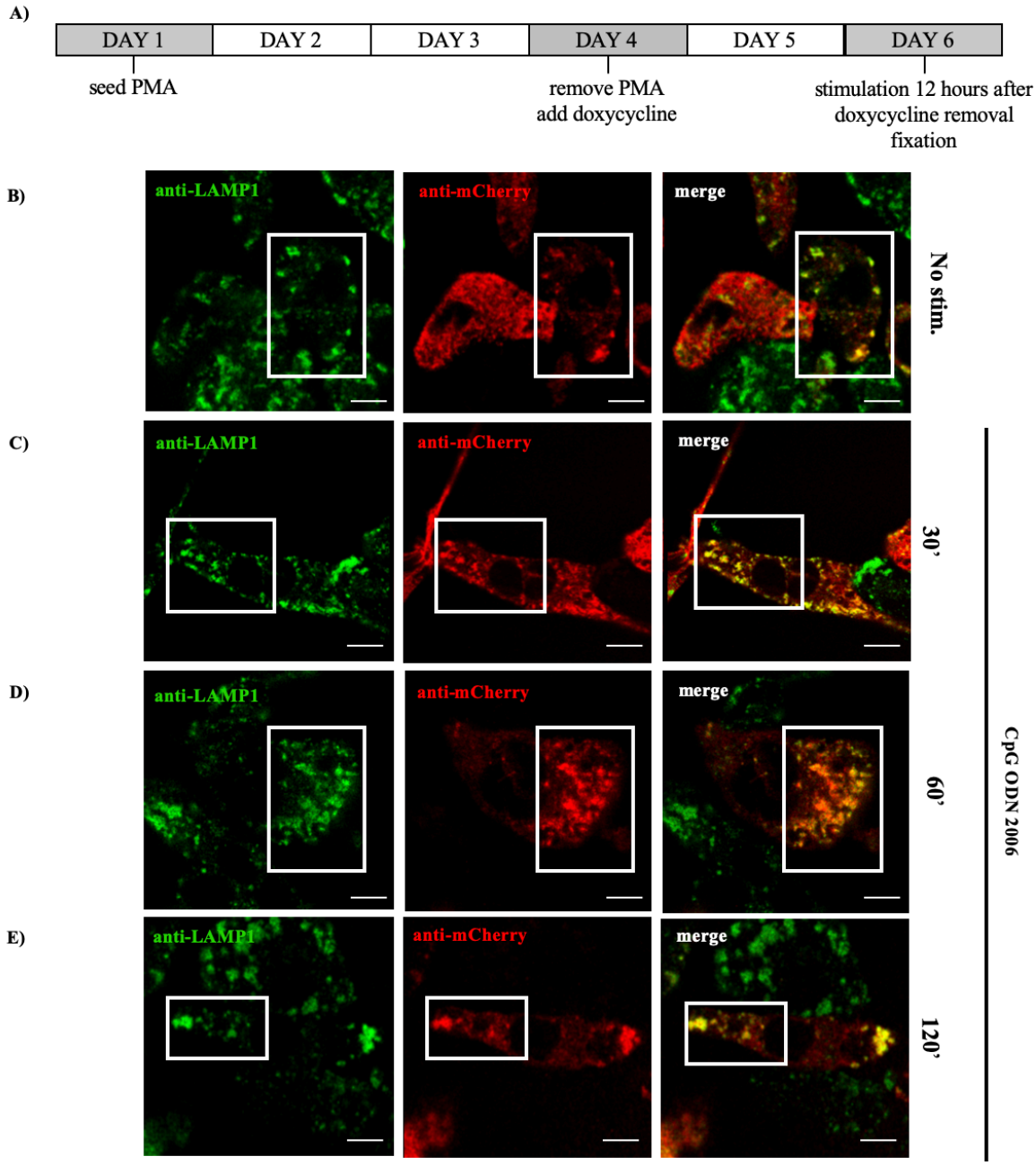

Figure 4.8 TLR9 colocalizes with LAMP1 before and after 30-, 60-, and 120-minute stimulation with CpG ODN 2006. A) THP-1 TLR9 mCherry cells (100 000 cells/well) were differentiated on poly-L-lysine-coated 24-well glass bottom plates with PMA (40ng/ml) for 72h. TLR9 expression was subsequently induced with doxycycline (1µg/ml) for 48h. After doxycycline removal cells were left to rest for 12 hours in fresh medium before being stimulated with **C, D, E)** 10µM CpG ODN 2006 for 30, 60 and 120 minutes. Cells were fixed and stained for **B, C, D, E)** TLR9 mCherry and LAMP1. Experiment was done once. Quantification of colocalization was not possible due to having too few TLR9-positive cells. White frames indicate areas of TLR9 and LAMP1 colocalization. Scale bars are 15µm.

4.7 TLR9-induced secretion of IFNβ1 and TNFα

To understand how trafficking regulates TLR9 signaling, it is first necessary to understand what components play part in TLR9 signaling and how exactly this receptor responds to its ligands. Once it was established that TLR9 expression could be studied by western blot and confocal microscopy in THP-1 TLR9 mCherry cell line, it was also necessary to confirm that these cells were able to produce cytokines. However, previous findings in the lab indicated that PMA-differentiated cells were not able to express IFNβ1 upon stimulation with either Class A or Class B CpG ODN (Wang, Grøvdal, Unpublished data). Therefore, our focus shifted to the differentiation method described by Berges at al. that results in generation of immature and mature dendritic-like THP-1 TLR9 mCherry cells[100]. In addition, signaling was also studied in pDC-like CAL-1 TLR9 mCherry cells that express both endogenous TLR9 and doxycycline-inducible TLR9 mCherry.

4.7.1 THP-1 TLR9 mCherry cells

4.7.1.1 THP-1 TLR9 mCherry differentiation

To determine which cells have the best ability to induce IFNβ1 and TNFα upon TLR9 stimulation with synthetic CpG ligands, three THP-1 differentiation protocols were assessed and compared: PMA differentiation that results in generation of macrophage-like cells; IL-4 and GM-CSF differentiation that gives rise to immature dendritic-like cells; IL-4, GM-CSF and ionomycin differentiation that generates mature dendritic-like cells.

THP-1 TLR9 mCherry cells were differentiated with PMA (40ng/ml) for 72h into macrophage-like cells (Figure 4.9A). Immature dendritic-like cells were generated by differentiation of THP-1 TLR9 mCherry cells with recombinant human IL-4 (rhIL-4) (200ng/ml) and recombinant human GM-CSF (rhGM-CSF) (100ng/ml) for five days (Figure 4.9B). Likewise, THP-1 TLR9 mCherry cells were differentiated into mature dendritic-like cells with rh-IL4 (200ng/ml), rhGM-CSF (100ng/ml) and ionomycin (200ng/ml) for five days (Figure 4.9C). rhIL-4 and rhGM-CSF (and ionomycin for mature dendritic-like cells) were replenished 48h after beginning of differentiation. In all cells TLR9 mCherry expression was induced with doxycycline (1µg/ml) for 48h prior to stimulation (Figure 4.9A, B, C). After doxycycline removal, cells were stimulated with 10µM CpG ODN 2006 for 3h and lysed. IFNβ1 and TNFα mRNA levels were subsequently measured by RT-qPCR to assess ability of the above-mentioned cells to respond to CpG ligands.

The results showed that CpG stimulation did not induce IFNβ1 in PMA-differentiated THP-1 TLR9 mCherry cells (Figure 4.9D), which is consistent with previously obtained results (Wang, Grøvdal, Unpublished data). TNFα was weakly induced by CpG stimulation of PMA-differentiated cells (Figure 4.9D). Differentiation of THP-1 TLR9 mCherry cells with IL-4 and GM-CSF resulted in generation of immature dendritic-like cells that are able to strongly secrete both IFNβ1 and TNFα upon stimulation with CpG ODN 2006 (Figure 4.9D). However, RT-qPCR-measured mRNA levels showed that administration of IL-4, GM-CSF and ionomycin to THP-1 TLR9 mCherry cells resulted in generation of mature dendritic-like cells that had diminished ability to secrete IFNβ1 and TNFα when compared to cells differentiated without ionomycin (Figure 4.9D). Summary of different THP-1 TLR9 mCherry differentiation methods and their outcomes is shown in Table 4.1.

Overall these results indicate that immature dendritic-like cells generated through IL-4 and GM-CSF-differentiation of THP-1 TLR9 mCherry cells are much stronger inducers of both IFNβ1 and TNFα than macrophage- or mature dendritic-like THP-1 TLR9 mCherry cells. Therefore, IL-4 and GM-CSF differentiation protocol was used in the rest of the project.

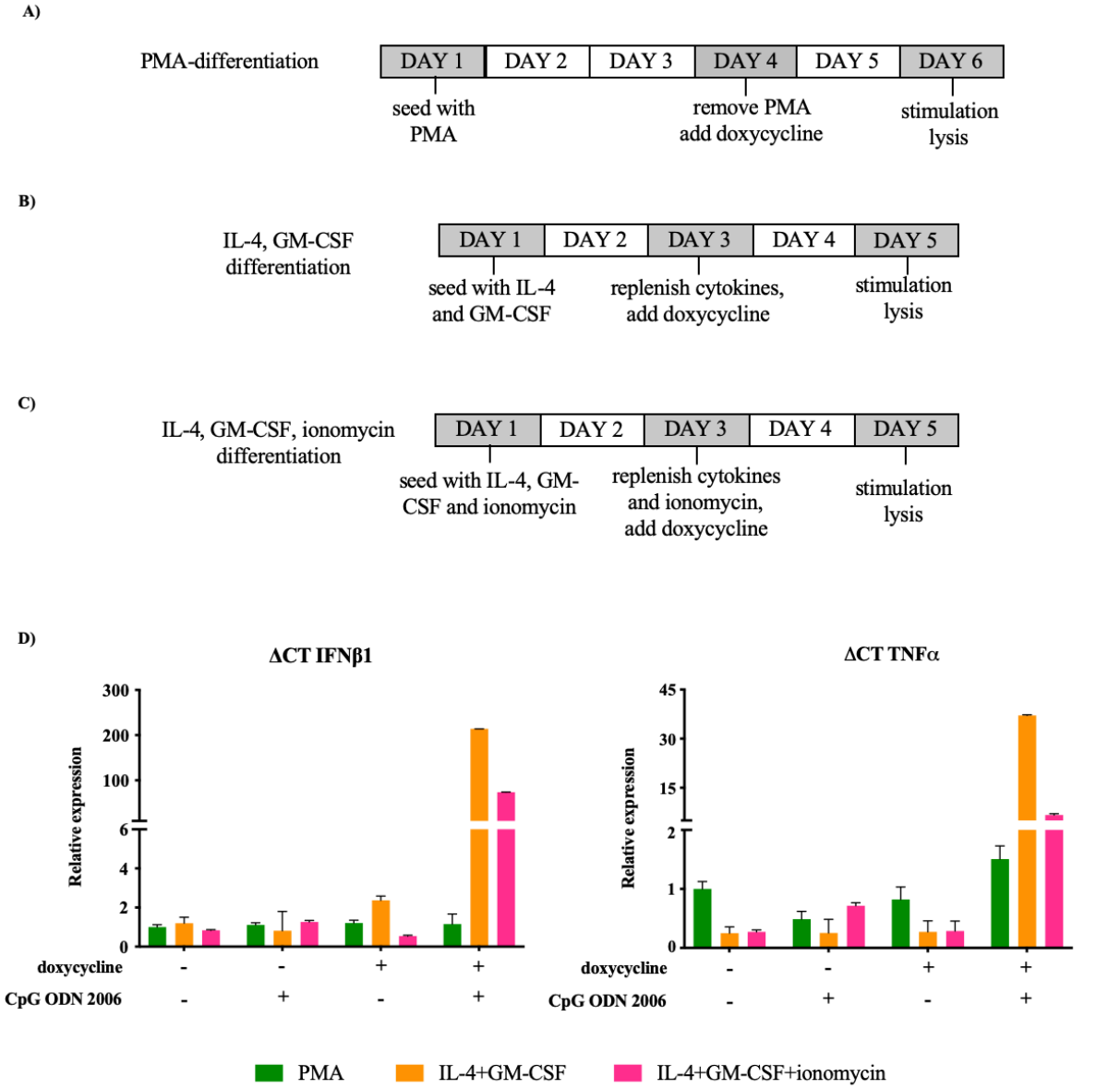

Figure 4.9 IL-4, GM-CSF-differentiated THP-1 TLR9 mCherry cells stimulated with CpG ODN 2006 strongly induce IFNβ1 and TNFα. THP-1 TLR9 mCherry cells (400 000 cells/well) were differentiated with **A)** PMA (40ng/ml) for 72h, after which doxycycline (1µg/ml) was added for 48h, **B)** rhIL-4 (200ng/ml) and rhGM-CSF (100ng/ml). After 48h, cytokines were replenished and doxycycline (1µg/ml) was added for 48h; **C)** rhIL-4 (200ng/ml), rhGM-CSF (100ng/ml) and ionomycin (200ng/ml). After 48h, cytokines and ionomycin were replenished, and doxycycline (1µg/ml) was added for 48h. **A, B, C)** After removal of doxycycline, cells were stimulated with 10µM CpG ODN 2006 for 3h, lysed and **D)** mRNA levels of IFNβ1 and TNFα were measured by RT-qPCR. TBP was used as an endogenous control. Results shown represent fold induction relative to PMA-differentiated untreated (- doxycycline, - CpG ODN 2006) cells. Error bars represent standard deviation between two technical replicates. Experiment was done once.

Differentiation protocol	Resulting cell type	Adherence properties	TLR9 expression	CpG stimulation	Cytokine secretion	
					IFNβ1	TNFα
Undifferentiated	Monocytes	Non-adherent	-	0	-	-
			-	2006	-	+
			-	2216	-	+
			+	0	-	-
			+	2006	-	++
			+	2216	-	+
PMA	Macrophage-like	Adherent	-	0	-	-
			-	2006	-	-
			-	2216	-	-
			+	0	-	-
			+	2006	-	+++
			+	2216	-	-
IL-4 + GM-CSF	Immature dendritic cell-like	Non-adherent	-	0	-	-
			-	2006	+	+
			-	2216	+	+
			+	0	-	-
			+	2006	+++	+++
			+	2216	+++	++
IL-4 + GM-CSF + ionomycin	Mature dendritic cell-like	Loosely adherent/non-adherent	-	0	-	-
			-	2006	-	+
			+	0	-	-
			+	2006	+++	-

Legend

No induction	<5-fold induction	10-40-fold induction	>40-fold induction
-	+	++	+++

Table 4.1 Summary of THP-1 TLR9 mCherry differentiation protocols and the resulting cytokine production. Results reflect RT-qPCR-measured mRNA levels of IFNβ and TNFα. Under TLR9 expression: "-" indicates no doxycycline induction of TLR9, "+" indicates doxycycline induction of TLR9. Under CpG stimulation: "0" refers to no stimulation, "2006" to CpG ODN 2006, "2216" to CpG ODN 2216. Under cytokine secretion "-" indicates no cytokine production, "+" indicates <5-fold induction; "++" indicates 5-40-fold induction; "+++" indicates >40-fold induction.

4.7.1.2 IFNβ1 and TNFα expression is induced by CpG ODN 2006

To optimize stimulation conditions, THP-1 TLR9 mCherry cells were differentiated with IL-4 and GM-CSF for 5 days. Cytokines were replenished 48h after beginning of differentiation, and TLR9 expression was induced with 1μg/ml of doxycycline for 48h. 10μM CpG ODN 2006 was previously identified as a very potent inducer of both IFNβ1 and TNFα (Supplementary Figure 5B), so stimulation was done with this concentration of ligand for up to 5h (Figure 4.10A). Cells were lysed and mRNA levels of IFNβ1 and TNFα were measured by RT-qPCR (Figure 4.10B). Proteins were isolated from cell lysates and TLR9 expression was assayed by western blot using anti-mCherry (Figure 4.10C) and anti-TLR9 (D9M9H) (Figure 4.10D) antibodies. Protein expression of phospho-TBK1 (Figure 4.10E), phospho-p38 (Figure 4.10F) and phospho-STAT1 (Figure 4.10G) was assessed to determine which signaling pathways were getting activated downstream of TLR9.

RT-qPCR-measured mRNA levels of IFNβ1 and TNFα showed that strongest cytokine response 3h post-stimulation with CpG ODN 2006 (Figure 4.10B). Western blot of protein extracts stained with anti-mCherry antibody detected two bands –$TLR9_{FL}$ mCherry found at 150kDa and mCherry-tagged short TLR9 fragment ($TLR9_S$ mCherry) found at 115kDa (Figure 4.10C). The expression of $TLR9_{FL}$ mCherry and $TLR9_S$ mCherry slightly increased 2h after stimulation with CpG ODN 2006. Protein extracts stained with anti-TLR9 antibody yielded a 150kDa band corresponding to $TLR9_{FL}$ mCherry and a 130kDa band corresponding to $TLR9_{FL}$ (Figure 4.10D). The expression of $TLR9_{FL}$ mCherry slightly increased after 2 hours of stimulation (Figure 4.10D), validating the observation seen for $TLR9_{FL}$ mCherry band on anti-mCherry antibody-stained western blot (Figure 4.10C). Strongest $TLR9_{FL}$ expression was observed 3h after stimulation (Figure 4.10D).

TBK1 is found downstream of TLR9. When phosphorylated, it can activate IRF3 and lead to its translocation to the nucleus and induction of IFNβ[39]. Therefore, protein expression of phospho-TBK1 (pTBK1) was assessed to determine whether TBK1-IRF3- IFNβ1 was being activated by TLR9 stimulation. Results showed that pTBK1 levels increased upon stimulation with CpG ODN 2006 (Figure 4.10E), suggesting activation of the TBK1-IRF3-IFNβ1 pathway. Unstimulated samples express low levels of pTBK1 (Figure 4.10E) indicating that IL-4 and GM-CSF differentiation, or doxycycline induction of TLR9 expression may be pre-activating these cells.

p38 is a serine/threonine kinase can be activated by various extracellular and intracellular stressors (such as PRR-mediate recognition of a ligand), as well as inflammatory

cytokines[122,123]. However, to exert its functions it first has to be phosphorylated by a member of MAP kinase kinase family. Expression of phospho-p38 (p-p38) was assessed by western to determine whether MAPK pathway was getting activated upon TLR9 stimulation. The results showed that phosphorylation of p38 increases with stimulation of TLR9 with CpG ODN 2006 (Figure 4.10F), indicating activation of the MAPK pathway.

STAT1 is a transcription factor that gets phosphorylated (pSTAT1) upon activation of type I IFN receptor (IFNAR). Increased phosphorylation of STAT1 was observed after 4h of stimulation (Figure 4.10G) indicating that IFNβ1 is also produced on protein level since it can activate this pathway.

Overall, the results of the experiment show that in IL-4, GM-CSF-differentiated THP-1 TLR9 mCherry cells, TNFα mRNA levels and IFNβ1 mRNA and protein levels are upregulated by stimulation of TLR9 with CpG ODN 2006.

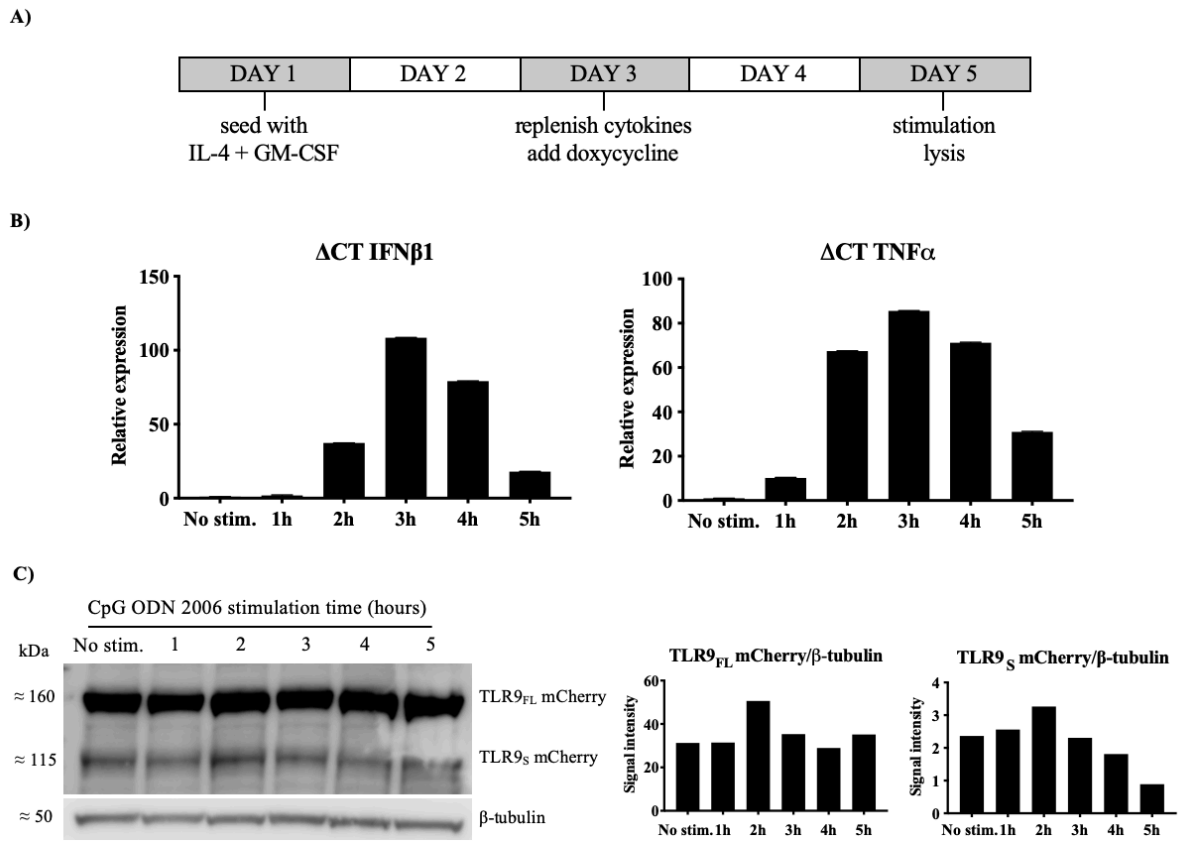

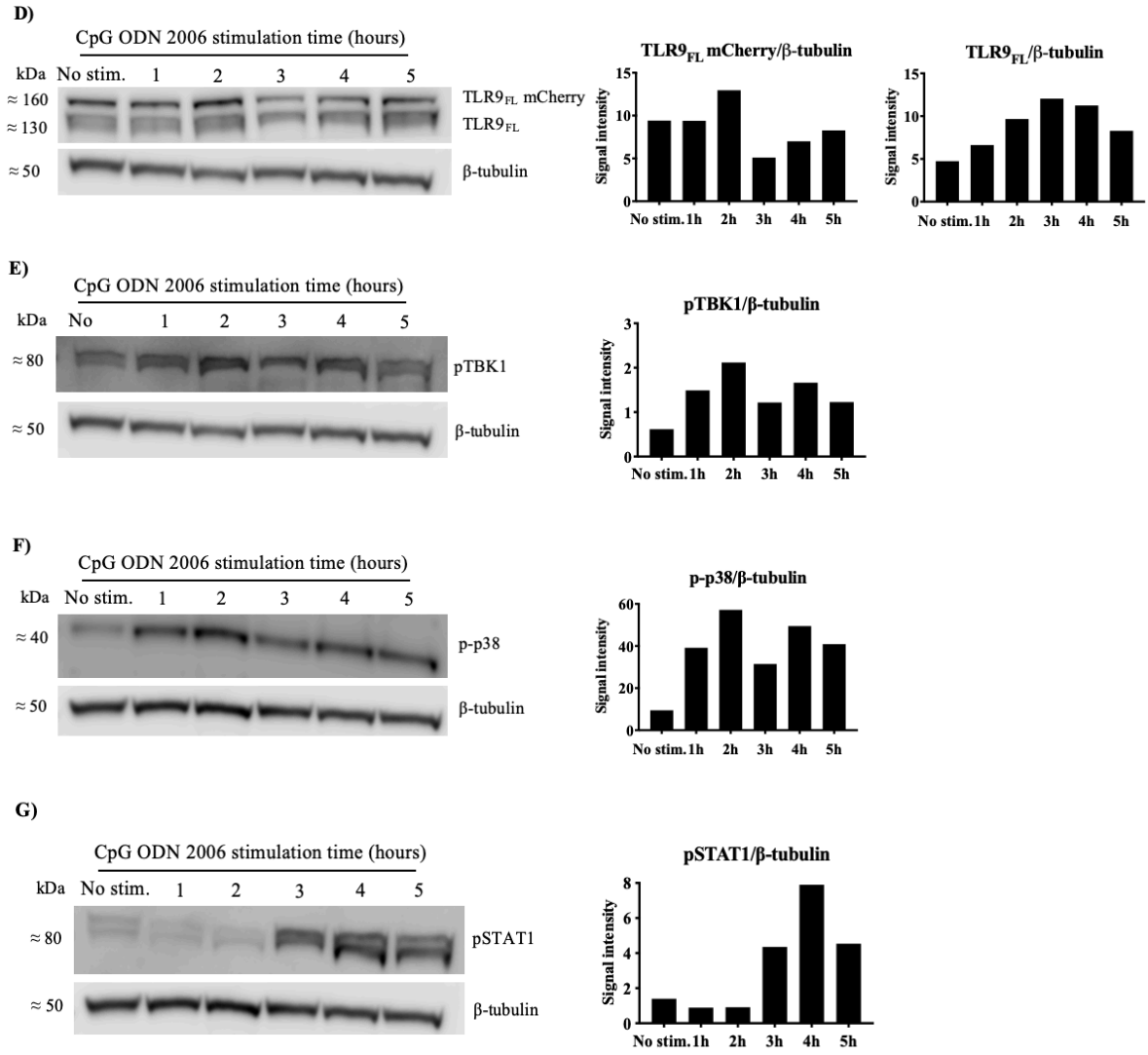

Figure 4.10 IFNβ1 and TNFα expression is induced by CpG ODN 2006 stimulation of IL-4, GM-CSF-differentiated THP-1 TLR9 mCherry cells. A) THP-1 TLR9 mCherry cells (400 000 cells/well) were differentiated with rhIL-4 (200ng/ml) and rhGM-CSF (100ng/ml) for 5 days. Cytokines were replenished after 48h of initiation of differentiation, and 1µg/ml doxycycline was added for 48h to induce TLR9 expression. After removal of doxycycline, cells were either left untreated or were stimulated with 10µM CpG ODN 2006 for 1, 2, 3, 4 and 5h. **B)** mRNA levels of IFNβ1 and TNFα were measured by RT-qPCR. TBP was used as an endogenous control. Results shown represent fold induction relative to unstimulated cells. Error bars represent standard deviation between two technical replicates. Proteins were isolated from QiAzol lysates and assayed to determine levels of **C)** TLR9 mCherry (anti-mCherry (RFP) antibody), **D)** TLR9 (anti-TLR9 (D9M9H) antibody), **E)** pTBK1, **F)** p-p38 and **G)** pSTAT1. Signal intensity was normalized to β-tubulin. Figure reflects results obtained in a single experiment. Phosphorylated proteins are designated with the prefix "p".
$TLR9_{FL}$- full length TLR9, $TLR9_{FL}$ mCherry - full length TLR9 mCherry, $TLR9_S$ mCherry– short TLR9 mCherry

4.7.1.3 CpG ODN 2006 and 2216 induce similar IFNβ1 and TNFα expression

Dendritic cells have been shown to be able to preferentially secrete IFNβ1 upon stimulation with CpG ODN 2216 (Class A CpG ODN)[100]. Since IL-4, GM-CSF

differentiation generates immature dendritic-like THP-1 TLR9 mCherry cells, we wanted to find out if these cells would be able to induce IFNβ1 and TNFα upon stimulation with CpG ODN 2216, and whether there would be any difference in the extent of cytokine responses upon stimulation of these cells with CpG ODN 2006 or CpG ODN 2216. To that end, THP-1 TLR9 mCherry cells were first differentiated with rhIL-4 and rhGM-CSF for 5 days, with cytokine replenishment on day 3 (Figure 4.11A). After cytokines were replenished, cells were either left untreated or were treated with doxycycline for 48h to induce TLR9 expression. After removal of doxycycline, cells were stimulated with 10μM CpG ODN 2006 or CpG ODN 2216 for 3h and lysed before RNA and proteins were isolated from lysates. IFNβ1 and TNFα expression was initially assessed by RT-qPCR, while western blot was used to assess TLR9 expression with anti-mCherry and anti-TLR9 (D9M9H) antibodies. Lysates were additionally assessed for signaling molecules pTBK1 and p38 found downstream of TLR9.

The results show that IFNβ1 levels are higher in IL-4, GM-CSF-differentiated THP-1 TLR9 mCherry cells stimulated with CpG ODN 2216 (Figure 4.11B). IFNβ1 expression is not markedly upregulated when TLR9 expression is not induced, indicating that IFNβ1 synthesis in response to CpG ODN 2006 and 2216 is dependent on doxycycline induction of TLR9 (Figure 4.11B). Both CpG ligands appeared to induce relatively similar levels of TNFα (Figure 4.11B). TNFα expression was upregulated upon stimulation with either CpG ligand in cells that were not treated with doxycycline (Figure 4.11B), suggesting that TNFα response seen in these cells may potentially be TLR9-independent (Figure 4.11B).

Protein extracts stained with anti-mCherry antibody showed a 150kDa and a 115kDa band in doxycycline-treated cells (Figure 4.11C). The 150kDa band corresponds to full length TLR9 ($TLR9_{FL}$) mCherry and it appears to be equally expressed after stimulation with either CpG ligand (Figure 4.11C). The expression of $TLR9_{FL}$ mCherry decreases after stimulation, suggesting increased cleavage of full-length TLR9 upon its interactions with CpG ligands (Figure 4.11C). The 115kDa band ($TLR9_S$ mCherry) is also equally expressed when cells are stimulated with CpG ODN 2006 or 2216 and its expression is decreased compared to unstimulated cells (Figure 4.11C). This suggests that this band could correspond to a full length TLR9 mCherry isoform, found at lower levels in the cells, that was also being cleaved upon interactions with CpG ligands.

Western blots of protein lysates stained with anti-TLR9 (D9M9H) antibody detected two bands (150kDa corresponding to $TLR9_{FL}$ mCherry and 130kDa corresponding to $TLR9_{FL}$) in doxycycline-treated cells (Figure 4.11D). $TLR9_{FL}$ mCherry and $TLR9_{FL}$ expression did not change markedly upon stimulation with CpG ligands (Figure 4.11D). This

is not fully in concordance with expression levels of $TLR9_{FL}$ mCherry detected on anti-mCherry antibody-stained western blot (Figure 4.11C), therefore it is not possible to draw a conclusion regarding doxycycline-induced TLR9 expression after CpG ODN 2006 or 2216 stimulation. A weak 150kDa band, corresponding to full length TLR9, was also detected in unstimulated and CpG ODN 2006-stimulated cells that were not treated with doxycycline (Figure 4.11D). This suggests that IL-4, GM-CSF-differentiated THP-1 TLR9 mCherry cells may express low levels of endogenous TLR9 that could potentially respond to CpG ligands and result in upregulation of TNFα expression (Figure 4.11B), even in the absence of doxycycline.

Protein lysates were also assayed for pTBK1 to see whether there were any differences in TBK1-IRF3-IFNβ pathway activation upon stimulation with different CpG ligands (Figure 4.11E). The results showed that after 3 hours of stimulation, CpG ODN 2006 was a stronger inducer of pTBK1 expression in doxycycline-treated cells (Figure 4.11E). However, in cells that were not treated with doxycycline, both ligands induced similar expression of pTBK1 (Figure 4.11E). In addition, both doxycycline-induced and non-induced cells expressed low levels of pTBK1 prior to stimulation (Figure 4.11E). This was also observed in the previous section in unstimulated, doxycycline-treated IL-4, GM-CSF-differentiated cells (Figure 4.10E). Together, these results indicate that IL-4, GM-CSF differentiation may be pre-activating THP-1 TLR9 mCherry cells.

Western blots of protein extracts were also stained with anti-p-p38 antibody to determine if CpG ODN 2006 and 2216 had different effects on MAPK pathway activation. The results show that stimulation with CpG ODN 2006 induces stronger expression of p-p38 in both doxycycline-treated and untreated cells (Figure 4.10F), supporting the results seen for TNFα upregulation upon stimulation of cells with this ligand (Figure 4.10B).

More than half (60%) of CpG ODN 2216-stimulated cells in which TLR9 expression had not been induced with doxycycline, died during 3-hour stimulation. This was also observed by very faint β-tubulin expression (Figure 4.11D, E, F, G) and absence of GAPDH (Figure 4.11C) on western blots (Figure 4.5.2). This indicates that 10μM CpG ODN 2216 may be toxic to IL-4, GM-CSF-differentiated THP-1 TLR9 mCherry cells, and that induction of TLR9 expression by doxycycline may rescue the cells from its toxic effects.

Overall, these results suggest that both CpG ODN 2006 and 2216 induce similar responses upon interactions with doxycycline-induced TLR9 in IL-4, GM-CSF-differentiated cells. They also show that these cells may express low endogenous levels of TLR9 that could interact with CpG ODNs to induce TNFα expression in the absence doxycycline.

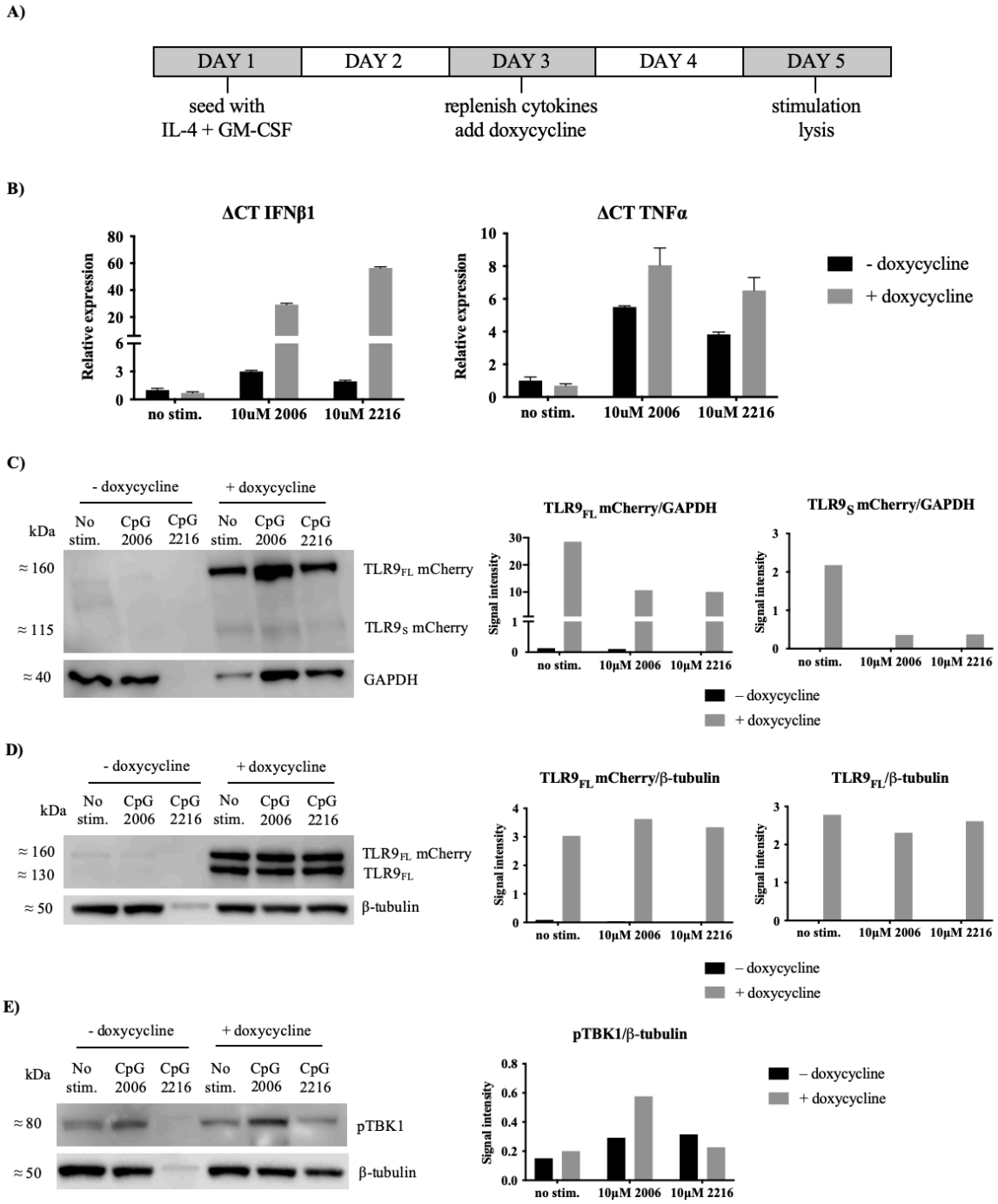
A)
DAY 1
DAY 2
DAY 3
DAY 4
DAY 5
seed with
IL-4 + GM-CSF
replenish cytokines
add doxycycline
stimulation
lysis
B)
ΔCT IFNβ1
ΔCT TNFα
Relative expression
no stim.
10uM 2006
10uM 2216
- doxycycline
+ doxycycline
C)
- doxycycline
+ doxycycline
kDa
No stim.
CpG 2006
CpG 2216
≈ 160
≈ 115
≈ 40
TLR9FL mCherry
TLR9S mCherry
GAPDH
TLR9FL mCherry/GAPDH
TLR9S mCherry/GAPDH
Signal intensity
10μM 2006
10μM 2216
– doxycycline
+ doxycycline
D)
≈ 130
TLR9FL
β-tubulin
TLR9FL mCherry/β-tubulin
TLR9FL/β-tubulin
E)
≈ 80
pTBK1
pTBK1/β-tubulin

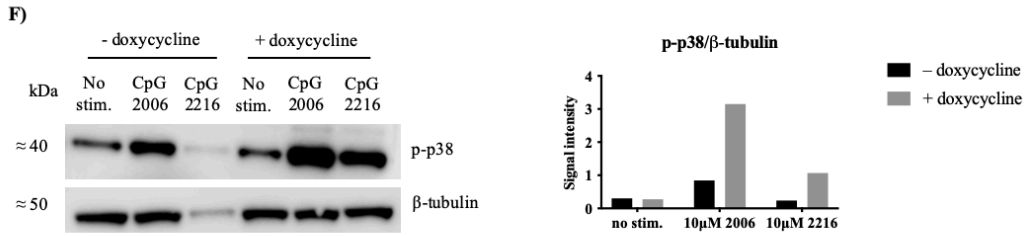

Figure 4.11 CpG ODN 2006 and 2216 both induce IFNβ1 and TNFα expression IL-4, GM-CSF-differentiated cells. A) THP-1 TLR9 mCherry cells (400 000 cells/well) were differentiated with rhIL-4 (200ng/ml) and rhGM-CSF (100ng/ml) for 5 days. Cytokines were replenished on day 3, and doxycycline (1μg/ml) was added for 48h to induce TLR9 expression. After removal of doxycycline, cells were either left untreated or were stimulated with 10μM CpG ODN 2006 or 2216 for 3 hours. **B)** mRNA levels of IFNβ1 and TNFα were measured by RT-qPCR. TBP was used as an endogenous control. Results shown represent fold induction relative to non-doxycycline-treated, unstimulated cells. Error bars represent standard deviation between two technical replicates. Proteins were isolated from QiAzol lysates and assayed for **C)** mCherry (anti-mCherry (RFP) antibody), **D)** TLR9 (anti-TLR9 (D9M9H) antibody), **E)** pTBK1 and **F)** p-p38 expression. Blots were stained with anti-β-tubulin as a loading reference. Figure reflects results obtained in a single experiment. Phosphorylated proteins are designated with the prefix "p".

$TLR9_{FL}$- full length TLR9, $TLR9_{FL}$ mCherry - full length TLR9 mCherry, $TLR9_{S}$ mCherry– short TLR9 mCherry

4.7.1.4 IL-4, GM-CSF-differentiated cells treated with PMA have high basal levels of IFNβ1 and TNFα

IL-4, GM-CSF-differentiated THP-1 TLR9 mCherry cells adopt immature dendritic-cell like morphology and properties. Unlike PMA differentiation, IL-4 and GM-CSF do not halt cell growth, nor do they render cells adherent. Suspension cells freely float in the observation field leading to the loss of focus during cell imagine, making studying subcellular localization of TLR9 by confocal microscopy difficult. Therefore, the aim of this experiment was to use PMA to induce adherence in IL-4, GM-CSF-differentiated THP-1 TLR9 mCherry cells.

THP-1 TLR9 mCherry cells were treated with rhIL-4 and rhIL-GM-CSF, and cytokines were replenished 48h after seeding (Figure 4.12A). Doxycycline was added during medium change for 48h to induce TLR9 expression. One day prior to cell stimulation and lysis, PMA (60ng/ml) was administered to the cells. After 24h, PMA and doxycycline were removed, and cells were stimulated with 1μM CpG ODN 2006 for 3h. Cells were subsequently lysed, and IFNβ1 and TNFα levels were assessed by RT-qPCR to determine whether PMA administration affected their ability to signal.

The results showed that stimulation of both IL-4, GM-CSF- and IL-4, GM-CSF, PMA-differentiated cells with CpG ODN 2006 leads to upregulation of IFNβ1 and TNFα (Figure

4.12B). Cells treated with IL-4, GM-CSF and PMA expressed higher levels of IFNβ1 and TNFα upon stimulation (Figure 4.12B). However, unstimulated IL-4, GM-CSF, PMA-differentiated cells also had 5- and 10-fold higher basal levels of IFNβ1 and TNFα, respectively, when compared to only IL-4, GM-CSF-differentiated unstimulated cells (Figure 4.12B), indicating that administration of PMA was activating cells and upregulating cytokine expression.

In addition, after 24h of PMA treatment, only a portion of cells (40%) became adherent. Since IL-4, GM-CSF, PMA-differentiated cells failed to become fully adherent and PMA administration was upregulating IFNβ1 and TNFα in resting conditions, we therefore decided to proceed with IL-4 and GM-CSF differentiation only.

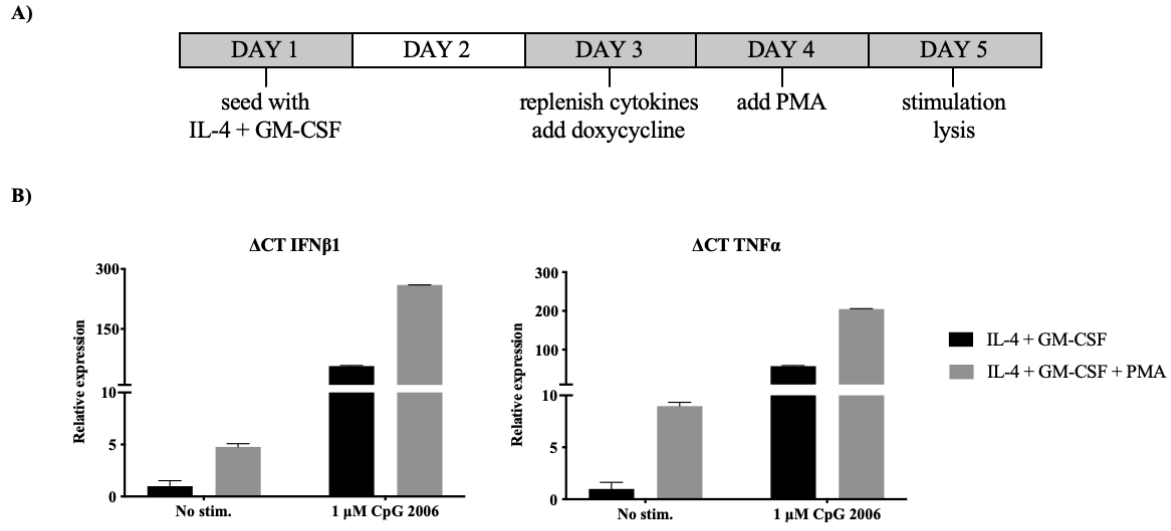

Figure 4.12 PMA, IL-4, GM-CSF-differentiated THP-1 TLR9 mCherry cells express high levels of IFNβ1 and TNFα under resting conditions. A) THP-1 TLR9 mCherry cells (400 000 cells/well) were seeded with rhIL-4 (200ng/ml) and rhGM-CSF (100ng/ml). Cytokines were replenished after 48h, and at the same time doxycycline (1µg/ml) was added for 48h to induce TLR9 expression. 24h prior to stimulation and lysis, PMA (60 ng/ml) was added to IL-4, GM-CSF, PMA-differentiated cells. After removal of doxycycline and PMA, cells were either left untreated or were stimulated with 1µM CpG ODN 2006 for 3 hours. Cells were subsequently lysed and **B)** IFNβ1 and TNFα mRNA levels were assayed by RT-qPCR. TBP was used as an endogenous control. Results shown represent fold induction relative to IL-4, GM-CSF-differentiated, unstimulated cells. Error bars represent standard deviation between two technical replicates. The experiment was done once.

4.7.2 CAL-1 TLR9 mCherry cells

4.7.2.1 CAL-1 TLR9 mCherry cells are stronger inducers of IFNβ1 expression than CAL-1

CAL-1 TLR9 mCherry cells, in addition to endogenous TLR9, also express doxycycline-inducible TLR9 mCherry. Strongest TLR9 mCherry expression in these cells is

detected after administration of doxycycline (0.5µg/ml) for 48h (Figure 4.3). Since wild type CAL-1 cells predominantly express TLR9, CpG-induced signaling in wild type cells and CAL-1 TLR9 mCherry was compared to determine whether TLR9 mCherry expression enhances immune response.

Undifferentiated CAL-1 and CAL-1 TLR9 mCherry cells were either treated with doxycycline (0.5µg/ml) or kept in fresh culture medium for 48h, before stimulation with 10µM CpG ODN 2006 or 2216 for 3h (Figure 4.13A). Cells were subsequently lysed and assayed for IFNβ1 and TNFα levels by RT-qPCR.

Results showed that both CpG ligands potently induce IFNβ1 in CAL-1 and CAL-1 TLR9 mCherry cells (Figure 4.13B), which is consistent with the literature[39]. CAL-1 TLR9 mCherry cells that expressed doxycycline-induced TLR9 showed stronger IFNβ1 response upon CpG stimulation than wild type CAL-1 and non-doxycycline-treated CAL-1 TLR9 mCherry cells (Figure 4.13B). CAL-1 TLR9 mCherry cells with doxycycline-induced TLR9 also showed similar IFNβ1 expression in response to CpG ODN 2006 and 2216 (Figure 4.13B). Neither ligand was able to induce TNFα in these cell lines (Supplementary Figure 6B), although several groups have shown that CAL-1 cells produce TNFα for up to 12h after stimulation with Class B CpG ligands[89].

Overall, these results show that after TLR9 induction with doxycycline, CAL-1 TLR9 mCherry cells are more potent inducers of IFNβ1 expression than wild type CAL-1 cells.

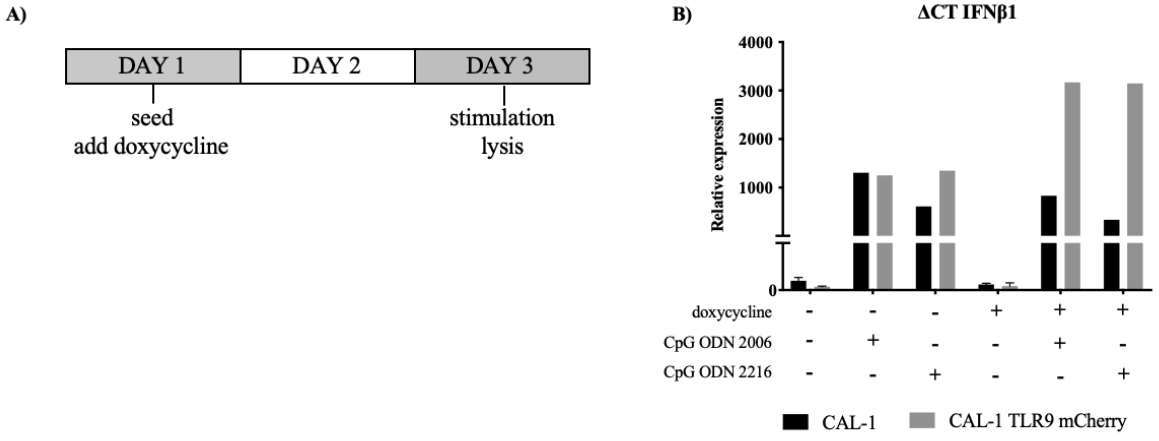

Figure 4.13 CAL-1 TLR9 mCherry cells with doxycycline-induced TLR9 expression are potent inducers of IFNβ1 in response to CpG ligands A) CAL-1 and CAL-1 TLR9 mCherry cells (400 000 cells/well) were initially treated with doxycycline (0.5µg/ml) or left untreated in fresh culture medium for 48h. After doxycycline withdrawal, cells were either left unstimulated or were stimulated with 10µM CpG ODN 2006 or 2216 for 3 hours. Cells were lysed and **B)** IFNβ1 mRNA levels were assayed by RT-qPCR and normalized to TBP. Results shown represent fold induction relative to unstimulated, non-doxycycline induced CAL-1 cells. Error bars represent standard deviation between two technical replicates. The experiment was done once.

4.7.2.2 Differentiation of CAL-1 TLR9 mCherry cells

Undifferentiated CAL-1 TLR9 mCherry cells have a small, round morphology and are found in suspension. They potently induce IFNβ1 expression in response to both CpG ODN 2006 and 2216 (Figure 4.12B). Due to their non-adherence, studying TLR9 subcellular localization and trafficking by confocal microscopy is very challenging. Therefore, our next goal was to induce adherence by differentiating CAL-1 TLR9 mCherry cells into mature dendritic-like cells and to ensure that the cells retain their signaling ability.

CAL-1 cells were seeded and left undifferentiated or were differentiated with either rhIL-3 (10ng/ml) or rhGM-CSF (100pg/ml) for 72h (Figure 4.14A). Doxycycline (0.5μg/ml) was added to the cells for 48h to induce TLR9 expression, prior to stimulation. Cells were stimulated with 10μM CpG ODN 2006 for 3h, lysed and subsequently assayed for IFNβ1 and TNFα mRNA expression by RT-qPCR.

The results showed that in the presence of doxycycline-induced TLR9 mCherry all cells (undifferentiated, IL-3- or GM-CSF-differentiated cells) induced IFNβ1 expression (Figure 4.14B). Undifferentiated and GM-CSF-differentiated cells both showed upregulated IFNβ1 expression after CpG stimulation in the absence of doxycycline-induced TLR9 mCherry. GM-CSF-differentiated cells also had higher levels of IFNβ1 under resting conditions (Figure 4.14B), indicating that this differentiation method may be activating CAL-1 TLR9 mCherry cells. TNFα expression was not markedly upregulated after stimulation in any of the cells, regardless of TLR9 mCherry expression (Figure 4.14B). In addition, differentiation of cells into mature dendritic-like cells did not induce their adherence to culture plates.

These results showed that CAL-1 TLR9 mCherry cells are poor inducers of TNFα, but strong inducers of IFNβ1 in response to CpG ODN 2006. Differentiation of these cells failed to induce adherence and to increase ability of the cells to induce IFNβ1 and TNFα expression in response to CpG stimulation. Therefore, only undifferentiated CAL-1 TLR9 mCherry cells were used in the rest of the project.

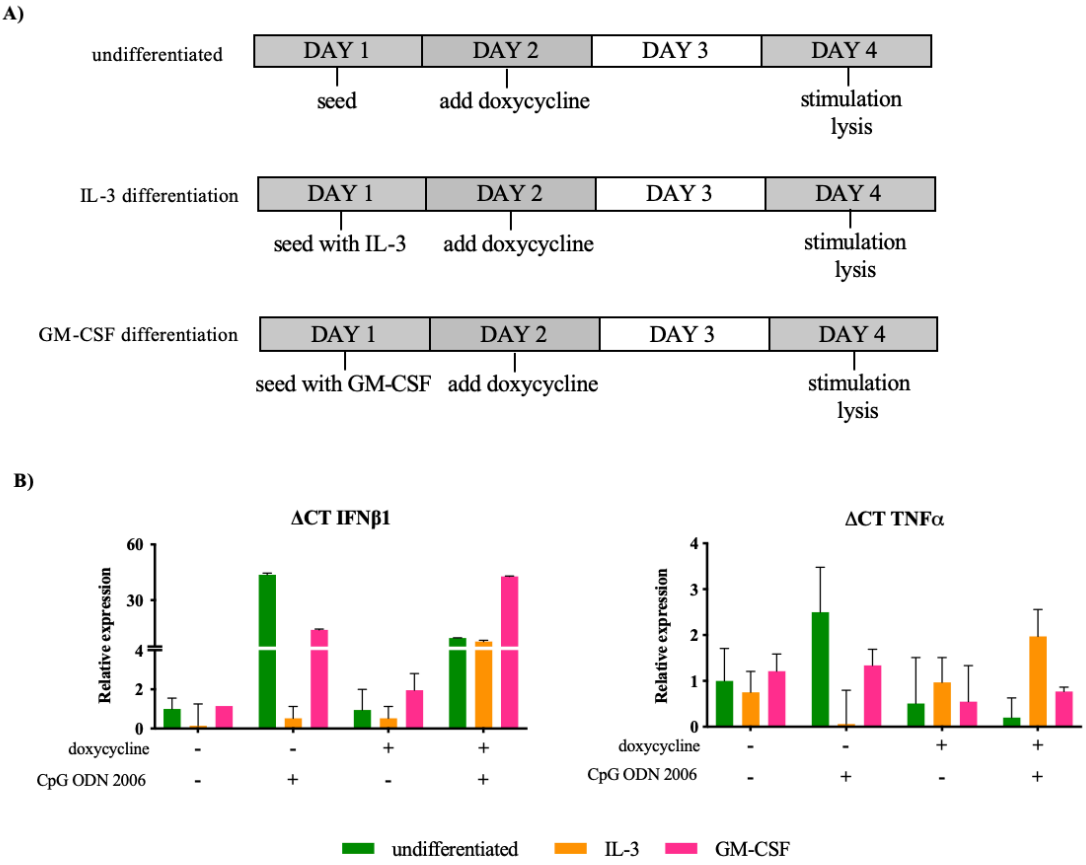

Figure 4.14 Differentiation of CAL-1 TLR9 mCherry cells fails to markedly increase cells ability to express IFNβ1 and TNFα in response to CpG ODN 2006. A) CAL-1 TLR9 mCherry cells (400 000 cells/well) were seeded and left undifferentiated or were differentiated with rhIL-3 (10ng/ml) or rhGM-CSF (100pg/ml). To induce TLR9 mCherry expression doxycycline (0.5µg/ml) was administered 48 prior to 3h stimulation with 10µM CpG ODN 2006. After stimulation, cells were lysed and **B)** IFNβ1 and TNFα mRNA levels were measured by RT-qPCR and normalized to TBP. Results shown represent fold change relative to untreated (- doxycycline, - CpG ODN 2006) cells. The experiment was done once. Error bars in **B)** represent standard deviation between two technical replicates.

4.8 Confocal microscopy analysis of TLR9 subcellular localization

Cytokine milieu generated upon TLR9 activation is dependent on the type of the ligand initiating the response, its internalization method and the endosomal compartment in which TLR9 encounters it. TLR9 is thought to preferentially interact with Class A CpG ODNs and signal from early endosomes to induce the production of type I IFNs[39,124]. TLR9 that interacts with Class B CpG ODNs is thought to signal from late endosomes to induce the production of pro-inflammatory cytokines, such as TNFα and IL-12, via NF-κB[39,78]. As we had previously established that IL-4, GM-CSF-differentiated THP-1 TLR9 mCherry and undifferentiated CAL-1 TLR9 mCherry cells can signal upon stimulation with both Class A and B CpG ODNs, confocal microscopy was done to determine the subcellular localization of

TLR9 in both of these cell lines before and after CpG ODN stimulation. EEA1 and LAMP1 were used to determine whether TLR9 localizes to early endosomes or late endosomes/ lysosomes, respectively.

4.8.1 TLR9 primarily colocalizes with LAMP1 in IL-4, GM-CSF-differentiated THP-1 TLR9 mCherry cells

Cells were differentiated with rhIL-4 and rhGM-CSF for 5 days. Cytokines were replenished after first 48h of differentiation, and at the same time doxycycline (1µg/ml) was administered for 48h to induce TLR9 mCherry expression (Figure 4.15A, F; Figure 4.16A). After doxycycline removal, cells were stimulated with 10µM CpG ODN 2006 or 2216 for 3h. Cells were then fixed and stained for TLR9 mCherry and EEA1 (Figure 4.15B, C, D), or TLR9 mCherry and LAMP1 (Figure 4.16B, C, D). Confocal images were taken with cells in PBS. The extent of colocalization between TLR9 and LAMP1, and TLR9 and EEA1 was determined by Pearson's correlation coefficient calculated by using Just Another Colocalization Plugin (JACoP) in Fiji.

The results show that there is little colocalization between TLR9 and EEA1, before or after stimulation with either CpG ligand (Figure 4.15B, C, D). The extent of colocalization between TLR9 and EEA1, as represented by Pearson's correlation coefficient, does not markedly change with CpG ODN stimulation (Figure 4.15E). There is some colocalization between TLR9 and LAMP1 both before and after stimulation with CpG ligands (Figure 4.16B, C, D). The extent of colocalization between TLR9 and LAMP1 is similar in resting conditions, and when cells are stimulated with different classes of CpG ligands (Figure 4.16E). This is a surprising finding, since CpG ODN 2216 is thought to interact with TLR9 and induce type I IFNs from early endosomes[78].

Overall, these results suggest that under resting conditions TLR9 is found in LAMP1-positive vesicles (late endosomes/lysosomes) of IL-4, GM-CSF-differentiated THP-1 TLR9 mCherry cells, and that it remains there 3h after stimulation, regardless of the ligand it was stimulated with.

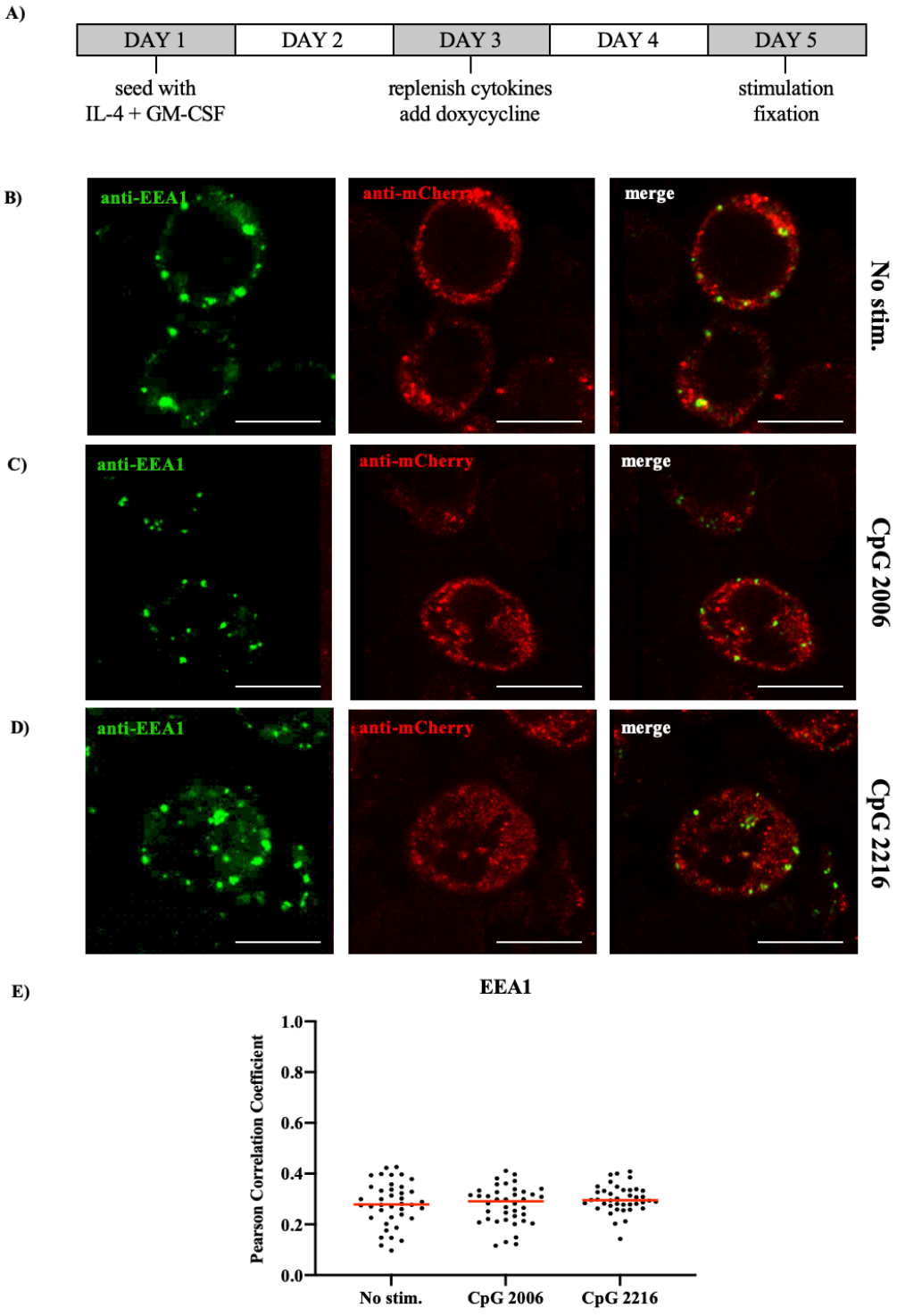

Figure 4.15 There is little colocalization between TLR9 and EEA1 in before and after stimulation. A) THP-1 TLR9 mCherry cells (600 000 cells/well) were differentiated with rhIL-4 (200ng/ml) and rhGM-CSF (100ng/ml). Cytokines were replenished 48h after seeding, and doxycycline (1µg/ml) was added to induce TLR9 mCherry expression. After 48h doxycycline was removed, and cells were either left **B)** unstimulated or were stimulated with 10µM **C)** CpG ODN 2006 or **D)** 2216 for 3 hours. Then they were fixed and stained for TLR9 mCherry and EEA1. Scale bars are 10µm. **E)** Colocalization is expressed as Pearson's correlation coefficient measured for individual cells using JACoP in Fiji. Median values for each condition are shown in red.

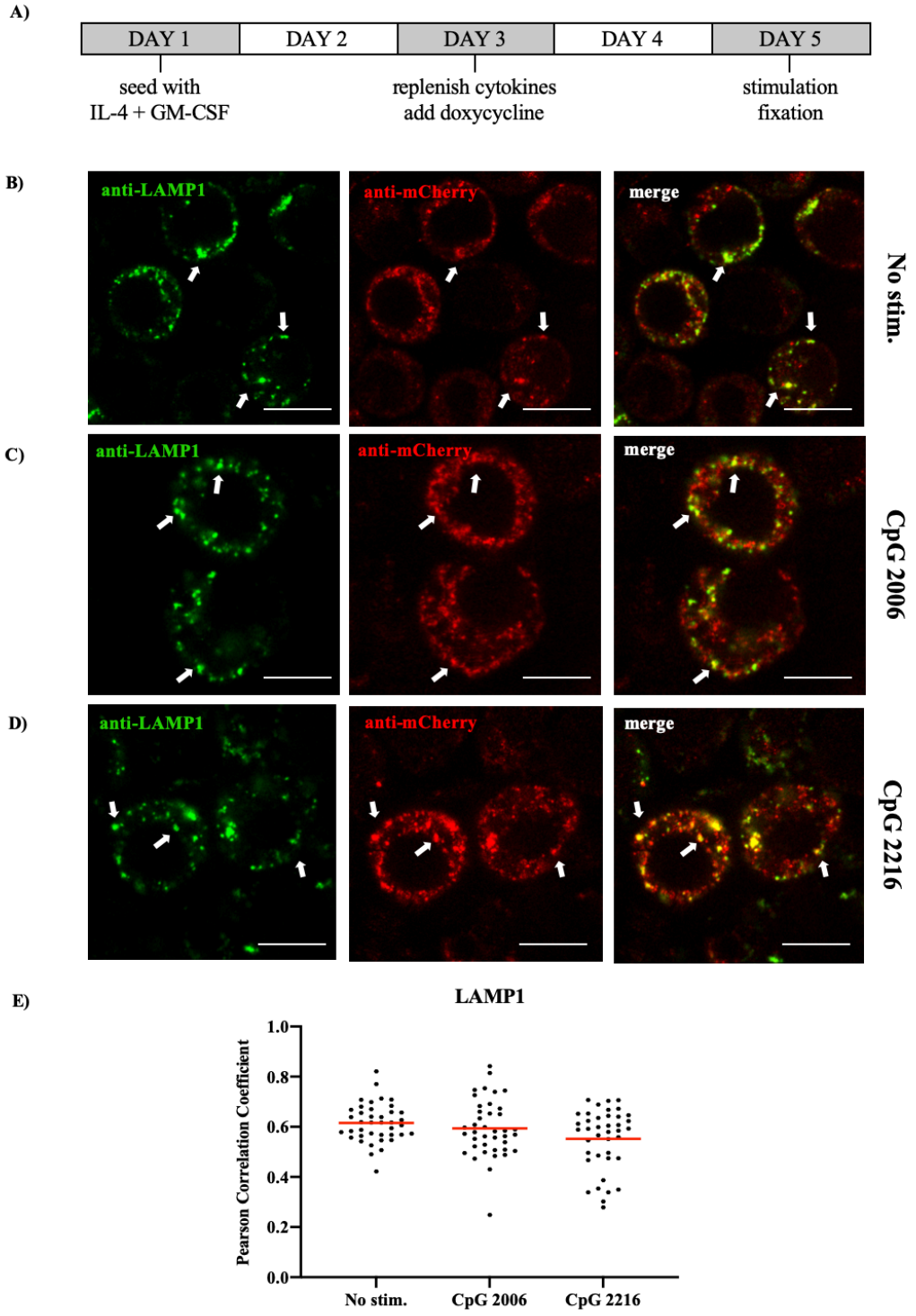

Figure 4.16 There is some colocalization between TLR9 and LAMP1 before and after stimulation. A) THP-1 TLR9 mCherry cells (600 000 cells/well) were differentiated with rhIL-4 (200ng/ml) and rhGM-CSF (100ng/ml). Cytokines were replenished 48h after seeding, and doxycycline (1µg/ml) was added to induce TLR9 mCherry expression. After 48h doxycycline was removed, and cells were either left **B)** unstimulated or were stimulated with 10µM **C)** CpG ODN 2006 or **D)** 2216 for 3 hours. Then they were fixed and stained for TLR9 mCherry and LAMP1. Arrows indicate colocalization sites between TLR9 and LAMP1. Scale bars are 10µm. **E)** Colocalization is expressed as Pearson's correlation coefficient measured for individual cells using JACoP in Fiji. Median values for each condition are shown in red.

4.8.2 TLR9 predominantly colocalizes with LAMP1 before and after CpG ODN 2216 stimulation of CAL-1 TLR9 mCherry cells

CAL-1 TLR9 mCherry cells were treated with doxycycline (0.5μg/ml) for 48h to induce TLR9 mCherry expression (Figure 4.17A, Figure 4.18A). Cells were then stimulated with 10μM CpG ODN 2006 or 2216 for 3h, fixed and subsequently stained for TLR9 mCherry and EEA1 (Figure 4.17B, C, D), or TLR9mCherry and LAMP1 (Figure 4.18B, C, D). Confocal microscopy images were taken with cells in PBS. The extent of colocalization between TLR9 and LAMP1, and TLR9 and EEA1 was determined by Pearson's correlation coefficient calculated using JACoP in Fiji.

The results show very little colocalization between TLR9 and EEA1 in undifferentiated CAL-1 TLR9 mCherry cells, both before and after stimulation with either CpG ligand (Figure 4.17B, C, D). The extent of colocalization between TLR9 and EEA1, as measured by Pearson's correlation coefficient, did not appear to vary markedly between resting and stimulated cells (Figure 4.17E). TLR9 strongly colocalizes with LAMP1 before and after stimulation of CAL-1 TLR9 mCherry cells with CpG ODN 2216 (Figure 4.18B, D). The extent of colocalization between TLR9 and LAMP1 reduces by half approximately, when TLR9 is stimulated with CpG ODN 2006 (Figure 4.18B, C, E), indicating that TLR9 might be signaling from some other endosomal compartment. This is an interesting finding, as TLR9 has been thought to preferentially interact with CpG ODN 2006 in late endosomes[39,125].

Together, these results indicate that in undifferentiated CAL-1 TLR9 mCherry cells, TLR9 predominately resides in LAMP1-postive vesicles and there it mainly interacts with CpG ODN 2216. CpG ODN 2006 may potentially be interacting with TLR9 elsewhere in the cell at this stimulation time point.

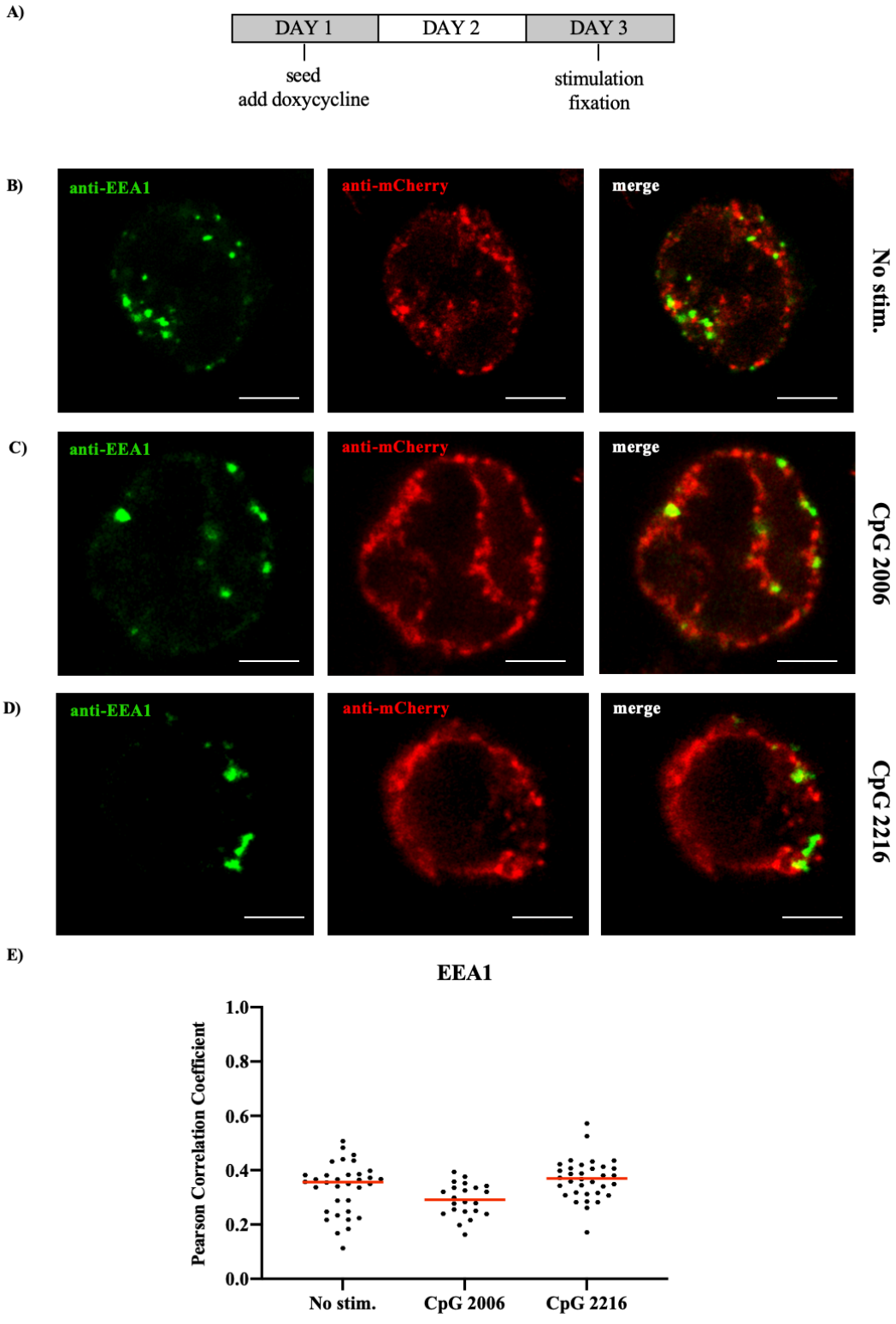

Figure 4.17 There is little colocalization with EEA1 before and after stimulation. A) CAL-1 TLR9 mCherry (600 000 cells/well) were treated with doxycycline (1µg/ml) for 48h to induce TLR9 mCherry expression. Cells were then either left **B)** unstimulated or were stimulated with 10µM **C)** CpG ODN 2006 or **D)** 2216 for 3 hours. Cells were fixed and stained for TLR9 mCherry and LAMP1. Arrows indicate colocalization sites between TLR9 and EEA1. Scale bars are 10µm. **E)** Colocalization is expressed as Pearson's correlation coefficient measured for individual cells using JACoP in Fiji. Median values for each condition are shown in red.

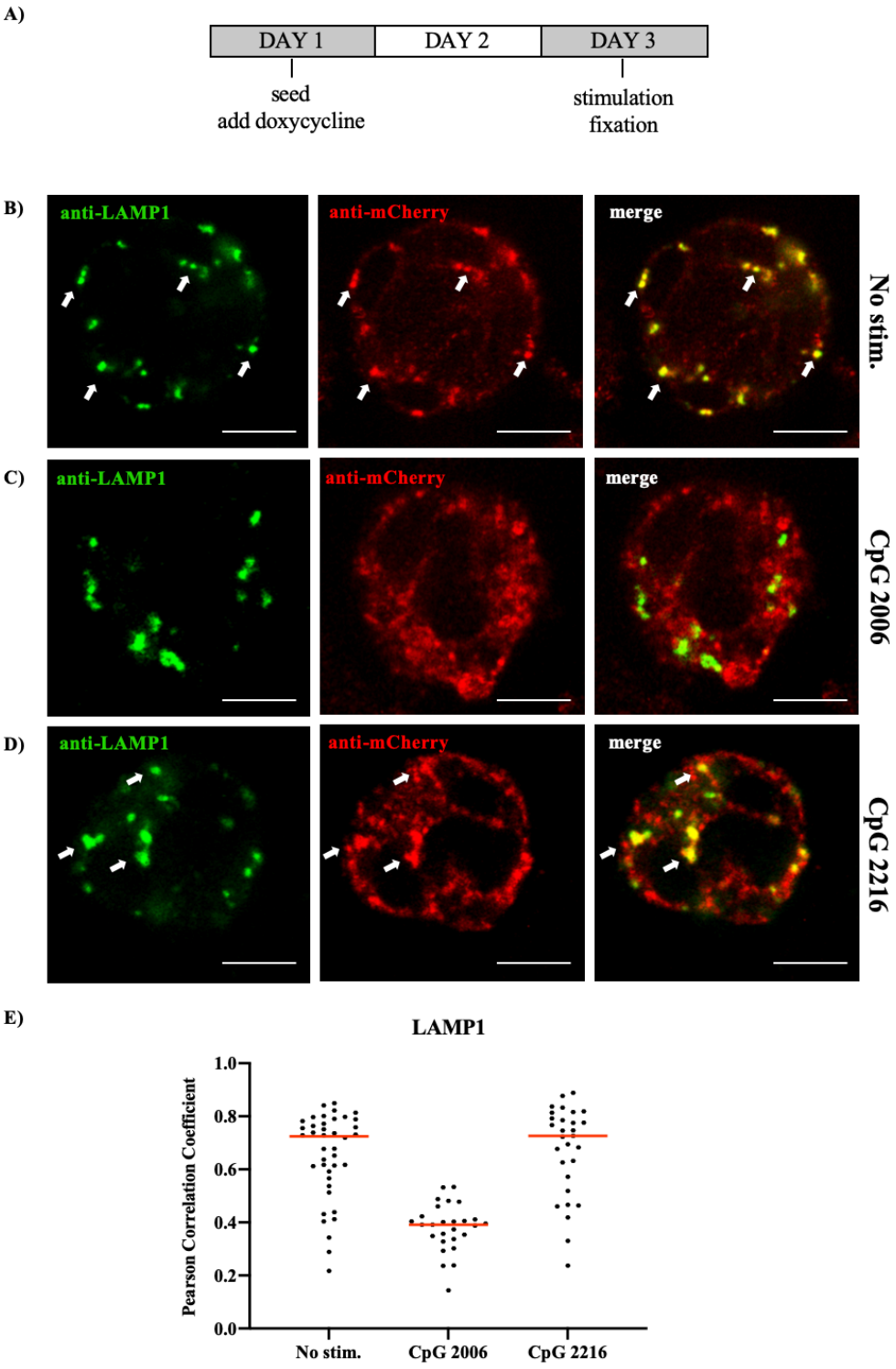

Figure 4.18 TLR9 primarily colocalizes with LAMP1 before and after stimulation with CpG ODN 2216
A) CAL-1 TLR9 mCherry (600 000 cells/well) were treated with doxycycline (1µg/ml) for 48h to induce TLR9 mCherry expression. Cells were then either left **B)** unstimulated or were stimulated with 10µM **C)** CpG ODN 2006 or **D)** 2216 for 3 hours. Cells were then fixed and stained for TLR9 mCherry and LAMP1. Arrows indicate colocalization sites between TLR9 and LAMP1. Scale bars are 10µm. E) Colocalization is expressed as Pearson's correlation coefficient measured for individual cells using JACoP in Fiji. Median values for each condition are shown in red.

4.9 siRNA-mediated gene silencing in undifferentiated CAL-1 TLR9 mCherry and IL-4, GM-CSF-differentiated THP-1 TLR9 mCherry cells

One of the goals of this project was to use siRNA-mediated gene silencing to transiently knockdown various mediators of endosomal trafficking to determine the role they may play in TLR9 trafficking and signaling. To be able to do this, it was first necessary to establish and optimize a protocol for siRNA-mediated gene silencing in undifferentiated CAL-1 TLR9 mCherry and IL-4, GM-CSF-differentiated THP-1 TLR9 mCherry cells. siRNA oligonucleotides targeting Rab11a and Rab39a were used in this project.

Rab11a regulates TLR4 trafficking and TLR4-induced IFNβ production[76,126,127]. It also maintains homeostatic intracellular distribution of TLR9 in murine intestinal epithelia[77]. Rab39a is a 217aa protein that was identified as a potential regulator of TLR9 signaling and trafficking (Grøvdal, Unpublished data). Its localization in the cell is not clear, but it has been shown that is associates with LAMP1 in late endosomes/lysosomes as well as the Golgi[128-130]. Given their roles in trafficking of other TLRs or in endosomal sorting, we were interested in further studying these two Rab proteins to determine whether they could regulate TLR9 trafficking and signaling.

4.9.1 Undifferentiated CAL-1 TLR9 mCherry cells are difficult to transfect

CAL-1 TLR9 mCherry cells resemble pDCs, which are extremely fragile and difficult to modify genetically. pDC siRNA transfections usually result in rapid cell death or induction of TLR7- or TLR9-mediated immune respones[131]. However, Smith et al. have recently shown that DOTAP liposomal transfection reagent can be used to successfully transfect human pDCs without inducing cell death or immune response[132]. Therefore, DOTAP was used to transfect CAL-1 TLR9 mCherry cells with Rab11a oligonucleotide.

CAL-1 TLR9 mCherry cells were treated with DOTAP-siRNA complexes for 5h in antibiotic-free medium. Final siRNA concentration was 160nM. After 5h, cells were placed in fresh, antibiotic-free culture medium. The following day, cells were either left untreated, or were treated with doxycycline (0.5μg/ml) to induce TLR9 mCherry expression (Figure 4.19A). CAL-1 TLR9 mCherry cells divide very quickly, so induction of TLR9 expression was only done for 24h to prevent generation of a large pool of cells that were not treated with DOTAP-siRNA complexes. Cells were then lysed, and knockdown efficiency was determined by assaying Rab11a mRNA levels by RT-qPCR.

The results show that 5h incubation of undifferentiated CAL-1 TLR9 mCherry cells with DOTAP-siRNA complexes results in 50% knockdown of Rab11a (Figure 4.19C). Allstar

oligonucleotide was used as a negative control, as it does not bind to any mRNA. There appeared to be increased cell death when CAL-1 TLR9 mCherry cells were incubated with DOTAP-siRNA complexes, but not in cells incubated only with DOTAP (no siRNA sample) (Figure 4.19B). Together, these results suggested that high siRNA oligonucleotide concentrations (160nM) may be toxic to these cells, and that knockdown efficiency could be improved by further optimizing siRNA concentration, DOTAP-siRNA incubation time or that alternative transfection methods should be explored. To that end, several other transfection methods were tried, but unfortunately, they all resulted either in reduced cell viability or low knockdown efficiency. Summary of alternative transfection methods with Rab11a siRNA oligonucleotide and the outcomes is shown in Table 4.2.

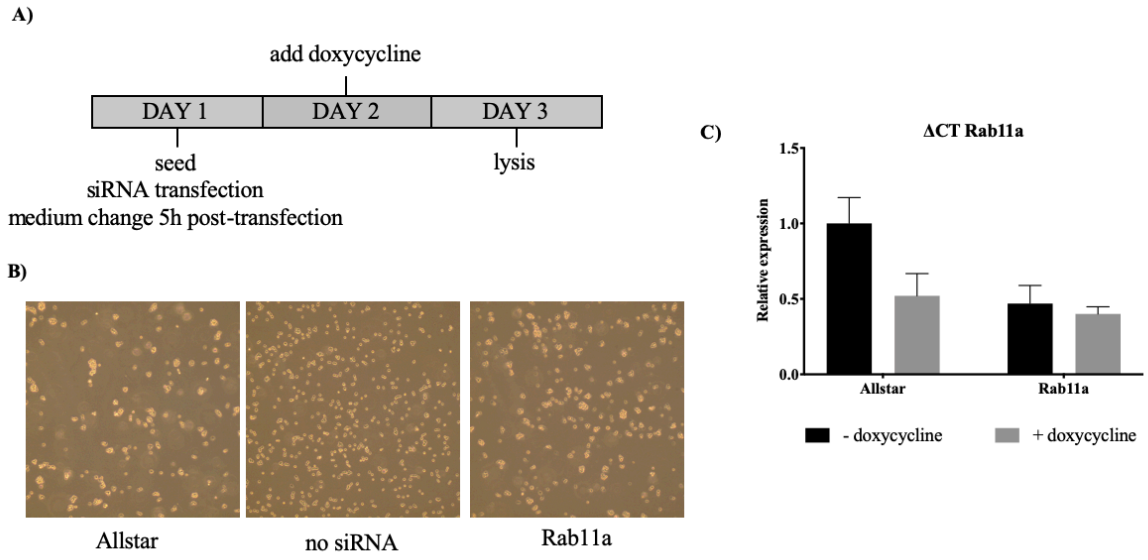

Figure 4.19 50% knockdown of Rab11a in CAL-1 TLR9 mCherry cells is achieved by 5-hour transfection with DOTAP-siRNA complex. **A)** CAL-1 TLR9 mCherry cells (400 000 cells/well) were seeded in antibiotic-free medium and siRNA transfection was performed with DOTAP on the same day. Final siRNA concentration was 160nM. Medium was changed 5h after transfection. Doxycycline (0.5µg/ml) was added the following day. Cells were lysed on 24h later. **B)** Cell morphology as examined by light-inverted microscope 5h after transfection, magnification 20X. **C)** mRNA levels of Rab11a were measured by RT-qPCR and normalized to TBP. Results shown represent fold change relative to Allstar-treated cells. Error bars in **C)** represent standard deviation between two independent experiments. mRNA levels could not be measured for no siRNA sample due to low concentration and purity of isolated RNA.

Transfection reagent/type of transfection	Final siRNA concentration	Incubation with siRNA (hours)	Rab11a knockdown (%)	Comments
DOTAP/forward	160nM	3 hours	no knockdown	– High cell viability after 3h incubation with transfection complexes – Supplementary Figure 7
		6 hours	30%	– Some cell death was observed following 6h incubation with transfection complexes – Supplementary Figure 8
		7 hours	no knockdown	– DOTAP-siRNA complexation was done in sterile glass tubes (as recommended by manufacturer's protocol to increase silencing efficiency) – Some cell death was observed following 7h incubation with transfection complexes – Supplementary Figure 9
		20 hours	no knockdown	– Significant reduction in cell viability (>80% of cells died following 20h incubation with transfection complexes) . – Supplementary Figure 10
Viromer BLUE/reverse	100nM	48 hours	no knockdown	– No apparent reduction in cell viability – Not suitable for confocal microscopy as TLR9 expression cannot be induced with doxycycline (silencing effects on mRNA level wear off 48-72h post transfection, according to manufacturer's guide) – Supplementary Figure 11
Viromer GREEN/reverse	100nM	48 hours	60%	
Lipofectamine 3000/forward	33nM	72 hours	50%	– High reduction in cell viability (>60% cells died following incubation with transfection complexes) – TLR9 expression was not induced with doxycycline – Supplementary Figure 12
Lipofectamine 3000/reverse	33nM	48 hours	no knockdown	– High reduction in cell viability (>60% cells died following incubation with transfection complexes) – Supplementary Figure 13
Lipofectamine 3000/forward	33nM	24 hours	70%	– Cells were pre-treated with GM-CSF (10pg/ml) for 72h – No apparent reduction in cell viability – Knockdown was only observed in cells not-treated with doxycycline – Supplementary Figure 14
RNAiMAX/ reverse	16nM	48 hours	no knockdown	– High reduction in cell viability (>50% cells died following incubation with transfection complexes) – Supplementary Figure 15

Table 4.2 Summary of siRNA transfection methods that failed to silence Rab11a in CAL-1 TLR9 mCherry cells.

4.9.2 siRNA-mediate gene silencing in IL-4, GM-CSF-differentiated THP-1 TLR9 mCherry cells

IL-4, GM-CSF-differentiated THP-1 TLR9 mCherry cells grow very densely during 5 days of differentiation, but cell growth is slowed down when they are fully differentiated into immature dendritic-like cells. When cells are transfected with siRNA during differentiation,

knockdown efficiency is low due to generation of new pool of cells that were not siRNA-treated (Supplementary Figure 16). To overcome this issue cells were treated with siRNA after being fully differentiated. Basal levels of IFNβ1 and TNFα were increased 2-3 days after differentiation, so cells had to be stimulated and corresponding cytokine responses had to be assessed 4-5 days after differentiation when IFNβ1 and TNFα expression returned to pre-differentiation levels (Supplementary Figure 17, Supplementary Figure 18).

4.9.2.1 Rab11a may play a role in TLR9-induced IFNβ1 signaling

The goal of the experiment was to determine whether Rab11a silencing affects TLR9-induced IFNβ1 and TNFα levels. THP-1 TLR9 mCherry cells were differentiated with rhIL-4 and rhGM-CSF for 5 days in antibiotic-free medium. When cells were fully differentiated on day 5, they were transfected with siRNA (33nM) using Lipofectamine 3000 (Figure 4.20A). Cells were incubated with Lipofectamine 3000-siRNA complexes for 72h, after which medium was changed, and doxycycline was added for 24h to induce TLR9 mCherry expression (Figure 4.20A). After doxycycline removal, cells were stimulated with 10μM CpG ODN 2006 for 3h and subsequently lysed. Rab11a, IFNβ1 and TNFα mRNA levels were then assayed by RT-qPCR. Rab11a mRNA expression was used to determine knockdown efficiency. The effects of Rab11a silencing on TLR9-induced signaling were assessed by IFNβ1 and TNFα mRNA expression.

The results show that Lipofectamine 3000 mediated 90% knockdown of Rab11a in IL-4, GM-CSF-differentiated THP-1 TLR9 mCherry cells (Figure 4.20C). Stimulation of Rab11a-silenced cells led to a marked decrease in IFNβ1 expression (Figure 4.20C), indicating that Rab11a may play a role in TLR9 signaling. TNFα expression did not appear to be markedly decreased in CpG-stimulated Rab11a silenced cells (Figure 4.20C), suggesting that Rab11a may not have a role in TLR9-induced TNFα expression. In addition, prior to stimulation, all cells were found in suspension, exhibiting small, round morphology, characteristic of IL-4, GM-CSF-differentiated monocytes into immature dendritic cells. After stimulation with CpG ODN 2006, a small percentage of cells adopts a stellate-like phenotype, characteristic of mature dendritic cells (Figure 4.20B).

These results suggest that Rab11a may primarily play a role in IFNβ1 production induced by CpG ODN 2006 stimulation of TLR9.

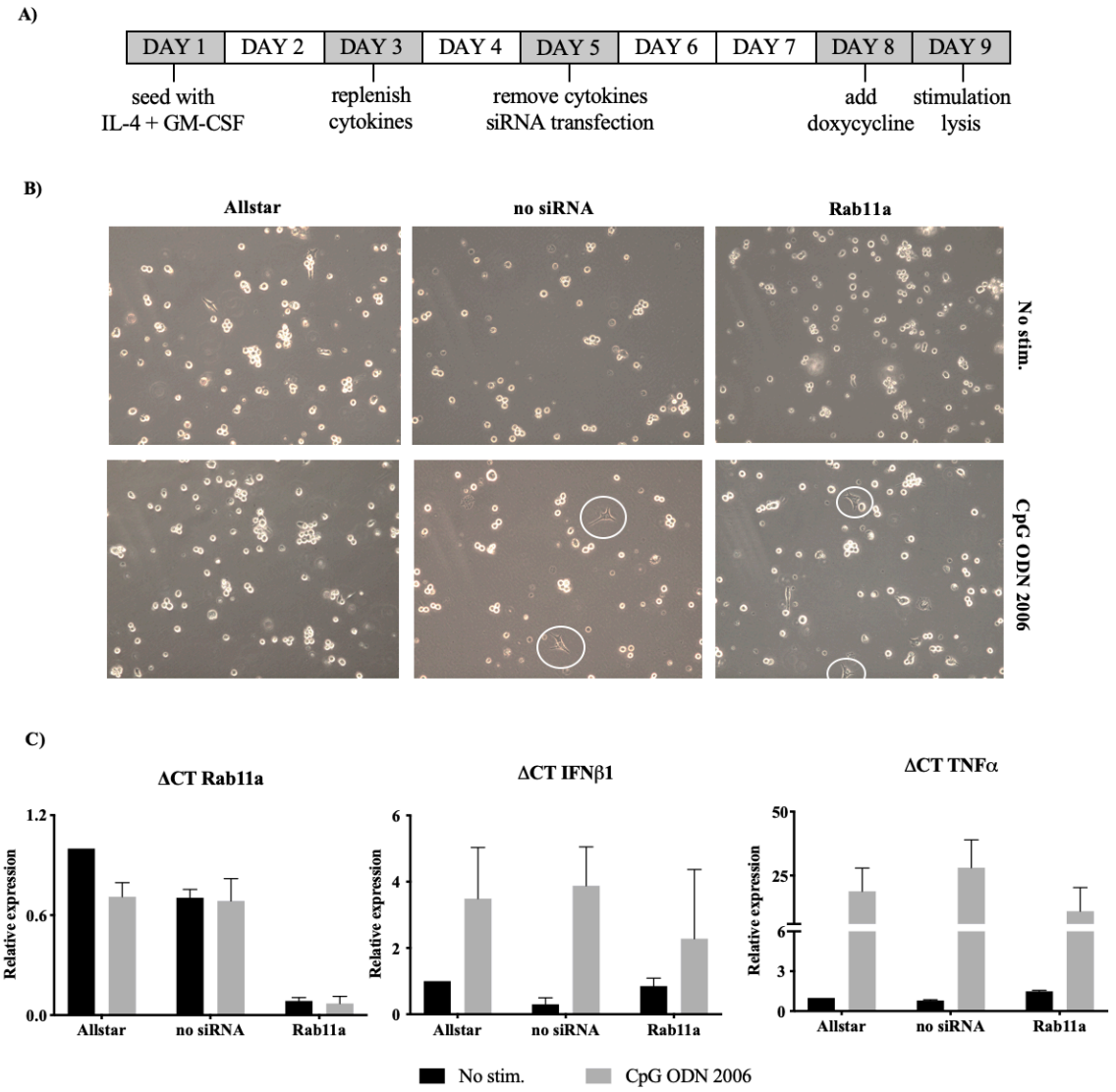

Figure 4.20 90% knockdown of Rab11a results in decreased IFNβ1 expression after stimulation with CpG ODN 2006. **A)** THP-1 TLR9 mCherry cells were differentiated with rhIL-4 (200 ng/ml) and rhGM-CSF (100 ng/ml) in antibiotic-free medium for 5 days. Cytokines were replenished 48h after seeding and removed 5 days after beginning of differentiation. Cells (400 000 cells/well) were then transfected with Lipofectamine 3000 on day 5 and incubated for 72h. Cells were then placed in fresh medium, and doxycycline (1µg/ml) was added for 24h to induce TLR9 mCherry expression. 24h after administration of doxycycline, cells were stimulated with 10µM CpG ODN 2006 for 3 hours. **B)** Cell morphology as examined by light-inverted microscope right before and after stimulation, magnification 20X. Prior to stimulation cells are in suspension, and exhibit small, round morphology. Upon stimulation some of the cells morphologically begin to resemble mature dendritic cells that adhere to the culture plate (indicated by white circles). **C)** mRNA levels of Rab11a, IFNβ1 and TNFα were measured by RT-qPCR and normalized to TBP. Results shown represent fold change relative to unstimulated, Allstar-treated cells. Error bars in **C)** represent standard deviation between two independent experiments. no siRNA – mock treated sample, incubated with Lipofectamine 3000 only.

4.9.2.2 Reverse transfection with Lipofectamine 3000 results in partial Rab39a knockdown

Achieving satisfactory Rab39a knockdown in IL-4, GM-CSF-differentiated cells proved to be more difficult than with Rab11a siRNA oligonucleotide. Several liposomal

reagents (DOTAP, RNAiMAX, Lipofectamine 3000) were used to transfect these cells, but they either resulted in reduced cell viability or low to none knockdown efficiency (Table 4.3). As IL-4, GM-CSF-differentiated cells are found in suspension, we hypothesized that low knockdown efficiency seen in forward transfections could be caused by low surface area available for interactions between the cells and transfection complexes. In reverse transfection, transfection reagent-siRNA mix is complexed in the culture plate after which cells are added to the plate. In theory, reverse transfection would then increase the interaction surface area, as suspension cells would be completely surrounded by the transfection complexes. Therefore, the goal of the next experiment was to test whether reverse transfection of Rab39a siRNA oligonucleotide would improve silencing outcomes.

THP-1 TLR9 mCherry cells were differentiated with rhIL-4 and rhGM-CSF in antibiotic-free medium for 5 days, with cytokine replenishment on day 3 (Figure 4.21A). After differentiation was complete on day 5, Lipofectamine 3000-siRNA complexes were assembled and incubated in culture plates for 10-15 minutes, after which differentiated cells (400 000 cells/well) were added to the complexes. Final siRNA concentration was 33nM. Allstar oligonucleotide was used as a negative control, and two Rab39a siRNA oligonucleotides (#5 and #7), that do not have a known off-target effect, were tested for their ability to silence Rab39a. Cells were incubated with transfection complexes for 72h, after which they were removed from culture medium and doxycycline (1μg/ml) was added for 24h to induce TLR9 mCherry expression. Cells were subsequently lysed and assayed for Rab39a expression by RT-qPCR to determine knockdown efficiency.

The results showed that reverse transfection with Lipofectamine 3000 was somewhat successful in silencing of Rab39a (Figure 4.21C). Approximately 70% knockdown of Rab39a was achieved with siRNA oligonucleotide #5 and a mix of two oligonucleotides (#5 and #7) (Figure 4.21C). Oligonucleotide #7 on its own was not particularly successful in Rab39a silencing. A decrease in cell viability was not observed at any point during the experiment and approximately 40% of cells adhered to culture plates after incubation with transfection complexes (Figure 4.21B).

These results show that a partial Rab39a knockdown can be achieved in IL-4, GM-CSF-differentiated THP-1 TLR9 mCherry cells by reverse transfection with Lipofectamine 3000. As this was the most successful Rab39a transfection method, it was used in further experiments to study the role of Rab39a in TLR9 signaling.

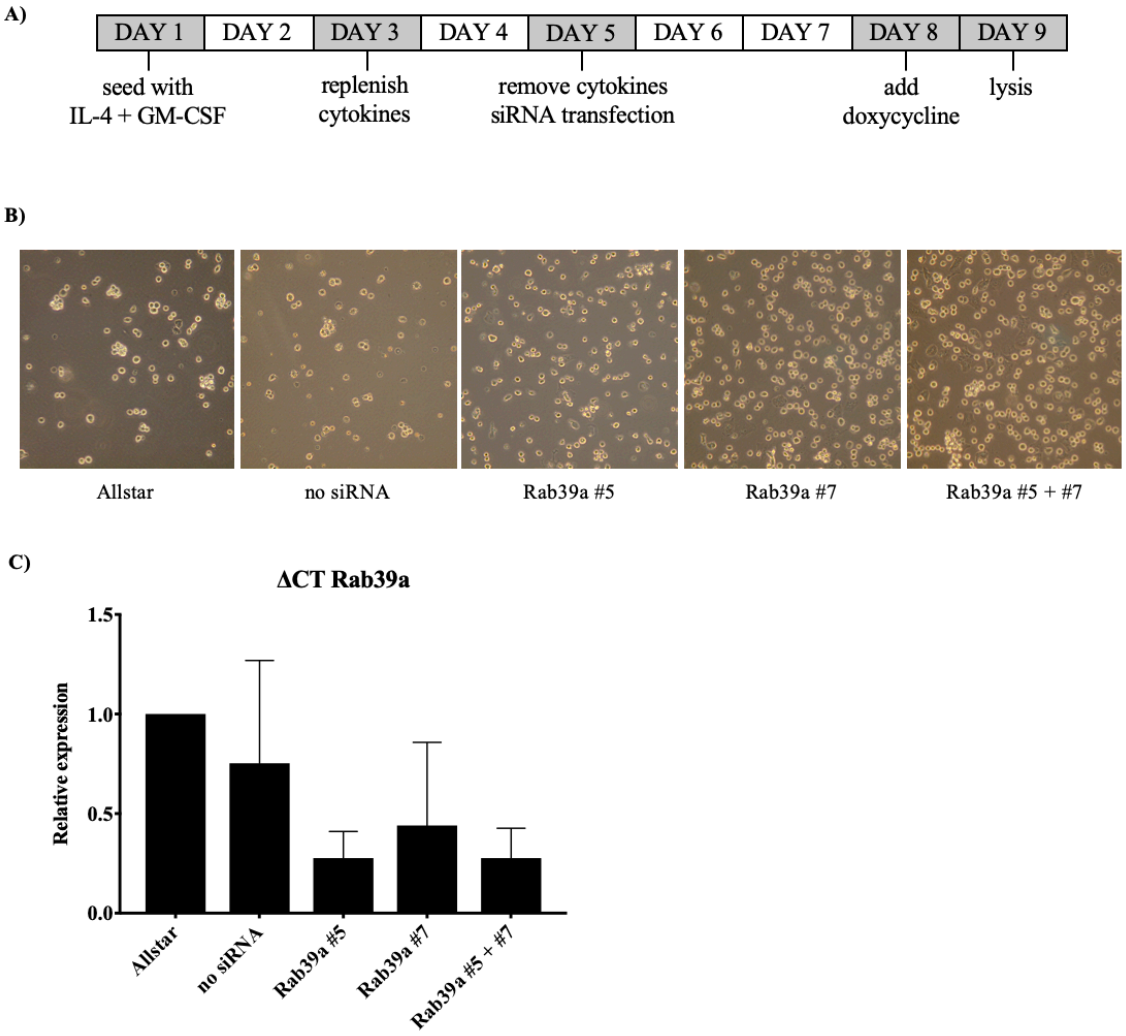

Figure 4.21 Reverse siRNA transfection with Lipofectamine 3000 results in 50% Rab39a knockdown. A) THP-1 TLR9 mCherry cells were differentiated in antibiotic-free medium with rhIL-4 (200ng/ml) and rhGM-CSF (100ng/ml) for 5 days. Cytokines were replenished on day 3 and reverse transfection with Lipofectamine 3000 was done on day 5, after removal of cytokines. Final siRNA concentration was 33nM. Cells were incubated with transfection complexes for 72h after which medium was changed and doxycycline (1µg/ml) was added for 24h. Cells were harvested and lysed 24h after doxycycline administration. **B)** Cell morphology as examined under light-inverted microscope on day 9, magnification 20X. Cells treated with Rab39a siRNA oligos grew more densely and attached more firmly to culture plate than Allstar-treated and untreated cells. **C)** Rab39a mRNA levels were measured by RT-qPCR and normalized to TBP to determine silencing efficiency. Results shown represent fold change relative to Allstar-treated cells. The experiment was done three times. Error bars in **C)** represent standard deviation between three biological replicates.

no siRNA – mock treated sample, incubated with Lipofectamine 3000 only.

Transfection reagent/type of transfection	Final siRNA concentration	Incubation with siRNA (hours)	Rab11a knockdown (%)	Comments
RNAiMAX/forward	16nM	2 x 24 hours	no knockdown	– Cells were transfected twice during 5-day differentiation with IL-4 and GM-CSF and incubated for 24h each time – High reduction in cell viability (>80% cells died possibly due to co-administration of siRNA and doxycycline required for TLR9 induction) – Supplementary Figure 16
Lipofectamine 3000/forward	33nM	72 hours	40%	– Supplementary Figure 19C
Lipofectamine 3000/forward	33nM	2 x 24 hours	50%	– Cells were transfected twice after differentiation with IL-4 and GM-CSF was complete. – Marked reduction in cell viability (<30% cells died after second transfection) – Supplementary Figure 20
DOTAP/forward	160nM	5 hours	50%	– High reduction in cell viability (>60% of cells died after 5h incubation with transfection complexes) – Supplementary Figure 21

Table 4.3 siRNA transfection methods that failed to silence Rab39a in IL-4, GM-CSF-differentiated THP-1 TLR9 mCherry cells.

4.9.2.3 Rab39a may play a role in TLR9-induced IFNβ1 signaling

Having established that partial silencing of Rab39a was possible in IL-4, GM-CSF-differentiated THP-1 TLR9 mCherry cells with Lipofectamine 3000-mediated reverse siRNA transfection, the next experiment focused on studying the effect of Rab39a knockdown on TLR9 signaling. To that end, cells were differentiated with rhIL-4 and rhGM-CSF in antibiotic-free medium for 5 days, with cytokine replenishment on day 3 (Figure 4.22A). Fully differentiated cells were then reverse transfected with Lipofectamine 3000-siRNA complexes and incubated for 72h (Figure 4.22A). Final siRNA concentration was 33nM. Allstar oligonucleotide was used as a negative control and oligonucleotides #5 and #7 were used to silence Rab39a. Doxycycline (1μg/ml) was administered 24h prior to 3h stimulation with 10μM CpG ODN 2006 (Figure 4.22A). Cells were then lysed and assayed for Rab39a, IFNβ1 and TNFα expression by RT-qPCR. Rab39a mRNA levels were used to determine knockdown efficiency, while IFNβ1 and TNFα were used to determine if Rab39a affected cytokine responses mediated by TLR9.

The results show that a partial Rab39a knockdown reduced IFNβ1 expression in stimulated cells (Figure 4.22B). This was a marked decrease, considering that Rab39a knockdown was modest (≈40%) (Figure 4.22B). Two Rab39a oligonucleotides resulted in similar silencing effects in stimulated cells, but IFNβ1 response was lower with

oligonucleotide #7 silencing, indicating that this Rab39a oligonucleotide may have an off-target effect on a regulator of the IFNβ1 signaling. TNFα expression in stimulated cells appeared less affected by Rab39a silencing, indicating that Rab39a may not be important for TLR9-mediated TNFα induction (Figure 4.22B). In addition, Rab39a silencing was not as successful as it had been previously observed (Figure 4.21C), indicating that further optimization of current transfection method should be done or that alternative silencing methods should be considered.

Overall these results suggest that Rab39a is a potential regulator of IFNβ1 signaling initiated from TLR9. However, further experiments need to be done to verify this finding.

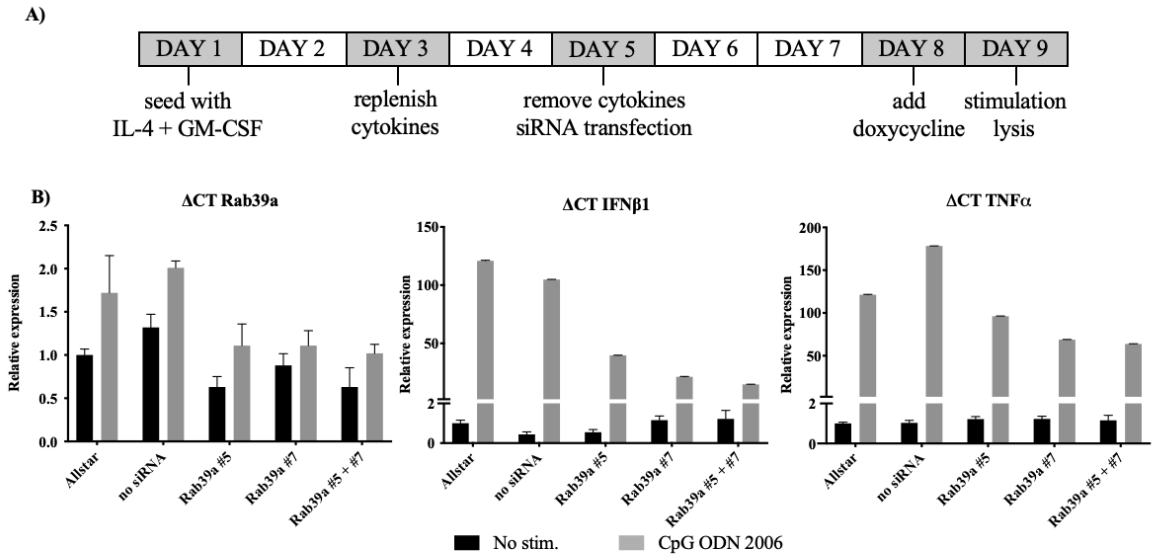

Figure 4.22 Partial Rab39a knockdown results in decreased IFNβ1 expression upon TLR9 stimulation with CpG ODN 2006. A) THP-1 TLR9 mCherry cells were differentiated with rhIL-4 (200ng/ml) and rhGM-CSF (100ng/ml) in antibiotic-free medium. Cytokines were replenished on day 3. After removal of cytokines on day 5, cells (400 000 cells/well) were reverse transfected with Lipofectamine 3000. Final siRNA concentration was 33nM. 72h later transfection complexes were removed and doxycycline (1µg/ml) was added for 24h to induce TLR9 mCherry expression. After removal of doxycycline, cells were stimulated with 10µM CpG ODN 2006 for 3h. **B)** mRNA levels of Rab39a, IFNβ1 and TNFα were measured by RT-qPCR and normalized to TBP. Results shown represent fold change relative to Allstar-treated, unstimulated cells. Error bars represent standard deviation between two technical replicates

no siRNA – mock treated sample, incubated with Lipofectamine 3000 only.

5 DISCUSSION

In this project two experimental cell lines with doxycycline-inducible TLR9 (THP-1 TLR9 mCherry and CAL-1 TLR9 mCherry) were characterized with regards to TLR9 expression and signaling. Signaling pathways down-stream of TLR9 activation were studied and Rab11a and Rab39a were identified as potential regulators of TLR9-induced IFNβ1 signaling. TLR9 subcellular localization was studied by confocal microscopy in both cell lines and it was determined that TLR9 may predominantly localize to LAMP1-positive endosomes under resting conditions.

5.1 TLR9 protein expression under resting conditions

Several human monocytic cell lines, including THP-1 cells, have been shown to produce cytokines in response to bacterial DNA and CpG ODNs, but whether they express a functional TLR9 endogenously is still unclear. On the other hand, CAL-1 cells are pDC-like and known to predominantly express high levels of TLR9 mRNA. In this project, western blot analysis of THP-1, THP-1 TLR9 mCherry, CAL-1 and CAL-1 TLR9 mCherry cells showed that under resting conditions TLR9 levels are not high enough to be detected in these cell lines. However, when doxycycline is added to THP-1 TLR9 mCherry and CAL-1 TLR9 mCherry cells it potently induces TLR9 expression via Tet-On gene expression system and allows for expression of TLR9-induced cytokines in response to CpG ODNs.

In both cell lines, two TLR9 mCherry-specific bands are detected by western blots stained with anti-mCherry antibody. The larger band (150kDa) likely corresponds to full length TLR9 mCherry, while the identity of the shorter band (115kDa), named $TLR9_S$ mCherry, is not clear. TLR9 is heavily post-transcriptionally modified, cleaved by several proteolytic enzymes and exists in many different isoforms, so $TLR9_S$ mCherry could correspond to the C-terminus fragment associated with the mCherry tag generated through proteolytic cleavage of TLR9 mCherry, TLR9-B variant associated with the mCherry tag, phosphorylated TLR9 mCherry or deglycosylated TLR9 mCherry.

In THP-1 TLR9 mCherry cells, the full length TLR9 is less stable than the shorter TLR9 detected by western blot. Decreased stability of full length TLR9 is consistent with what was described by Fukui et al. who showed that murine full length TLR9 is more prone to degradation than cleaved TLR9 fragments[133]. Another group has also shown that cleaved TLR9 fragment is highly stable and that it can be detected for up to 12h after the cleavage

event, further supporting the assumption that TLR9$_S$ mCherry corresponds to cleaved TLR9 mCherry[25].

TLR9-B is an alternatively spliced isoform of TLR9 first reported following gene cloning from THP-1 cells[14,134]. It is a truncated variant, 42 aa shorter than the canonical sequence, predicted to recognize mitochondrial DNA (mtDNA)[14]. However, information regarding this variant is severely lacking so it can only by hypothesized that the shorter band corresponds to TLR9-B mCherry variant whose expression is weakly upregulated upon doxycycline induction.

In addition to being stable for 12h after induction in unstimulated lysates, the shorter band is also detected and has stable expression in lysates stimulated with CpG ODN 2006, indicating that this ligand does not necessarily affect its stability. TLR9 in murine macrophages becomes phosphorylated by Src kinases on tyrosine residues found in its cytoplasmic tail. This modification has been shown to stabilize the receptor, so the 12-hour stability of the shorter band raises a possibility that it corresponds to phosphorylated TLR9.

In addition to phosphorylation, TLR9 is also heavily glycosylated. Sato et al. have shown that glycosylation of TLRs (TLR5, TLR7 and TLR9 in particular) may play an important role in stability of these proteins. This was further confirmed by Hasan et. al who demonstrated that tunicamycin, an inhibitor of N-linked glycosylation, leads to loss of TLR9 within 4 hours of its administration to mouse macrophages[135]. These findings indicate that the shorter band is least likely to correspond to deglycosylated TLR9 due to its low stability.

Overall, we cannot deduce the identity of this band with certainty. However, this band is never detected in non-doxycycline-treated cells, suggesting that it is TLR9-, and doxycycline-induction specific. If these cell lines are to be used as experimental models, understanding what this band corresponds to would be beneficial (e.g. inhibition of glycosylation or phosphorylation in doxycycline-induced cells to determine whether the stability or expression of the band are affected by either of those).

5.2 TLR9 protein expression in response to CpG ODN 2006

Upon stimulation, TLR9 is thought to be upregulated and proteolytically cleaved into two fragments, a C-terminal fragment that can activate downstream signaling, and an N-terminal fragment which may play a role in regulation of TLR9 responses[117,136]. Expression and cleavage of TLR9 before and after stimulation can be detected by western blot. In this project, it was observed that CpG ODN 2006 stimulation of PMA-differentiated cells does not have an effect on TLR9 protein levels, once they had been induced by doxycycline. These

cells were also able to upregulate TNFα expression only when TLR9 was induced, indicating that TNFα response seen on mRNA level was TLR9-dependent. Together, these results suggested that even though protein expression of TLR9 during stimulation remained stable, TLR9 was still responding to stimuli, supporting the finding described by Hasan et al. that TLR9 protein expression and cleavage do not necessarily correspond to signaling ability and the extent of immune response induced by the receptor[135].

Interestingly, when THP-1 TLR9 mCherry cells were differentiated into immature dendritic-like cells by administration of IL-4 and GM-CSF, and stimulated with the same ligand, full length TLR9 expression was moderately increased. It peaked at 2h after stimulation and subsequently decreased to levels below those observed in unstimulated cells. Similar findings were described by Zhang et al. for human lung tissue macrophages in which TLR9 was stimulated with mtDNA, however, the length of stimulation was much longer, and full length TLR9 expression returned to basal levels 24h after stimulation[137]. From the current literature and findings in this project it is apparent that TLR9 expression prior to and after stimulation is cell-type dependent, and the extent and length of TLR9 upregulation depend on the ligand that is activating the receptor. In addition, cleavage of TLR9 may not be an adequate measure of TLR9 activation, therefore other methods (e.g. mRNA and protein expression of downstream signaling molecules, levels of produced cytokines, etc.) need to be used to verify its activation and its ability to induce immune response.

5.3 TLR9-induced cytokine responses

PMA-differentiated THP-1 TLR9 mCherry cells resemble macrophages. When stimulated with CpG ligands, they failed to induce IFNβ1, but were potent inducers of TNFα. This was an unexpected finding given that PMA-differentiated THP-1 and THP-1 TLR9 mCherry cells both upregulate IFNβ1 upon TLR4 stimulation with LPS, regardless of doxycycline presence (Wang, Unpublished data). However, when THP-1 TLR9 mCherry cells were differentiated with IL-4 and GM-CSF into immature dendritic-like cells they resulted in potent upregulation of both IFNβ1 and TNFα. According to the literature, TLR9-induced production of type I IFNs requires activation of several IRF proteins (IRF1, IRF3, IRF5, IRF7)[40-43]. Increased phosphorylation of TBK1 after stimulation of TLR9, indicated that CpG ligands were activating TBK1-IRF3-IFNβ1 pathway and inducing IRF3 translocation to the nucleus to upregulate IFNβ1 expression. IFNβ1 was also produced on protein level and it activated IFNAR as reflected by increased phosphorylation of STAT1 protein. Stimulation of these cells also activated p38, leading to its phosphorylation. Together

with upregulation of TNFα expression, this suggested that AP-1, a transcription factor found downstream of p38 was inducing TNFα responses[122].

As demonstrated by Berges et al. differentiation of THP-1 TLR9 mCherry cells with IL-4 and GM-CSF into immature dendritic-like cells results in *de novo* synthesis of CD209 (DC-SIGN)[100]. CD209 is a C-type lectin receptor found on the surface of dendritic cells and macrophages. It has been shown that DC-SIGN can enhance internalization of pathogenic DNA and CpG ODNs, facilitate their delivery into endosomes and therefore activate TLR9[138]. This *de novo* synthesized cell surface protein could explain why THP-1 TLR9 mCherry cells were able to induce such potent cytokine expression after differentiation with IL-4 and GM-CSF. However, cell surface markers for immature dendritic-like THP-1 TLR9 mCherry cells were not assayed in this project and should therefore be examined if this cell line is to be used in future experiments.

The results obtained for cytokine responses in CAL-1 TLR9 mCherry cells were somewhat puzzling. CAL-1 cells resemble pDCs, and they have been found to secrete type I IFNs and TNFα in response to CpG ODN 2216, but not upon stimulation with CpG ODN 2006[89]. Our results show that upon stimulation with CpG ODN 2006 or 2216, undifferentiated CAL-1 and CAL-1 TLR9 mCherry cells were potent inducers of IFNβ1 expression but failed to induce TNFα. In the future experiments, signaling molecules found downstream of TLR9 should be studied in both CAL-1 TLR9 mCherry and THP-1 TLR9 mCherry cells as TLR9 is thought to engage different downstream signaling molecules, dependent on the cell type it is signaling from. For example, in addition to IRF3, IRF1 has been implicated in TLR9-induced IFNβ production in myeloid dendritic cells, while IRF5 is required for TLR9-induced IFNβ production in pDCs[38,39].

5.4 Rab39a is a potential regulator of TLR9-induced IFNβ1 signaling

In humans, Rab39a is a ubiquitously expressed 217 aa protein encoded on chromosome 11[128]. It contains a highly conserved caspase-1 cleavage site at Asp148 and upon incubation with caspase-1, it becomes cleaved into two fragments – a 25kDa and a 17kDa fragment[120]. As of now its main role is regulation of endocytosis and acidification of maturing phagosomes[129,130]. More specifically, it regulates LPS-induced autophagosome formation and secretion of pro-inflammatory cytokines and functions as a trafficking adaptor linking caspase-1 and IL-1β secretion[120,129]. Rab39a can be found in late endosomes and lysosomes, as shown by strong association between Rab39a and LAMP1-positive vesicles[128-130]. Tudela et al. have demonstrated that Rab39a tends to concentrate in acidic MVBs with low

degradative enzymatic activity[128]. In addition, Rab39a has been shown to localize in the Golgi and enhance endocytosis in HeLa cells, but its endocytic function seems to be cell-type dependent[139].

Our results show that partial Rab39a silencing leads to a marked decrease in IFNβ1 expression upon stimulation of IL-4, GM-CSF-differentiated THP-1 TLR9 mCherry cells with CpG ODN 2006. The effect of Rab39a silencing was not observed in TNFα expression. As Rab39a is found in late endosomes/lysosome, its partial silencing may lead to dysregulation in late endosome function or structure. CpG ODN 2006 is thought to predominantly signal from late endosomes, therefore, partial Rab39a silencing could reduce the availability of vesicles for TLR9 and CpG ODN 2006 interactions. In addition, it is also possible that knockdown of Rab39a may interfere with endocytosis of CpG in THP-1 cells, thus leading to a decrease in cytokine production. Further signaling and trafficking experiments should be done to verify this finding, and to determine where Rab39a is located under resting and stimulatory conditions in these cells, and how it behaves with regards to TLR9.

5.5 Rab11a may play a role in TLR9-induced IFNβ1 signaling

Rab11a is a Rab GTPase that plays a crucial role in regulation of endocytic membrane recycling, by acting as a component of recycling endosomes[126,127]. It has been shown that Rab11a regulates TLR4 trafficking in and out of the endocytic recycling compartment (ERC) and TLR4-induced IRF3 activation and IFNβ production[76]. In murine intestinal epithelial cells, Rab11a contributes to maintenance of homeostatic intracellular distribution of TLR9[77]. Loss of Rab11a leads to accumulation of TLR9 in intracellular compartments and a phenotype that resembles inflammatory bowel disease[77].

In this project it was shown that almost a complete Rab11a knockdown leads to a moderate decrease in IFNβ1, but not TNFα expression, suggesting that Rab11a may play a role in TLR9-induced IFNβ1 signaling. Rab11a may contribute to TLR9 signaling by facilitating its recycling under resting conditions, or by affecting IRF3-mediated IFNβ1 responses[76]. However, future experiments should be done to verify this finding, to determine whether TLR9 is located in Rab11a-positive endosomes, and how its silencing may affect signaling molecules found downstream of TLR9.

5.6 TLR9 is found in late endosomes/lysosomes under resting conditions

TLR9-induced cytokine responses are thought to be dependent on the type of the ligand it interacts with, its mode of internalization and the intracellular compartment in which TLR9-ligand interactions occur. Class A CpG ODNs (e.g. CpG ODN 2216) are thought to interact with TLR9 in early endosomes and predominantly induce type I IFNs, while Class B CpG ODNs (e.g. CpG ODN 2006) are thought to signal from late endosomes and induce pro-inflammatory cytokines (TNFα, IL-12)[78]. However, the results in this project show that both cell lines respond to both CpG ligands equally – IL-4, GM-CSF-differentiated THP-1 TLR9 mCherry cells similarly upregulate IFNβ1 and TNFα expression in response to both CpG 2216 and 2006, and undifferentiated CAL-1 TLR9 mCherry cells express IFNβ1 at relatively similar levels when stimulated with CpG ODN 2216 and 2006.

Confocal microscopy experiments that studied subcellular localization of TLR9 before and after stimulation resulted in some unexpected findings. In resting cells, TLR9 is thought to reside in the ER, from where it gets translocated to the endosomes upon stimulation[140]. However, in both resting IL-4, GM-CSF-differentiated THP-1 TLR9 mCherry and CAL-1 TLR9 mCherry cells, the majority of TLR9 was found colocalizing with LAMP1, a marker for late endosomes/lysosomes. After stimulation of IL-4, GM-CSF-differentiated THP-1 TLR9 mCherry cells with CpG ODN 2006 or 2216 for 3 hours, the same amount of colocalization was found with LAMP1 as before stimulation. This suggested that TLR9 in these cells possibly resides and signals from LAMP1-positive vesicles. Colocalization of CpG ODN 2006-stimulated TLR9 with late endosomes was expected, as this ligand is thought to signal from late endosomes. On the other hand, CpG ODN 2216-stimulated TLR9 was also found in LAMP1-positive endosomes, even though it is expected to activate TLR9 from the early endosomes. Upon 3h stimulation of CAL-1 TLR9 mCherry cells with CpG ODN 2216, the majority of TLR9 remained in LAMP1-positive endosomes. However, colocalization between CpG ODN 2006-stimulated TLR9 and LAMP1-positive endosomes decreased after 3h stimulation, indicating that CpG ODN 2006-stimulated TLR9 might be signaling from other endosomal compartments. However, at the same time point CpG ODN 2006-stimulated TLR9 did not signal from early endosomes, as there was no colocalization between TLR9 and EEA1.

These experiments were only done on unstimulated IL-4, GM-CSF-differentiated THP-1 TLR9 mCherry and CAL-1 TLR9 mCherry cells, and those stimulated for 3h so it is impossible to know whether TLR9 localized to different endosomal compartments at earlier stages of stimulation. For example, CpG ODN 2216 was found in late endosomes/lysosome in both cell lines after 3h of stimulation. This CpG ligand belongs to Class A CpG ODNs, a

family of ligands that tends to spontaneously form nanoparticle-like structures that get taken up slowly and result in pro-longed interactions with TLR9 in early endosomes[11,17]. It is possible that CpG ODN 2216 was found signaling from early endosomes in the first 1-2 hours of stimulation, and afterwards got transferred to LAMP1-positive endosomes. Additional experiments need to be done to verify these findings and further explore subcellular localization of TLR9. Colocalization or a lack of thereof should not be based on a single endosomal compartment marker, but instead, additional makers for the same compartment should be used to confirm. Further, both cells lines express mCherry-tagged TLR9, allowing us to use live microscopy to capture localization of TLR9 during different stages of stimulation. At the same time, fluorescent CpG ligands can be used to determine whether there is a difference in intracellular compartments in which TLR9 encounters its ligand.

Finally, while findings regarding TLR9 localization in these cells are interesting, one has to be aware that these cell lines overexpress TLR9 after doxycycline induction, therefore making it possible that some cell-line specific machinery, overexpression system or fluorescent-tagging of TLR9 are affecting localization and trafficking of TLR9 in these cells.

5.7 Application of experimental model cell lines in *in vitro* studies

TLR9 expression, signaling and trafficking all appear to be species-, tissue- and cell-type dependent. Due to difficulties associated with working with pDCs, most of the information we have about this receptor stems from murine models, which only partially mimic human immune response. Given the lack of suitable experimental models for studying TLR9, THP-1 TLR9 mCherry and CAL-1 TLR9 mCherry cells represent two models that have a potential to be used in studying TLR9 expression, signaling and trafficking. However, due to genetic manipulations and the sole nature of cancer cell lines, TLR9 properties in these cells may not reflect the “real-life” events that take place in *in vivo* equivalents of these cells. A potential use of these can be in conducting preliminary experiments and optimization for study of TLR9 in pDCs. Further, since THP-1 TLR9 mCherry cells can be differentiated into immature dendritic-like cells, and undifferentiated CAL-1 TLR9 mCherry cells closely resemble pDCs, these two models can be used simultaneously to study differences in TLR9 signaling and trafficking between myeloid and plasmacytoid DCs.

6 CONCLUSION

In this project, two experimental model cells lines (THP-1 TLR9 mCherry and CAL-1 TLR9 mCherry) were characterized for *in vitro* studies of TLR9 expression, signaling and trafficking. Under resting conditions and in the absence of doxycycline, TLR9 levels cannot be detected in these two cell lines. However, administration of doxycycline induces expression TLR9 mCherry that is not further affected by CpG ODN stimulation. PMA-differentiated THP-1 TLR9 mCherry cells are poor inducers of TLR9-dependnet IFNβ1 responses. THP-1 TLR9 mCherry cells that are differentiated with IL-4 and GM-CSF into immature dendritic-like cells strongly induce both IFNβ1 and TNFα expression in response to CpG ODN 2006 or 2216. Undifferentiated CAL-1 TLR9 mCherry cells share morphological and functional similarities with pDCs and potently induce IFNβ1 in response to CpG ODN 2006 and 2216. Rab39a and Rab11a have been shown to potentially play a role in regulation of TLR9-induced IFNβ1 signaling in immature dendritic-like THP-1 TLR9 mCherry cells. At the same time, a potential role of these Rab GTPases in CAL-1 TLR9 mCherry cells remains unknown, as CAL-1 TLR9 mCherry cells are very fragile, and difficult to transfect with siRNA. Confocal microscopy experiments revealed that PMA-differentiated under resting conditions TLR9 colocalizes with LAMP1-positive vesicles in both cell lines. After 3h stimulation of both cells types with CpG ODN 2216, TLR9 remains in late endosomes/lysosomes, while stimulation with CpG ODN 2006 results in marked loss of TLR9 from late endosomes in CAL-1 TLR9 mCherry cells.

Some of the results obtained for cytokine response and TLR9 localization before and after stimulation with CpG ligands were unexpected, considering available information regarding TLR9 signaling and trafficking. However, majority of literature available is based on murine models, therefore direct comparison with our results cannot be made. Instead, further experiments should be done to verify these findings in the context of human immune system. Further, this study showed that CAL-1 TLR9 mCherry and THP-1 TLR9 mCherry cells have a potential to be used in *in vitro* studies of TLR9 properties in pDC-like cells or to delineate differences in TLR9 expression, signaling and trafficking between myeloid dendritic cells and pDCs.

REFERENCES

1 Jiménez-Dalmaroni, M. J., Gerswhin, M. E. & Adamopoulos, I. E. The critical role of toll-like receptors — From microbial recognition to autoimmunity: A comprehensive review. *Autoimmunity reviews* **15**, 1-8, doi:https://doi.org/10.1016/j.autrev.2015.08.009 (2016).

2 Pradhan, V. D., Das, S., Surve, P. & Ghosh, K. Toll-like receptors in autoimmunity with special reference to systemic lupus erythematosus. *Indian Journal of Human Genetics* **18**, 155-160, doi:10.4103/0971-6866.100750 (2012).

3 Kawai, T. & Akira, S. Toll-like Receptors and Their Crosstalk with Other Innate Receptors in Infection and Immunity. *Immunity* **34**, 637-650, doi:https://doi.org/10.1016/j.immuni.2011.05.006 (2011).

4 Duffy, L. & O'Reilly, S. C. Toll-like receptors in the pathogenesis of autoimmune diseases: recent and emerging translational developments. *ImmunoTargets and Therapy* **5**, 69-80, doi:10.2147/ITT.S89795 (2016).

5 Kawai, T. & Akira, S. The role of pattern-recognition receptors in innate immunity: update on Toll-like receptors. *Nat Immunol* **11**, 373-384 (2010).

6 Kagan, J. C. *et al.* TRAM couples endocytosis of Toll-like receptor 4 to the induction of interferon-β. *Nature immunology* **9**, 361 (2008).

7 Mouchess, Maria L. *et al.* Transmembrane Mutations in Toll-like Receptor 9 Bypass the Requirement for Ectodomain Proteolysis and Induce Fatal Inflammation. *Immunity* **35**, 721-732, doi:https://doi.org/10.1016/j.immuni.2011.10.009 (2011).

8 Bonham, K. S. *et al.* A promiscuous lipid-binding protein diversifies the subcellular sites of toll-like receptor signal transduction. *Cell* **156**, 705-716, doi:10.1016/j.cell.2014.01.019 (2014).

9 Li, Y., Liantang, W. & Shangwu, C. Endogenous toll-like receptor ligands and their biological significance. *Journal of Cellular and Molecular Medicine* **14**, 2592-2603, doi:doi:10.1111/j.1582-4934.2010.01127.x (2010).

10 Goulopoulou, S., McCarthy, C. G. & Webb, R. C. Toll-like Receptors in the Vascular System: Sensing the Dangers Within. *Pharmacological Reviews* **68**, 142-167, doi:10.1124/pr.114.010090 (2016).

11 Hartmann, G. in *Advances in Immunology* Vol. 133 (ed Frederick W. Alt) 121-169 (Academic Press, 2017).

12 Harberts, E. & Gaspari, A. A. TLR Signaling and DNA Repair: Are They Associated? *Journal of Investigative Dermatology* **133**, 296-302, doi:https://doi.org/10.1038/jid.2012.288 (2013).

13 Krieg, A. M. Development of TLR9 agonists for cancer therapy. *The Journal of Clinical Investigation* **117**, 1184-1194, doi:10.1172/JCI31414 (2007).

14 McKelvey, K. J., Highton, J. & Hessian, P. A. Cell-specific expression of TLR9 isoforms in inflammation. *Journal of Autoimmunity* **36**, 76-86, doi:https://doi.org/10.1016/j.jaut.2010.11.001 (2011).

15 Krug, A. *et al.* Identification of CpG oligonucleotide sequences with high induction of IFN-α/β in plasmacytoid dendritic cells. *European Journal of Immunology* **31**, 2154-2163, doi:10.1002/1521-4141(200107)31:7<2154::Aid-immu2154>3.0.Co;2-u (2001).

16 Dalpke, A. H., Zimmermann, S., Albrecht, I. & Heeg, K. Phosphodiester CpG oligonucleotides as adjuvants: polyguanosine runs enhance cellular uptake and improve immunostimulative activity of phosphodiester CpG oligonucleotides in vitro and in vivo. *Immunology* **106**, 102-112, doi:10.1046/j.1365-2567.2002.01410.x (2002).

17 Kerkmann, M. *et al.* Spontaneous formation of nucleic acid-based nanoparticles is responsible for high interferon-alpha induction by CpG-A in plasmacytoid dendritic cells. *J Biol Chem* **280**, 8086-8093, doi:10.1074/jbc.M410868200 (2005).

18 Swiecki, M. & Colonna, M. The multifaceted biology of plasmacytoid dendritic cells. *Nature reviews. Immunology* **15**, 471-485, doi:10.1038/nri3865 (2015).

19 Ohto, U. *et al.* Structural basis of CpG and inhibitory DNA recognition by Toll-like receptor 9. *Nature* **520**, 702, doi:10.1038/nature14138 (2015).

20 Ohto, U. *et al.* Toll-like Receptor 9 Contains Two DNA Binding Sites that Function Cooperatively to Promote Receptor Dimerization and Activation. *Immunity* **48**, 649-658.e644, doi:10.1016/j.immuni.2018.03.013 (2018).

21 Pohar, J. *et al.* Short single-stranded DNA degradation products augment the activation of Toll-like receptor 9. *Nature Communications* **8**, 15363, doi:10.1038/ncomms15363 https://www.nature.com/articles/ncomms15363#supplementary-information (2017).

22 Pandey, S. & Kawai, T. in *Biological DNA Sensor* (eds Ken J. Ishii & Choon Kit Tang) 103-132 (Academic Press, 2014).

23 Ewald, S. E. *et al.* The ectodomain of Toll-like receptor 9 is cleaved to generate a functional receptor. *Nature* **456**, 658, doi:10.1038/nature07405

https://www.nature.com/articles/nature07405#supplementary-information (2008).
24 Park, B. *et al.* Proteolytic cleavage in an endolysosomal compartment is required for activation of Toll-like receptor 9. *Nature Immunology* **9**, 1407, doi:10.1038/ni.1669
https://www.nature.com/articles/ni.1669#supplementary-information (2008).
25 Ewald, S. E. *et al.* Nucleic acid recognition by Toll-like receptors is coupled to stepwise processing by cathepsins and asparagine endopeptidase. *J Exp Med* **208**, 643-651, doi:10.1084/jem.20100682 (2011).
26 Onji, M. *et al.* An essential role for the N-terminal fragment of Toll-like receptor 9 in DNA sensing. *Nature Communications* **4**, 1949, doi:10.1038/ncomms2949
https://www.nature.com/articles/ncomms2949#supplementary-information (2013).
27 Kawai, T. & Akira, S. TLR signaling. *Cell Death & Differentiation* **13**, 816-825, doi:10.1038/sj.cdd.4401850 (2006).
28 Latz, E. *et al.* Ligand-induced conformational changes allosterically activate Toll-like receptor 9. *Nat Immunol* **8**, 772-779, doi:10.1038/ni1479 (2007).
29 Mohammad Hosseini, A., Majidi, J., Baradaran, B. & Yousefi, M. Toll-Like Receptors in the Pathogenesis of Autoimmune Diseases. *Advanced Pharmaceutical Bulletin* **5**, 605-614, doi:10.15171/apb.2015.082 (2015).
30 Suzuki, N. *et al.* Severe impairment of interleukin-1 and Toll-like receptor signalling in mice lacking IRAK-4. *Nature* **416**, 750-756, doi:10.1038/nature736 (2002).
31 Kawagoe, T. *et al.* Sequential control of Toll-like receptor-dependent responses by IRAK1 and IRAK2. *Nat Immunol* **9**, 684-691, doi:10.1038/ni.1606 (2008).
32 Marongiu, L., Gornati, L., Artuso, I., Zanoni, I. & Granucci, F. Below the surface: The inner lives of TLR4 and TLR9. *Journal of Leukocyte Biology* **0**, doi:10.1002/jlb.3mir1218-483rr (2019).
33 Takaesu, G. *et al.* TAK1 is critical for IkappaB kinase-mediated activation of the NF-kappaB pathway. *J Mol Biol* **326**, 105-115 (2003).
34 Patel, H. *et al.* Toll-like receptors in ischaemia and its potential role in the pathophysiology of muscle damage in critical limb ischaemia. *Cardiology research and practice* **2012**, 121237, doi:10.1155/2012/121237 (2012).
35 Ninomiya-Tsuji, J. *et al.* The kinase TAK1 can activate the NIK-I kappaB as well as the MAP kinase cascade in the IL-1 signalling pathway. *Nature* **398**, 252-256, doi:10.1038/18465 (1999).
36 Negishi, H. *et al.* Evidence for licensing of IFN-gamma-induced IFN regulatory factor 1 transcription factor by MyD88 in Toll-like receptor-dependent gene induction program. *Proc Natl Acad Sci U S A* **103**, 15136-15141, doi:10.1073/pnas.0607181103 (2006).
37 Takaoka, A. *et al.* Integral role of IRF-5 in the gene induction programme activated by Toll-like receptors. *Nature* **434**, 243-249, doi:10.1038/nature03308 (2005).
38 Schmitz, F. *et al.* Interferon-regulatory-factor 1 controls Toll-like receptor 9-mediated IFN-beta production in myeloid dendritic cells. *Eur J Immunol* **37**, 315-327, doi:10.1002/eji.200636767 (2007).
39 Steinhagen, F. *et al.* IRF-5 and NF-κB p50 co-regulate IFN-β and IL-6 expression in TLR9-stimulated human plasmacytoid dendritic cells. *European Journal of Immunology* **43**, 1896-1906, doi:10.1002/eji.201242792 (2013).
40 Honda, K. *et al.* Role of a transductional-transcriptional processor complex involving MyD88 and IRF-7 in Toll-like receptor signaling. *Proc Natl Acad Sci U S A* **101**, 15416-15421, doi:10.1073/pnas.0406933101 (2004).
41 Yang, K. *et al.* Human TLR-7-, -8-, and -9-mediated induction of IFN-alpha/beta and -lambda Is IRAK-4 dependent and redundant for protective immunity to viruses. *Immunity* **23**, 465-478, doi:10.1016/j.immuni.2005.09.016 (2005).
42 Hacker, H. *et al.* Specificity in Toll-like receptor signalling through distinct effector functions of TRAF3 and TRAF6. *Nature* **439**, 204-207, doi:10.1038/nature04369 (2006).
43 Uematsu, S. *et al.* Interleukin-1 receptor-associated kinase-1 plays an essential role for Toll-like receptor (TLR)7- and TLR9-mediated interferon-{alpha} induction. *J Exp Med* **201**, 915-923, doi:10.1084/jem.20042372 (2005).
44 Kawai, T. *et al.* Interferon-alpha induction through Toll-like receptors involves a direct interaction of IRF7 with MyD88 and TRAF6. *Nat Immunol* **5**, 1061-1068, doi:10.1038/ni1118 (2004).
45 Honda, K. *et al.* IRF-7 is the master regulator of type-I interferon-dependent immune responses. *Nature* **434**, 772-777, doi:10.1038/nature03464 (2005).
46 Shinohara, M. L. *et al.* Osteopontin expression is essential for interferon-alpha production by plasmacytoid dendritic cells. *Nat Immunol* **7**, 498-506, doi:10.1038/ni1327 (2006).
47 Podinovskaia, M. & Spang, A. in *Endocytosis and Signaling* (eds Christophe Lamaze & Ian Prior) 1-38 (Springer International Publishing, 2018).
48 Corvera, S., D'Arrigo, A. & Stenmark, H. Phosphoinositides in membrane traffic. *Curr Opin Cell Biol* **11**, 460-465, doi:10.1016/s0955-0674(99)80066-0 (1999).

49 Naslavsky, N. & Caplan, S. The enigmatic endosome – sorting the ins and outs of endocytic trafficking. *Journal of Cell Science* **131**, jcs216499, doi:10.1242/jcs.216499 (2018).

50 Delevoye, C. & Goud, B. in *Methods in Cell Biology* Vol. 130 (ed Wei Guo) 235-246 (Academic Press, 2015).

51 Sönnichsen, B., De Renzis, S., Nielsen, E., Rietdorf, J. & Zerial, M. Distinct Membrane Domains on Endosomes in the Recycling Pathway Visualized by Multicolor Imaging of Rab4, Rab5, and Rab11. *The Journal of Cell Biology* **149**, 901-914, doi:10.1083/jcb.149.4.901 (2000).

52 Jones, M. C., Caswell, P. T. & Norman, J. C. Endocytic recycling pathways: emerging regulators of cell migration. *Current Opinion in Cell Biology* **18**, 549-557, doi:https://doi.org/10.1016/j.ceb.2006.08.003 (2006).

53 Maxfield, F. R. & McGraw, T. E. Endocytic recycling. *Nat Rev Mol Cell Biol* **5**, 121-132, doi:10.1038/nrm1315 (2004).

54 Naslavsky, N. & Caplan, S. C-terminal EH-domain-containing proteins: consensus for a role in endocytic trafficking, EH? *Journal of Cell Science* **118**, 4093-4101, doi:10.1242/jcs.02595 (2005).

55 Naslavsky, N. & Caplan, S. EHD proteins: key conductors of endocytic transport. *Trends Cell Biol* **21**, 122-131, doi:10.1016/j.tcb.2010.10.003 (2011).

56 Frankel, E. B. & Audhya, A. ESCRT-dependent cargo sorting at multivesicular endosomes. *Seminars in Cell & Developmental Biology* **74**, 4-10, doi:https://doi.org/10.1016/j.semcdb.2017.08.020 (2018).

57 Shaw, J. D., Hama, H., Sohrabi, F., DeWald, D. B. & Wendland, B. PtdIns(3,5)P2 is required for delivery of endocytic cargo into the multivesicular body. *Traffic* **4**, 479-490 (2003).

58 Matsuo, H. *et al.* Role of LBPA and Alix in Multivesicular Liposome Formation and Endosome Organization. *Science* **303**, 531-534, doi:10.1126/science.1092425 (2004).

59 Frederick, T. E., Chebukati, J. N., Mair, C. E., Goff, P. C. & Fanucci, G. E. Bis(monoacylglycero)phosphate forms stable small lamellar vesicle structures: insights into vesicular body formation in endosomes. *Biophys J* **96**, 1847-1855, doi:10.1016/j.bpj.2008.12.3892 (2009).

60 Hullin-Matsuda, F. *et al.* De novo biosynthesis of the late endosome lipid, bis(monoacylglycero)phosphate. *J Lipid Res* **48**, 1997-2008, doi:10.1194/jlr.M700154-JLR200 (2007).

61 Guerra, F. & Bucci, C. Multiple Roles of the Small GTPase Rab7. *Cells* **5**, 34 (2016).

62 Hutagalung, A. H. & Novick, P. J. Role of Rab GTPases in Membrane Traffic and Cell Physiology. *Physiological Reviews* **91**, 119-149, doi:10.1152/physrev.00059.2009 (2011).

63 Zerial, M. & McBride, H. Rab proteins as membrane organizers. *Nature Reviews Molecular Cell Biology* **2**, 107, doi:10.1038/35052055 (2001).

64 Jordens, I., Marsman, M., Kuijl, C. & Neefjes, J. Rab proteins, connecting transport and vesicle fusion. *Traffic* **6**, 1070-1077 (2005).

65 Schwartz, S. L., Cao, C., Pylypenko, O., Rak, A. & Wandinger-Ness, A. Rab GTPases at a glance. *Journal of Cell Science* **120**, 3905-3910, doi:10.1242/jcs.015909 (2007).

66 Grosshans, B. L., Ortiz, D. & Novick, P. Rabs and their effectors: Achieving specificity in membrane traffic. *Proceedings of the National Academy of Sciences* **103**, 11821-11827, doi:10.1073/pnas.0601617103 (2006).

67 Markgraf, D. F., Peplowska, K. & Ungermann, C. Rab cascades and tethering factors in the endomembrane system. *FEBS Lett* **581**, 2125-2130, doi:10.1016/j.febslet.2007.01.090 (2007).

68 Collins, R. N. "Getting it on"--GDI displacement and small GTPase membrane recruitment. *Mol Cell* **12**, 1064-1066 (2003).

69 Sivars, U., Aivazian, D. & Pfeffer, S. R. Yip3 catalyses the dissociation of endosomal Rab-GDI complexes. *Nature* **425**, 856-859, doi:10.1038/nature02057 (2003).

70 Ullrich, O. *et al.* Rab GDP dissociation inhibitor as a general regulator for the membrane association of rab proteins. *J Biol Chem* **268**, 18143-18150 (1993).

71 Wu, S. K., Zeng, K., Wilson, I. A. & Balch, W. E. Structural insights into the function of the Rab GDI superfamily. *Trends Biochem Sci* **21**, 472-476 (1996).

72 Pfeffer, S. R. Structural clues to Rab GTPase functional diversity. *J Biol Chem* **280**, 15485-15488, doi:10.1074/jbc.R500003200 (2005).

73 Chavrier, P. *et al.* Hypervariable C-terminal domain of rab proteins acts as a targeting signal. *Nature* **353**, 769-772, doi:10.1038/353769a0 (1991).

74 Yao, M. *et al.* Late Endosome/Lysosome-Localized Rab7b Suppresses TLR9-Initiated Proinflammatory Cytokine and Type I IFN Production in Macrophages. *The Journal of Immunology* **183**, 1751, doi:10.4049/jimmunol.0900249 (2009).

75 Wall, A. A. *et al.* Small GTPase Rab8a-recruited Phosphatidylinositol 3-Kinase γ Regulates Signaling and Cytokine Outputs from Endosomal Toll-like Receptors. *The Journal of biological chemistry* **292**, 4411-4422, doi:10.1074/jbc.M116.766337 (2017).

76 Husebye, H. *et al.* The Rab11a GTPase Controls Toll-like Receptor 4-Induced Activation of Interferon Regulatory Factor-3 on Phagosomes. *Immunity* **33**, 583-596, doi:10.1016/j.immuni.2010.09.010 (2010).
77 Yu, S. & Gao, N. Compartmentalizing intestinal epithelial cell toll-like receptors for immune surveillance. *Cellular and Molecular Life Sciences* **72**, 3343-3353, doi:10.1007/s00018-015-1931-1 (2015).
78 Lee, B. L. & Barton, G. M. Trafficking of endosomal Toll-like receptors. *Trends Cell Biol* **24**, 360-369, doi:10.1016/j.tcb.2013.12.002 (2014).
79 Yang, Y. *et al.* Heat Shock Protein gp96 Is a Master Chaperone for Toll-like Receptors and Is Important in the Innate Function of Macrophages. *Immunity* **26**, 215-226, doi:https://doi.org/10.1016/j.immuni.2006.12.005 (2007).
80 Takahashi, K. *et al.* A protein associated with Toll-like receptor (TLR) 4 (PRAT4A) is required for TLR-dependent immune responses. *The Journal of Experimental Medicine* **204**, 2963-2976, doi:10.1084/jem.20071132 (2007).
81 Marongiu, L., Gornati, L., Artuso, I., Zanoni, I. & Granucci, F. Below the surface: The inner lives of TLR4 and TLR9. *Journal of Leukocyte Biology* **0**, doi:10.1002/jlb.3mir1218-483rr.
82 Lee, B. L. *et al.* UNC93B1 mediates differential trafficking of endosomal TLRs. *Elife* **2**, e00291, doi:10.7554/eLife.00291 (2013).
83 Sasai, M., Linehan, M. M. & Iwasaki, A. Bifurcation of Toll-like receptor 9 signaling by adaptor protein 3. *Science* **329**, 1530-1534, doi:10.1126/science.1187029 (2010).
84 Shisheva, A. PIKfyve: Partners, significance, debates and paradoxes. *Cell Biol Int* **32**, 591-604, doi:10.1016/j.cellbi.2008.01.006 (2008).
85 Combes, A. *et al.* BAD-LAMP controls TLR9 trafficking and signalling in human plasmacytoid dendritic cells. *Nat Commun* **8**, 913, doi:10.1038/s41467-017-00695-1 (2017).
86 Latz, E. *et al.* TLR9 signals after translocating from the ER to CpG DNA in the lysosome. *Nat Immunol* **5**, 190-198, doi:http://www.nature.com/ni/journal/v5/n2/suppinfo/ni1028_S1.html (2004).
87 Park, B. *et al.* Granulin is a soluble cofactor for toll-like receptor 9 signaling. *Immunity* **34**, 505-513, doi:10.1016/j.immuni.2011.01.018 (2011).
88 Ivanov, S. *et al.* A novel role for HMGB1 in TLR9-mediated inflammatory responses to CpG-DNA. *Blood* **110**, 1970-1981, doi:10.1182/blood-2006-09-044776 (2007).
89 Maeda, T. *et al. A Novel Plasmacytoid Dendritic Cell Line, CAL-1, Established from a Patient with Blastic Natural Killer Cell Lymphoma*. Vol. 81 (2005).
90 Tsuchiya, S. *et al.* Establishment and characterization of a human acute monocytic leukemia cell line (THP-1). *Int J Cancer* **26**, 171-176 (1980).
91 Auwerx, J. The human leukemia cell line, THP-1: A multifacetted model for the study of monocyte-macrophage differentiation. *Experientia* **47**, 22-31, doi:10.1007/bf02041244 (1991).
92 Kiemer, A. K. *et al.* Attenuated Activation of Macrophage TLR9 by DNA from Virulent Mycobacteria. *Journal of Innate Immunity* **1**, 29-45, doi:10.1159/000142731 (2009).
93 Remer, K. A., Brcic, M., Sauter, K. S. & Jungi, T. W. Human monocytoid cells as a model to study Toll-like receptor-mediated activation. *J Immunol Methods* **313**, 1-10, doi:10.1016/j.jim.2005.07.026 (2006).
94 Hartmann, G. & Krieg, A. M. CpG DNA and LPS induce distinct patterns of activation in human monocytes. *Gene Ther* **6**, 893-903, doi:10.1038/sj.gt.3300880 (1999).
95 Sawamura, D. *et al.* Direct injection of plasmid DNA into the skin induces dermatitis by activation of monocytes through toll-like receptor 9. *J Gene Med* **7**, 664-671, doi:10.1002/jgm.709 (2005).
96 Mao, T. K. *et al.* Altered monocyte responses to defined TLR ligands in patients with primary biliary cirrhosis. *Hepatology* **42**, 802-808, doi:10.1002/hep.20859 (2005).
97 Hoene, V., Peiser, M. & Wanner, R. Human monocyte-derived dendritic cells express TLR9 and react directly to the CpG-A oligonucleotide D19. *J Leukoc Biol* **80**, 1328-1336, doi:10.1189/jlb.0106011 (2006).
98 Chanput, W., Peters, V. & Wichers, H. in *The Impact of Food Bioactives on Health: in vitro and ex vivo models* (eds Kitty Verhoeckx *et al.*) 147-159 (Springer International Publishing, 2015).
99 Chanput, W., Mes, J. J. & Wichers, H. J. THP-1 cell line: An in vitro cell model for immune modulation approach. *International Immunopharmacology* **23**, 37-45, doi:https://doi.org/10.1016/j.intimp.2014.08.002 (2014).
100 Berges, C. *et al.* A cell line model for the differentiation of human dendritic cells. *Biochem Biophys Res Commun* **333**, 896-907, doi:10.1016/j.bbrc.2005.05.171 (2005).
101 Thomas, P. & Smart, T. G. HEK293 cell line: A vehicle for the expression of recombinant proteins. *Journal of Pharmacological and Toxicological Methods* **51**, 187-200, doi:https://doi.org/10.1016/j.vascn.2004.08.014 (2005).

102 Martell, J. D. *et al.* Engineered ascorbate peroxidase as a genetically encoded reporter for electron microscopy. *Nature Biotechnology* **30**, 1143, doi:10.1038/nbt.2375 https://www.nature.com/articles/nbt.2375#supplementary-information (2012).
103 Zhang, M. *et al.* 121-133 (Springer Singapore).
104 Berens, C. & Hillen, W. Gene regulation by tetracyclines. *European Journal of Biochemistry* **270**, 3109-3121, doi:10.1046/j.1432-1033.2003.03694.x (2003).
105 Triezenberg, S. J., Kingsbury, R. C. & McKnight, S. L. Functional dissection of VP16, the trans-activator of herpes simplex virus immediate early gene expression. *Genes Dev* **2**, 718-729 (1988).
106 Clontech Laboratories, I. (2012).
107 Dana, H. *et al.* Molecular Mechanisms and Biological Functions of siRNA. *International journal of biomedical science : IJBS* **13**, 48-57 (2017).
108 Mahmood, T. & Yang, P.-C. Western blot: technique, theory, and trouble shooting. *North American journal of medical sciences* **4**, 429-434, doi:10.4103/1947-2714.100998 (2012).
109 Qiagen. *RNeasy Mini Handbook*, <http://www.bea.ki.se/documents/EN-RNeasy%20handbook.pdf> (2012).
110 Rio, D. C., Ares, M., Jr., Hannon, G. J. & Nilsen, T. W. Purification of RNA using TRIzol (TRI reagent). *Cold Spring Harb Protoc* **2010**, pdb.prot5439, doi:10.1101/pdb.prot5439 (2010).
111 ThermoFisher. *Reverse Transcription Reaction Setup*, <https://www.thermofisher.com/no/en/home/life-science/cloning/cloning-learning-center/invitrogen-school-of-molecular-biology/rt-education/reverse-transcription-setup.html> (
112 Pabinger, S., Rödiger, S., Kriegner, A., Vierlinger, K. & Weinhäusel, A. A survey of tools for the analysis of quantitative PCR (qPCR) data. *Biomolecular detection and quantification* **1**, 23-33, doi:10.1016/j.bdq.2014.08.002 (2014).
113 *Microscopy Techniques and Culture Surfaces*, <https://ibidi.com/content/216-confocal-microscopy> (
114 Rolls, G. *Process of Fixation and the Nature of Fixatives*, <https://www.leicabiosystems.com/pathologyleaders/fixation-and-fixatives-1-the-process-of-fixation-and-the-nature-of-fixatives/#c22456> (
115 Hoff, F. *How to Prepare Your Specimen for Immunofluorescence Microscopy*, <https://www.leica-microsystems.com/science-lab/how-to-prepare-your-specimen-for-immunofluorescence-microscopy/> (2015).
116 Held, P. *Sample Preparation for Fluorescence Microscopy: An Introduction*, <https://www.biotek.com/assets/tech_resources/Cell%20Fixation%20White%20Paper.pdf> (2015).
117 Sinha, S. S., Cameron, J., Brooks, J. C. & Leifer, C. A. Complex Negative Regulation of TLR9 by Multiple Proteolytic Cleavage Events. *J Immunol* **197**, 1343-1352, doi:10.4049/jimmunol.1502357 (2016).
118 Das, A. T., Tenenbaum, L. & Berkhout, B. Tet-On Systems For Doxycycline-inducible Gene Expression. *Current gene therapy* **16**, 156-167, doi:10.2174/1566523216666160524144041 (2016).
119 Onji, M. *et al.* An essential role for the N-terminal fragment of Toll-like receptor 9 in DNA sensing. *Nat Commun* **4**, 1949, doi:10.1038/ncomms2949 (2013).
120 Becker, C. E., Creagh, E. M. & O'Neill, L. A. Rab39a binds caspase-1 and is required for caspase-1-dependent interleukin-1beta secretion. *J Biol Chem* **284**, 34531-34537, doi:10.1074/jbc.M109.046102 (2009).
121 Liu, M. *et al.* Co-ordinated activation of classical and novel PKC isoforms is required for PMA-induced mTORC1 activation. *PloS one* **12**, e0184818-e0184818, doi:10.1371/journal.pone.0184818 (2017).
122 Escós, A., Risco, A., Alsina-Beauchamp, D. & Cuenda, A. p38γ and p38δ Mitogen Activated Protein Kinases (MAPKs), New Stars in the MAPK Galaxy. *Frontiers in Cell and Developmental Biology* **4**, doi:10.3389/fcell.2016.00031 (2016).
123 Dörner, T. & Lipsky, P. E. in *Handbook of Cell Signaling (Second Edition)* (eds Ralph A. Bradshaw & Edward A. Dennis) 2919-2932 (Academic Press, 2010).
124 Chaturvedi, A. & Pierce, S. K. How location governs Toll like receptor signaling. *Traffic* **10**, 621-628, doi:10.1111/j.1600-0854.2009.00899.x (2009).
125 Cox, D., Lee, D. J., Dale, B. M., Calafat, J. & Greenberg, S. A Rab11-containing rapidly recycling compartment in macrophages that promotes phagocytosis. *Proceedings of the National Academy of Sciences* **97**, 680-685, doi:10.1073/pnas.97.2.680 (2000).
126 Bhuin, T. & Roy, J. K. Rab11 in disease progression. *Int J Mol Cell Med* **4**, 1-8 (2015).
127 Jiang, C. *et al.* Inactivation of Rab11a GTPase in Macrophages Facilitates Phagocytosis of Apoptotic Neutrophils. *The Journal of Immunology* **198**, 1660-1672, doi:10.4049/jimmunol.1601495 (2017).
128 Gambarte Tudela, J. *et al.* Rab39a and Rab39b Display Different Intracellular Distribution and Function in Sphingolipids and Phospholipids Transport. *International Journal of Molecular Sciences* **20**, 1688 (2019).

129 Seto, S. *et al.* Rab39a interacts with phosphatidylinositol 3-kinase and negatively regulates autophagy induced by lipopolysaccharide stimulation in macrophages. *PLoS One* **8**, e83324, doi:10.1371/journal.pone.0083324 (2013).
130 Chano, T. & Avnet, S. RAB39A: a Rab small GTPase with a prominent role in cancer stemness. *The Journal of Biochemistry* **164**, 9-14, doi:10.1093/jb/mvy041 (2018).
131 Jangi, S. *et al.* Alterations of the human gut microbiome in multiple sclerosis. *Nature Communications* **7**, 12015, doi:10.1038/ncomms12015
https://www.nature.com/articles/ncomms12015#supplementary-information (2016).
132 Smith, N., Vidalain, P.-O., Nisole, S. & Herbeuval, J.-P. An efficient method for gene silencing in human primary plasmacytoid dendritic cells: silencing of the TLR7/IRF-7 pathway as a proof of concept. *Scientific Reports* **6**, 29891, doi:10.1038/srep29891
https://www.nature.com/articles/srep29891#supplementary-information (2016).
133 Fukui, R. *et al.* Cleavage of Toll-Like Receptor 9 Ectodomain Is Required for In Vivo Responses to Single Strand DNA. *Frontiers in Immunology* **9**, doi:10.3389/fimmu.2018.01491 (2018).
134 Du, X., Poltorak, A., Wei, Y. & Beutler, B. Three novel mammalian toll-like receptors: gene structure, expression, and evolution. *European cytokine network* **11**, 362-371 (2000).
135 Hasan, M., Gruber, E., Cameron, J. & Leifer, C. A. TLR9 stability and signaling are regulated by phosphorylation and cell stress. *Journal of Leukocyte Biology* **100**, 525-533, doi:10.1189/jlb.2A0815-337R (2016).
136 Chockalingam, A., Cameron, J. L., Brooks, J. C. & Leifer, C. A. Negative regulation of signaling by a soluble form of toll-like receptor 9. *Eur J Immunol* **41**, 2176-2184, doi:10.1002/eji.201041034 (2011).
137 Zhang, J. Z., Liu, Z., Liu, J., Ren, J. X. & Sun, T. S. Mitochondrial DNA induces inflammation and increases TLR9/NF-kappaB expression in lung tissue. *Int J Mol Med* **33**, 817-824, doi:10.3892/ijmm.2014.1650 (2014).
138 Sprokholt, J. K., Heineke, M. H., Kaptein, T. M., van Hamme, J. L. & Geijtenbeek, T. B. H. DCs facilitate B cell responses against microbial DNA via DC-SIGN. *PLOS ONE* **12**, e0185580, doi:10.1371/journal.pone.0185580 (2017).
139 Chen, T. *et al.* Rab39, a novel Golgi-associated Rab GTPase from human dendritic cells involved in cellular endocytosis. *Biochemical and Biophysical Research Communications* **303**, 1114-1120, doi:https://doi.org/10.1016/S0006-291X(03)00482-0 (2003).
140 Leifer, C. A. *et al.* TLR9 is localized in the endoplasmic reticulum prior to stimulation. *Journal of immunology (Baltimore, Md. : 1950)* **173**, 1179-1183, doi:10.4049/jimmunol.173.2.1179 (2004).

APPENDIX

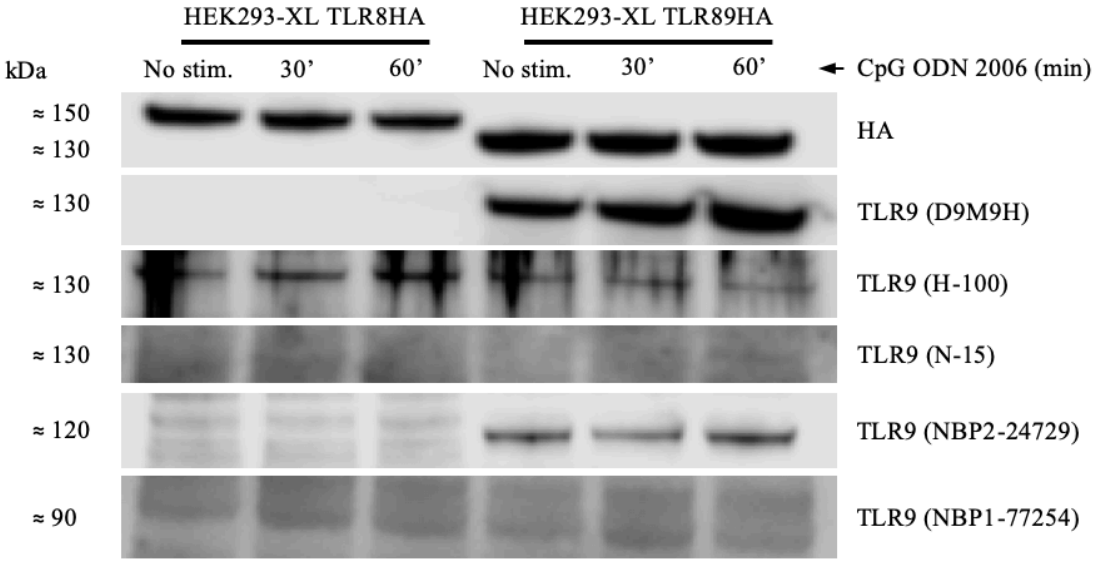

Supplementary Figure 1: Validation of anti-TLR9 antibodies by western blot analysis of TLR9 expression in HEK293-XL TLR8HA and HEK293-XL TLR9HA whole cell lysates before and after stimulation with CpG ODN 2006 for 30 and 60 minutes. Cells were seeded at a density of 500 000 cells/well in standard DMEM supplemented with 10% FCS, 2mM GlutaMAX, 0.5 mg/ml G418, 100 U/ml penicillin and 0.1 mg/ml streptomycin, stimulated with 1µM CpG ODN 2006 for 30 and 60 minutes and lysed in RIPA with protease and phosphatase inhibitors. Gel electrophoresis was performed using NuPAGE 4-12% Bis-Tris gels at 100V for 30 min, then 150V for 90 min. Proteins were transferred to a nitrocellulose membrane using iBlot 2 Gel Transfer Device program P0 (20V for 1 min, 23V for 4 min, 25V for 2 min). HEK293-XL TLR8HA was used as a negative control due to absence of TLR9, and HEK239-XL TLR9HA was used as a positive control. Presence of both HA-tagged TLR8 (≈150 kDa) and TLR9 (≈130 kDa) in respective cell lines was confirmed by staining a blot with anti-HA antibody. Anti-TLR9 (D9M9H) rabbit monoclonal antibody, predicted to recognize the full-length isoform of TLR9 (≈130 kDa) and anti-TLR9 (NBP2-24729) mouse monoclonal antibody, developed against amino acids 268-300 of human TLR9 isoform A, both appear specific for full-length TLR9 and recognize it before and after stimulation with CpG ODN 2006. Anti-TLR9 (H-100) rabbit polyclonal antibody, raised against amino acids 771-870 of TLR9 of human origin, anti-TLR9 (N-15) goat polyclonal antibody, raised against a peptide mapping area near the N-terminus of TLR9 of human origin, and anti-TLR9 (NBP1-77254) rabbit polyclonal antibody raised against 16 amino acids located within 960-1010 amino acids of TLR9, are not specific for TLR9 as shown by the blot.

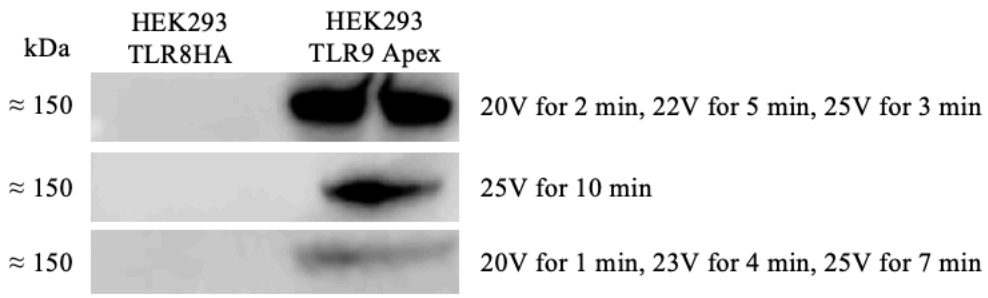

Supplementary Figure 2: High transfer efficiency of TLR9 is achieved upon transfer of proteins from a NuPAGE 4-12% Bis-Tris gel to nitrocellulose membrane using iBlot 2 Gel Transfer Device optimized program (20V for 2min, 22V for 5min, 25V for 3min). Cells were seeded at a density of 500 000 cells/well in DMEM supplemented with 10% FCS, 2mM GlutaMAX, 0.5 mg/ml G418, 100 U/ml penicillin and 0.1 mg/ml streptomycin and lysed in 200µl RIPA (containing protease and phosphatase inhibitors) on ice for 1 hour. Gel electrophoresis was performed using NuPAGE 4-12% Bis-Tris gels at 100V for 30 min, then 150V for 90 min. Blotting was done using 3 different programs on iBlot 2 Gel Transfer Device: 1) 20V for 2min, 22V for 5min, 25V for 3min, 2) 25V for 10min, 3) 10V for 1 min, 23V for 4 min, 25V for 7min. All membranes were probed with anti-TLR9 (NBP2-24729) antibody. No bands corresponding to $TLR9_{FL}$ or $TLR9_{FL}$ Apex were detected in HEK293 TLR8 (negative control) on any of the membranes, and a single band of 150kDa was detected in HEK293 TLR9 Apex (positive control) on all membranes.

$TLR9_{FL}$ – full length TLR9

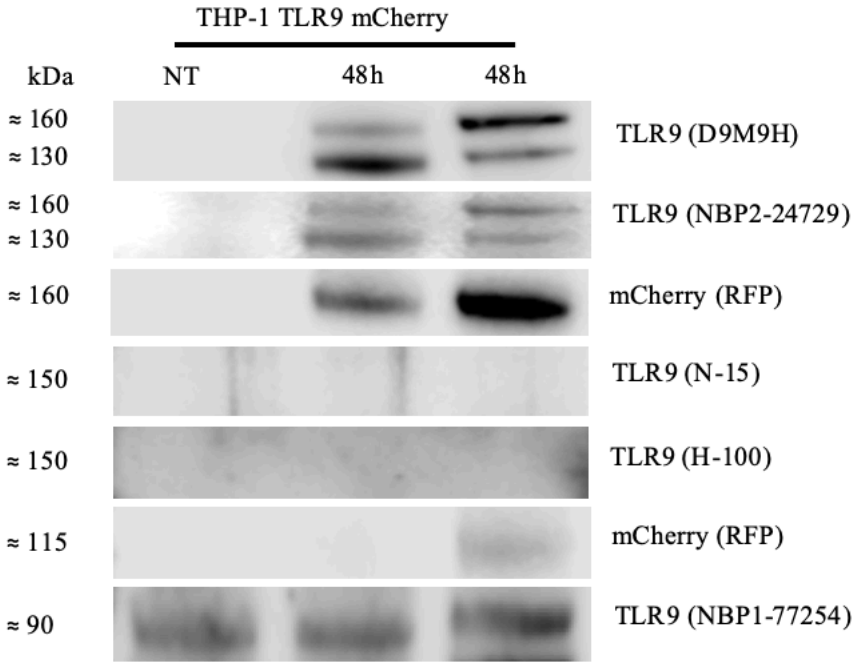

Supplementary Figure 3: Anti-TLR9 antibodies D9M9H and NBP2-24729 detect $TLR9_{FL}$ and $TLR9_{FL}$ mCherry, and anti-mCherry (RFP) antibody detects $TLR9_{FL}$ mCherry and $TLR9_{C}$ mCherry. THP-1 TLR9 mCherry (400 000 cells/well) were differentiated with PMA (40ng/ml) for 72h. After removal of PMA, doxycycline (1µg/ml) was added for 48h. After 48h cells were lysed in RIPA with protease and phosphatase inhibitors. Gel electrophoresis was performed using NuPAGE 4-12% Bis-Tris gels at 100V for 30 min, then 150V for 90 min. Proteins were transferred to a nitrocellulose membrane using iBlot 2 Gel Transfer Device optimized program (20V for 2 min, 23V for 5 min, 25V for 3 min). Anti-TLR9 D9M9H and NBP2-24729 antibodies detected two bands in both experimental replicates treated with doxycycline – a ≈160 kDa band corresponding to $TLR9_{FL}$ mCherry and a ≈130 kDa band corresponding to $TLR9_{FL}$. Other anti-TLR9 antibodies did not yield a signal of expected TLR9 size. Anti-mCherry antibody (RFP) detected two bands – a ≈160 kDa band corresponding to $TLR9_{FL}$ mCherry, and a ≈115 kDa corresponding to $TLR9_{C}$ mCherry.

NT – no doxycycline treatment; $TLR9_{FL}$ – full length TLR9; $TLR9_{FL}$ mCherry – full length TLR9 mCherry; $TLR9_{C}$ mCherry – cleaved TLR9 mCherry

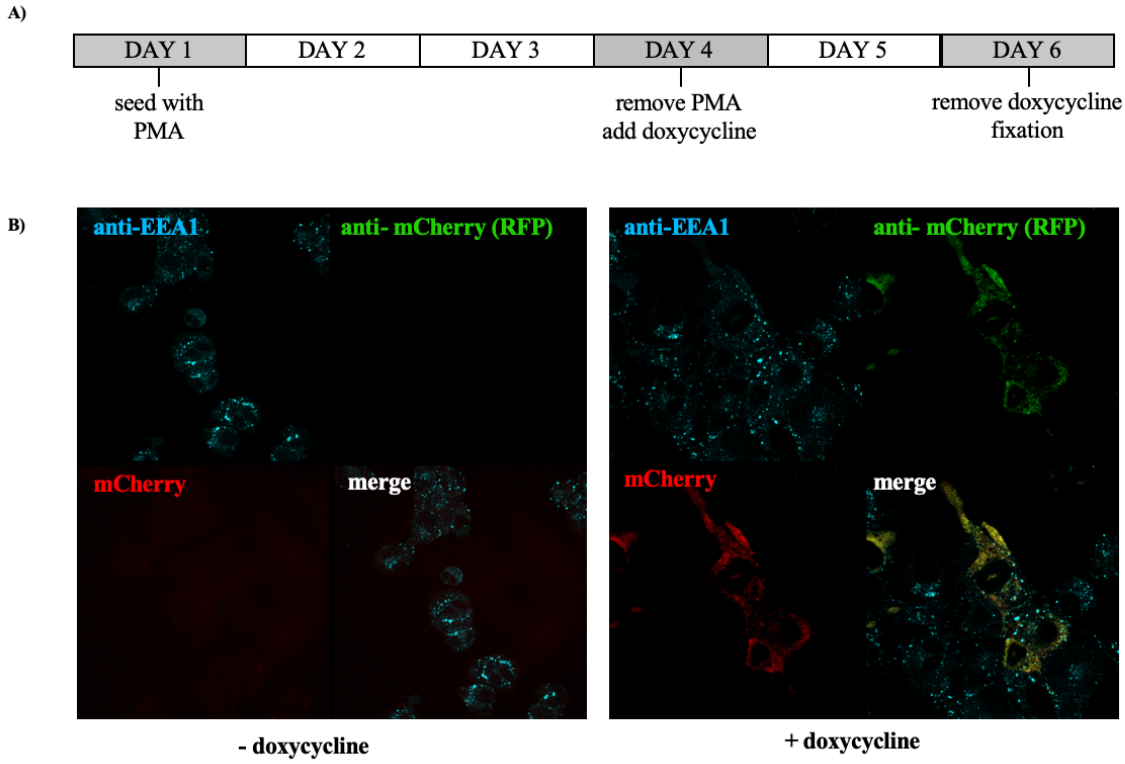

Supplementary Figure 4: **TLR9 does not colocalize with EEA1 in PMA-differentiated THP-1 TLR9 mCherry cells before stimulation**. **A)** Cells were seeded on poly-L-lysine-coated 8-well microscopy chamber at a density of 100 000 cells/well in THP-1 medium with PMA (40 ng/ml) and 0.25µg/ml puromycin. 1µg/ml doxycycline was added for 48h after removal of PMA. Cells were fixed with 4% PFA and stained with **B)** anti-mCherry (RFP) and **C)** anti-EEA1 antibodies. mCherry reflects signal from TLR9 mCherry tag. The experiment was done once.

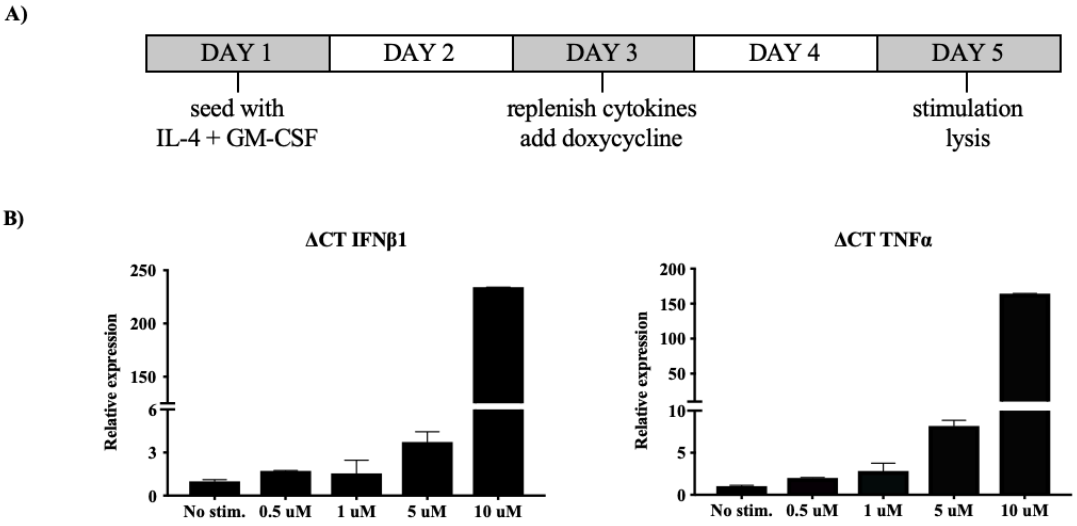

Supplementary Figure 5: **10µM CpG ODN 2006 is a potent inducer of IFNβ1 and TNFα responses in IL-4, GM-CSF-differentiated THP-1 TLR9 mCherry cells. A)** THP-1 TLR9 mCherry (400 000 cells/well) were differentiated with rhIL-4 (200 ng/ml), rhGM-CSF (100ng/ml) for 5 days with cytokines replenishment on day 3. Doxycycline (1µg/ml) was added for 48h on day 3. After removal of doxycycline on day 5, cells were either left untreated or were stimulated with CpG ODN 2006 (0.5µM, 1µM, 5µM and 10µM) for 3 hours. **B)** mRNA levels of IFNβ1 and TNFα were measured by RT-qPCR and normalized to TBP. Results shown represent fold induction relative to unstimulated cells. The experiment was done once. Error bars in **B)** represent standard deviation between two technical replicates.

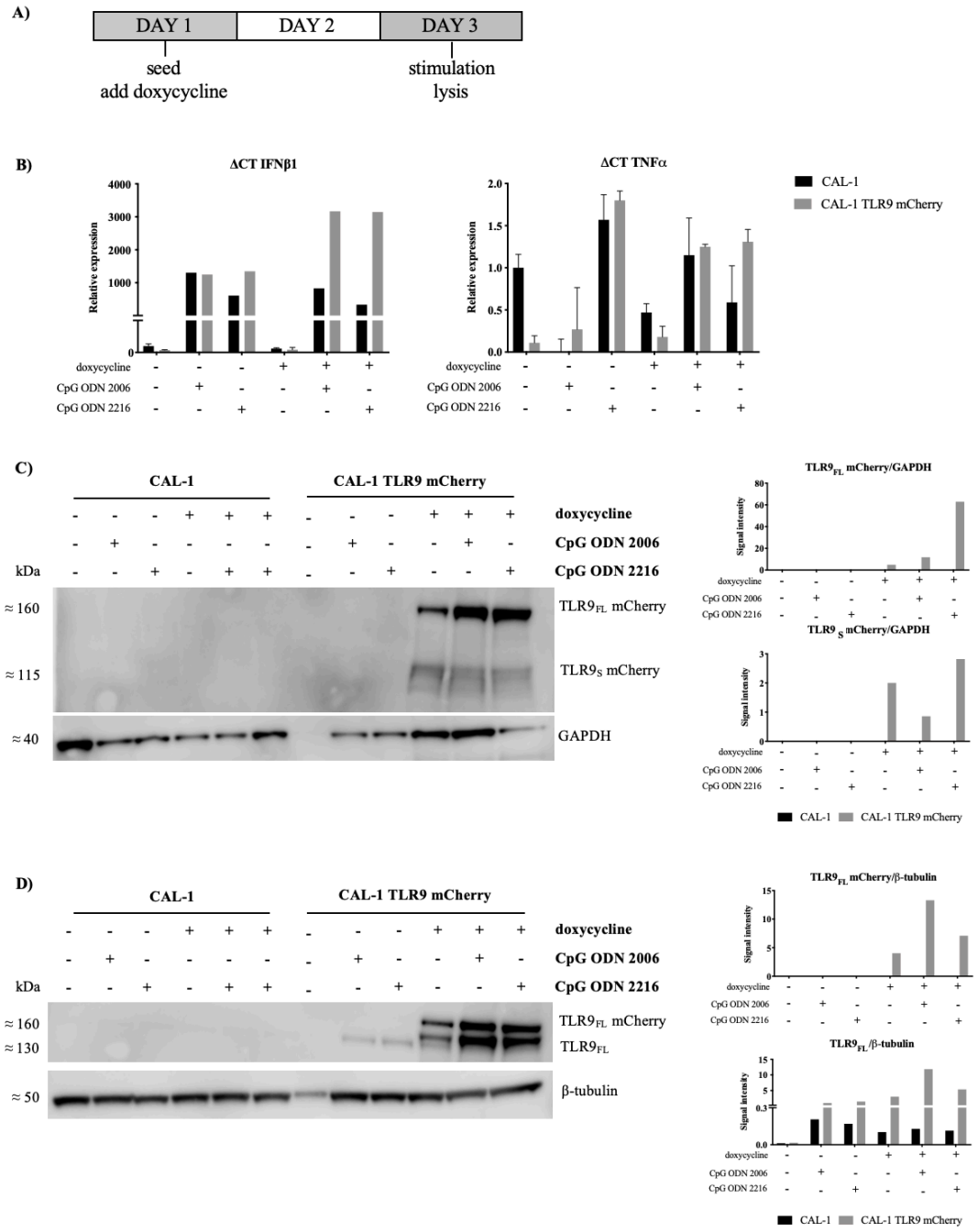

Supplementary Figure 6: **CAL-1 TLR9 mCherry cells treated with 0.5µg/ml doxycycline for 48h have stronger IFNβ1 and TNFα response to CpG ligands upon stimulation than CAL-1 cells. A)** CAL-1 and CAL-1 TLR9 mCherry cells (400 000 cells/well) were seeded with doxycycline (0.5µg/ml) or kept in culture medium without doxycycline. After 48h doxycycline was removed and cells were either left unstimulated or were stimulated with 10µM CpG ODN 2006 or 2216 for 3 hours. **B)** mRNA levels of IFNβ1 and TNFα were measured by RT-qPCR and normalized to TBP. Results shown represent fold induction relative to unstimulated, non-doxycycline induced CAL-1 cells. Error bars in represent standard deviation between two technical replicates. Proteins for western blot were isolated from QiAzol lysates and assayed with **C)** anti-mCherry (RFP) and **D)** anti-TLR9 (D9M9H) antibodies. GAPDH and β-tubulin were used as loading controls and for normalization of signal intensity. The experiment was done once.

$TLR9_{FL}$ mCherry – full length TLR9 mCherry, $TLR9_{FL}$ – full length TLR9, $TLR9_S$ mCherry– short TLR9 mCherry

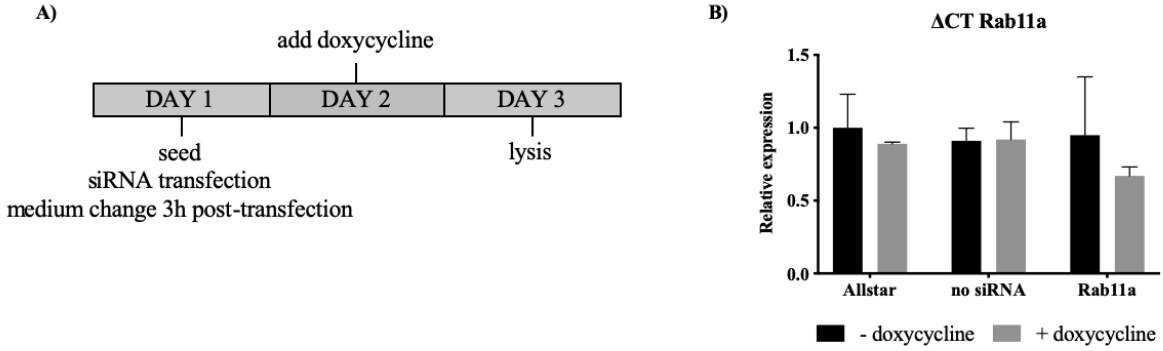

Supplementary Figure 7: Forward siRNA transfection with DOTAP for 3h in undifferentiated CAL-1 TLR9 mCherry cells does not result in Rab11a knockdown. **A)** CAL-1 TLR9 mCherry cells (400 000 cells/well) were transfected with DOTAP. Final siRNA concentration was 160nM. Medium was changed 3h after transfection. Doxycycline (0.5µg/ml) was added on day 2. Cells were lysed 24h after administration of doxycycline. **B)** mRNA levels of Rab11a were measured by RT-qPCR and normalized to TBP. Results shown represent fold change relative to non-induced, Allstar-treated cells. The experiment was done once. Error bars in **B)** represent standard deviation between two technical replicates.

no siRNA – mock treated samples with DOTAP only

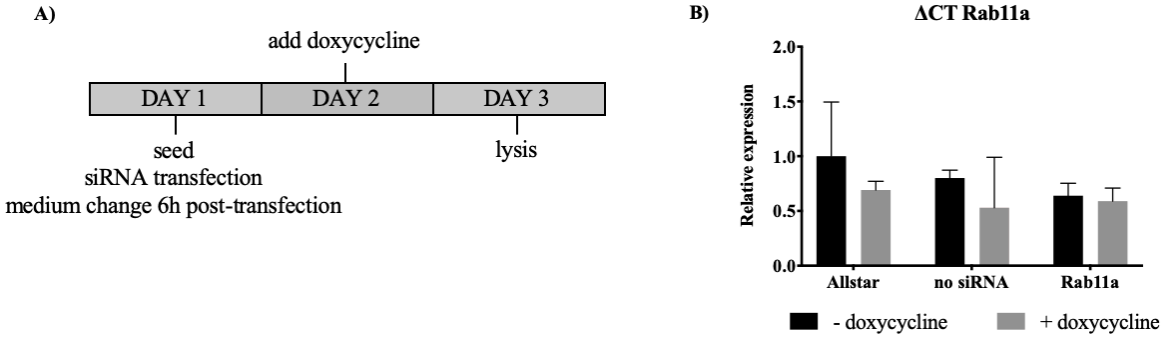

Supplementary Figure 8: Forward siRNA transfection with DOTAP for 6h in undifferentiated CAL-1 TLR9 mCherry cells results in ≈30% Rab11a knockdown. **A)** CAL-1 TLR9 mCherry cells (400 000 cells/well) were transfected with DOTAP. Final siRNA concentration was 160nM. Medium was changed 6h after transfection. Doxycycline (0.5µg/ml) was added on day 2. Cells were lysed 24h after administration of doxycycline. **B)** mRNA levels of Rab11a were measured by RT-qPCR and normalized to TBP. Results shown represent fold change relative to non-induced, Allstar-treated cells. The experiment was done once. Error bars in **B)** represent standard deviation between two technical replicates.

no siRNA – mock treated samples with DOTAP only

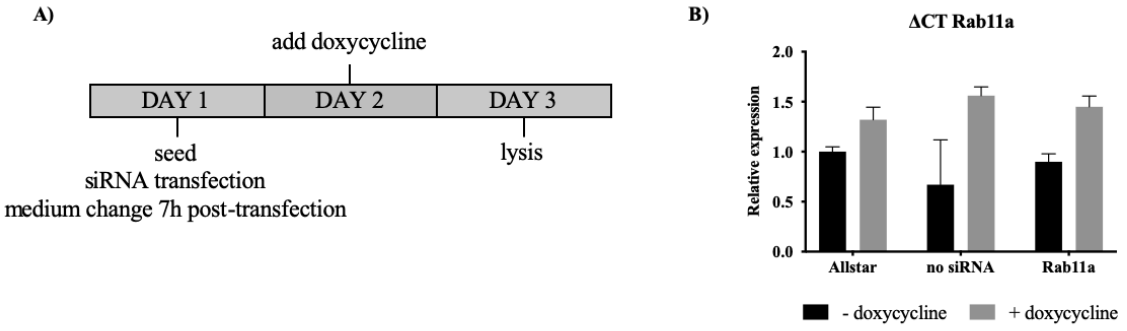

Supplementary Figure 9: Forward siRNA transfection with DOTAP for 7h in undifferentiated CAL-1 TLR9 mCherry cells does not silence Rab11a. **A)** CAL-1 TLR9 mCherry cells (400 000 cells/well) were transfected with DOTAP. Final siRNA concentration was 160nM. Medium was changed 7h after transfection. Doxycycline (0.5µg/ml) was added on day 2. Cells were lysed 24h after administration of doxycycline. **B)** mRNA levels of Rab11a were measured by RT-qPCR and normalized to TBP. Results shown represent fold change relative to non-induced, Allstar-treated cells. The experiment was done once. Error bars in **B)** represent standard deviation between two technical replicates.

no siRNA – mock treated samples with DOTAP only

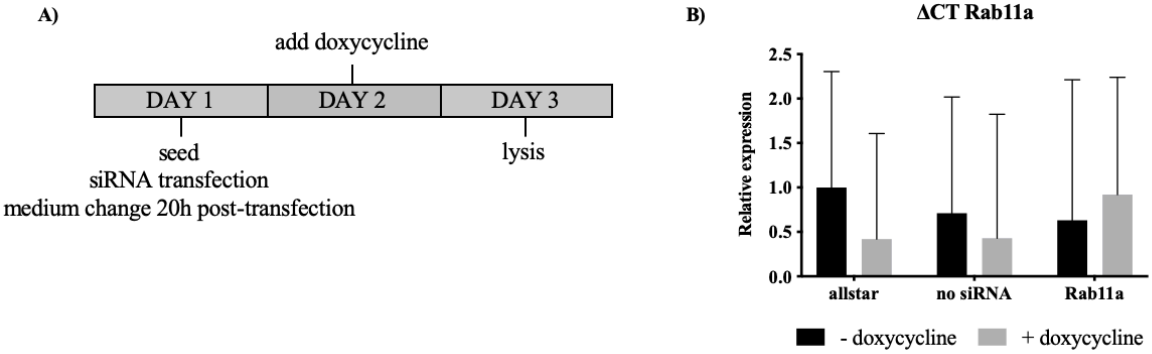

Supplementary Figure 10: **Forward siRNA transfection with DOTAP for 20h in undifferentiated CAL-1 TLR9 mCherry cells does not give a knockdown of Rab11a**. **A)** CAL-1 TLR9 mCherry cells (400 000 cells/well) were transfected with DOTAP. Final siRNA concentration was 160nM. Medium was changed 20h after transfection. Doxycycline (0.5µg/ml) was added on day 2. Cells were lysed 24h after administration of doxycycline. **B)** mRNA levels of Rab11a were measured by RT-qPCR and normalized to TBP. Results shown represent fold change relative to non-induced, Allstar-treated cells. The experiment was done once. Error bars in **B)** represent standard deviation between two technical replicates.

no siRNA – mock treated samples with DOTAP only

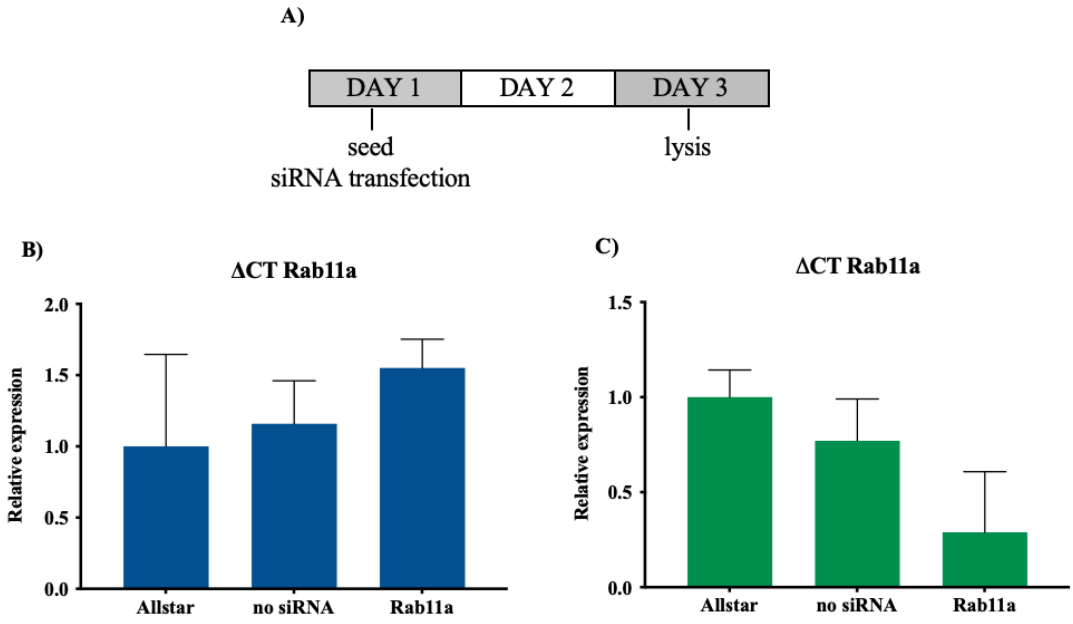

Supplementary Figure 11: **Reverse siRNA transfection with ViromerGREEN in undifferentiated CAL-1 TLR9 mCherry cells results in ≈60% knockdown of Rab11a**. **A)** CAL-1 TLR9 mCherry cells (600 000 cells/well) were reverse transfected with **B)** ViromerBLUE or **C)** ViromerGREEN and incubated for 48h. Final siRNA concentration was 100nM. Cells were then lysed and **B, C)** mRNA levels of Rab11a were measured by RT-qPCR and normalized to TBP. Results shown represent fold change relative to Allstar-treated cells. Each experiment was done once. Error bars in **B, C)** represent standard deviation between two technical replicates.

no siRNA – mock treated samples with ViromerBLUE/ViromerGREEN only

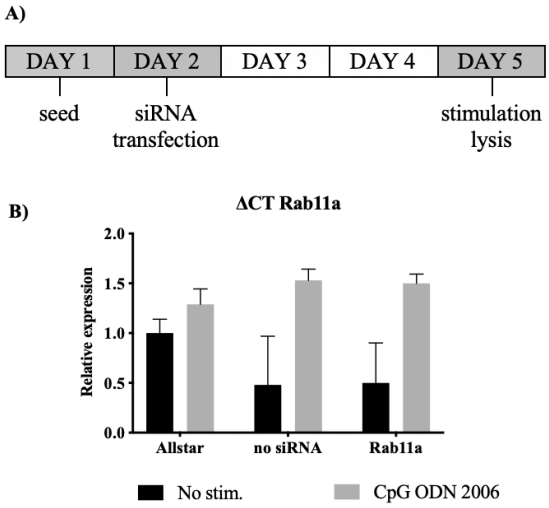

Supplementary Figure 12: **Forward Lipofectamine 3000-mediate transfection in undifferentiated CAL-1 TLR9 mCherry cells results in ≈50% knockdown of Rab11a, but reduces cell viability A)** CAL-1 TLR9 mCherry cells (400 000 cells/well) were transfected with siRNA (33nM) a day after seeding and incubated with transfection complexes for 72h. Cells were stimulated with 10µM CpG ODN 2006 for 3 hours, subsequently lysed and **B)** Rab11a mRNA levels were assayed by RT-qPCR and normalized to TBP. Results shown represent fold change relative to unstimulated, Allstar-treated cells. The experiment was done once. Error bars in **B)** represent standard deviation between two technical replicates.

no siRNA – mock treated sample with Lipofectamine 3000 only

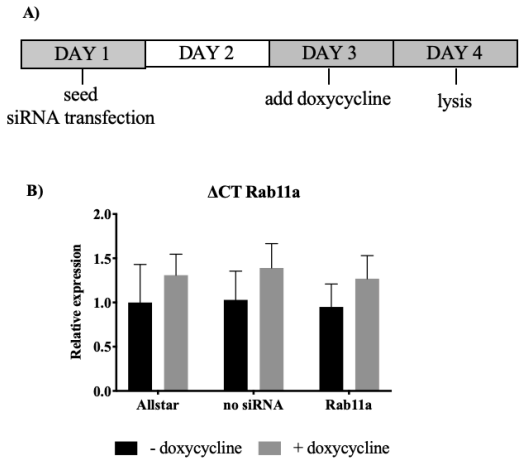

Supplementary Figure 13: **Reverse siRNA transfection with Lipofectamine 3000 in undifferentiated CAL-1 TLR9 mCherry cells does not silence Rab11a**. **A)** CAL-1 TLR9 mCherry (400 000 cells/well) were reverse transfected with Lipofectamine 3000 and incubated for 48h. Final siRNA concentration was 33nM. Doxycycline (0.5µg/ml) was added for 24h after removal of transfection complexes to induce TLR9 expression. Cells were lysed the following day. **B)** mRNA levels of Rab11a were measured by RT-qPCR and normalized to TBP. Results shown represent fold change relative to Allstar-treated cells. The experiment was done once. Error bars in **B)** represent standard deviation between two technical replicates

no siRNA – mock treated samples with Lipofetamine 3000 only

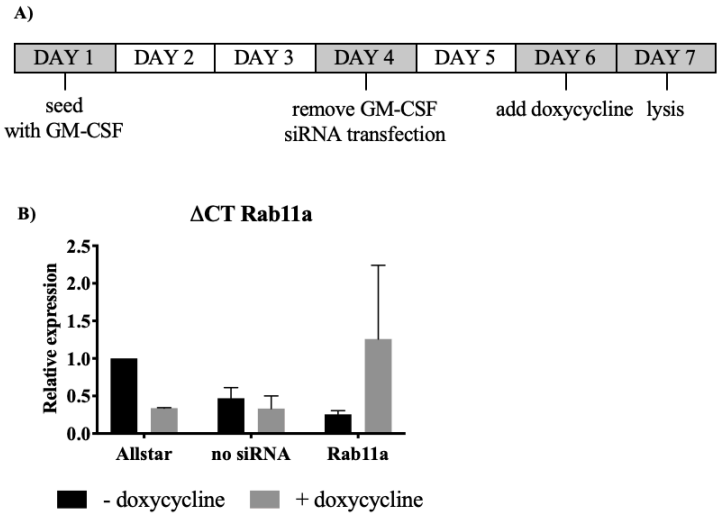

Supplementary Figure 14: **Forward siRNA transfection with Lipofectamine 3000 in GM-CSF-treated CAL-1 TLR9 mCherry cells results in Rab11a knockdown only prior to doxycycline induction**. **A)** CAL-1 TLR9 mCherry cells (400 000 cells/well) were treated with rhGM-CSF (10 pg/ml) for 72h. Cells were transfected with Lipofectamine 3000 after removal of GM-CSF and incubated for 24h. Final siRNA concentration was 33nM. When transfection complexes were removed, doxycycline (0.5µg/ml) was added for 24h. Cells were subsequently lysed and **B)** mRNA levels of Rab11a were measured by RT-qPCR and normalized to TBP. Results shown represent fold change relative to non-induced, Allstar-treated cells. The experiment was done twice. Error bars in **B)** represent standard deviation between two biological replicates.

no siRNA – mock treated samples with Lipofectamine only

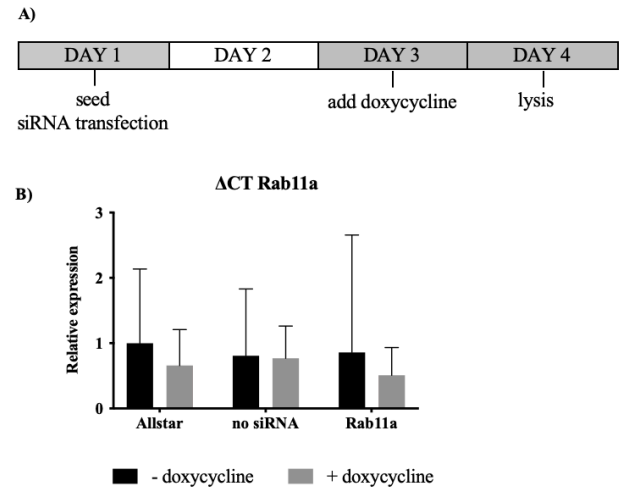

Supplementary Figure 15: **Reverse siRNA transfection with RNAiMAX in undifferentiated CAL-1 TLR9 mCherry cells does silence Rab11a**. **A)** CAL-1 TLR9 mCherry cells (400 000 cells/well) were transfected with RNAiMAX and incubated for 48h. Final siRNA concentration was 16nM. Doxycycline (0.5µg/ml) was added for 24h, after removal of transfection complexes. Cells were then lysed and assayed for **B)** Rab11a mRNA levels by RT-qPCR and normalized to TBP. Results shown represent fold change relative to non-induced, Allstar-treated cells. The experiment was done once. Error bars in **B)** represent standard deviation between two technical replicates.

no siRNA – mock treated samples with RNAiMAX only

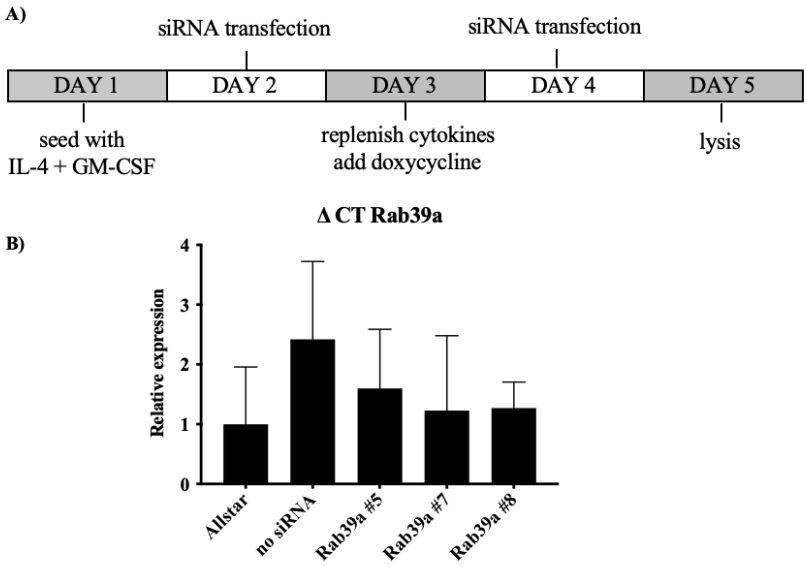

Supplementary Figure 16: **Forward siRNA transfections with RNAiMAX on days 2 and 4 of IL-4-, GM-CSF-differentiation do not silence Rab39a and result in cell death. A)** THP-1 TLR9 mCherry cells (400 000 cells/well) with rhIL-4 (200ng/ml) and rhGM-CSF (100ng/ml) in antibiotic-free medium. Cytokines were replenished 48h after seeding. Cells were transfected with RNAiMAX on days 2 and 4 and incubated for 24h each time. Final siRNA concentration was 16nM. Doxycycline (1µg/ml) was added on day 3 for 48h, after which cells were lysed and assayed for **B)** Rab39a mRNA levels by RT-qPCR and normalized to TBP. Results shown represent fold change relative to Allstar-treated cells. The experiment was done once. Error bars in **B)** represent standard deviation between two technical replicates.

no siRNA – mock treated samples with RNAiMAX only

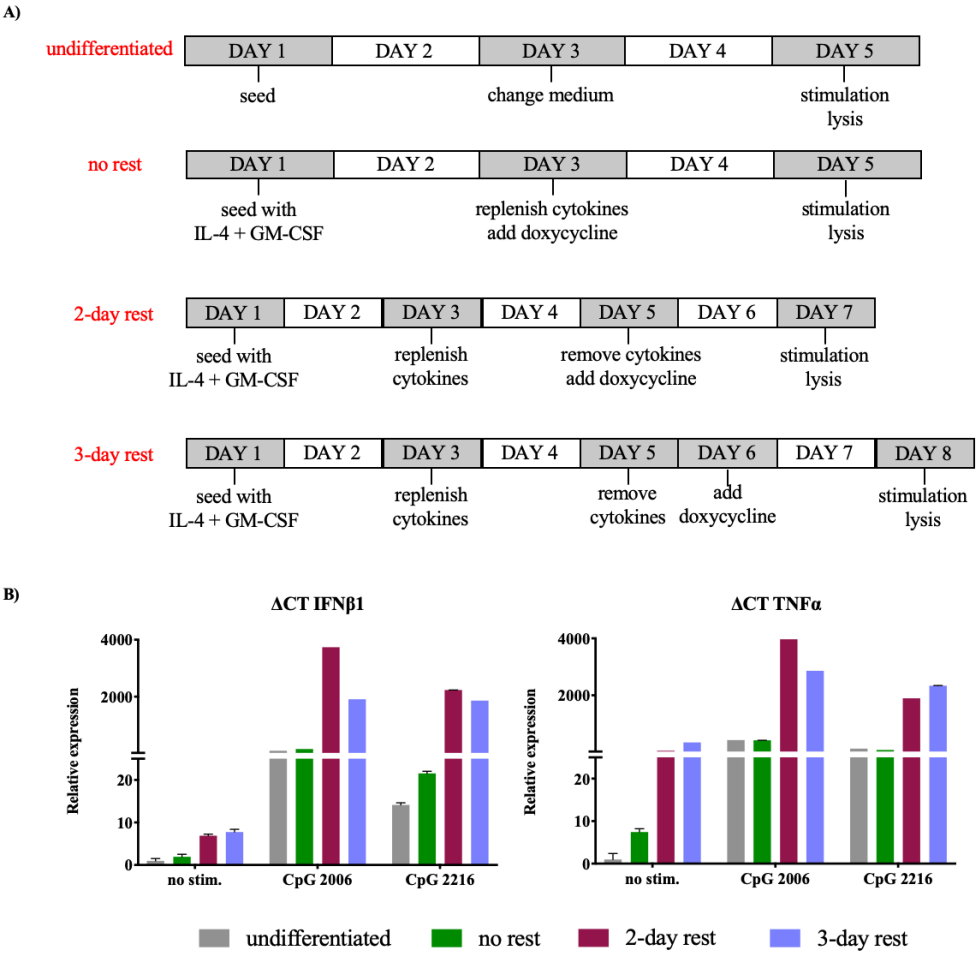

Supplementary Figure 17: **2- and 3-day rest following IL-4, GM-CSF differentiation results in increased background levels of IFNβ1 and TNFα. A)** THP-1 TLR9 mCherry cells (400 000 cells/well) were supplemented with rhIL-4 (200 ng/ml) and rhGM-CSF (100ng/ml) on day 1 and 3. Cytokines were removed on day 5, and cells were either stimulated and lysed right away or allowed to rest in culture medium for 2-3 days prior to stimulation and lysis. Undifferentiated cells were kept in standard culture medium throughout the experiment. TLR9 expression was induced with 1µg/ml doxycycline 48h prior to stimulation and lysis. Stimulation was done with 10µM CpG ODN 2006 or 2216 for 3 hours. **B)** mRNA levels of IFNβ1 and TNFα were measured by RT-qPCR and normalized to TBP. Results shown represent fold induction relative to undifferentiated, unstimulated cells. The experiment was done once. Error bars in **B)** represent standard deviation between two technical replicates.

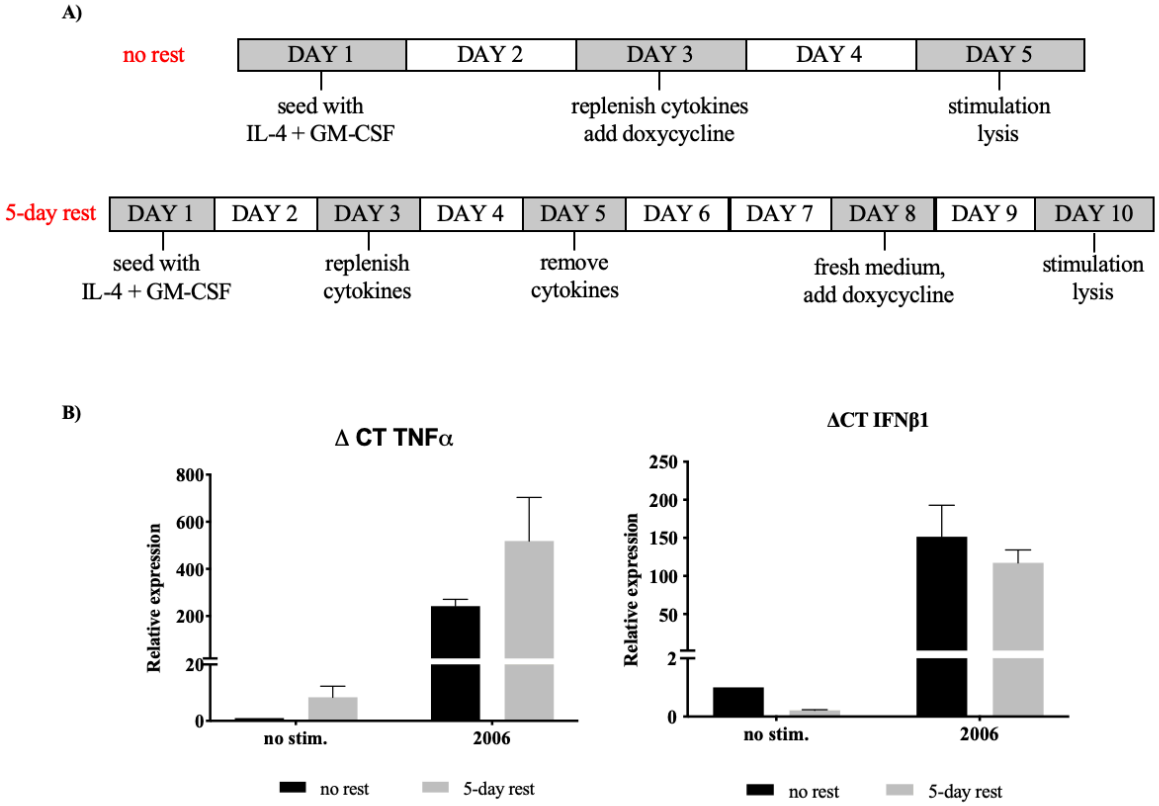

Supplementary Figure 18: **5-day rest following IL-4, GM-CSF differentiation results in reduced IFNβ1 and a slight increase in TNFα basal levels**. **A)** THP-1 TLR9 mCherry cells (400 000 cells/well) were differentiated with rhIL-4 (200ng/ml), rhGM-CSF (100ng/ml) with cytokine replenishment on day 3. Doxycycline (1µg/ml) was added on day 3 (for 5-day differentiation, no rest protocol) and on day 8 (for 5-day rest protocol) for 48h. On the last day, cells were either left unstimulated or were stimulated with 10µM CpG ODN 2006. **B)** mRNA levels of IFNβ1 and TNFα were measured by RT-qPCR and normalized to TBP. Results shown represent fold induction relative to undifferentiated, unstimulated cells. The experiment was done once. Error bars in **B)** represent standard deviation between two technical replicates.

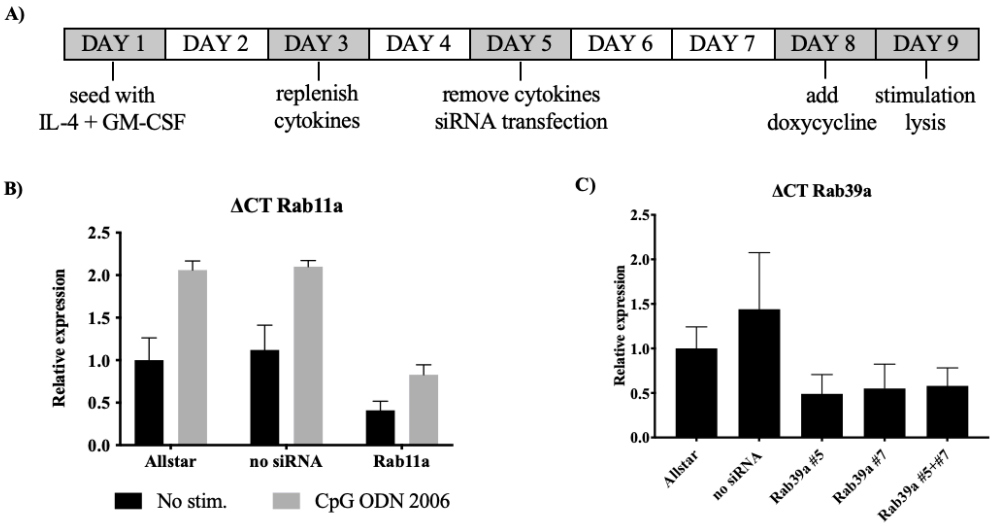

Supplementary Figure 19: **Forward siRNA transfections with Lipofectamine 3000 in IL-4-, GM-CSF-differentiated cells results in ≈50% knockdown of Rab11a and ≈45% knockdown of Rab39a.** **A)** THP-1 TLR9 mCherry (400 000 cells/well) were differentiated with rhIL-4 (200ng/ml) and rhGM-CSF (100ng/ml) in antibiotic-free medium. Cytokines were replenished on day 3. Cells were transfected with Lipofectamine 3000 on day 5 and incubated for 72h. 1µg/ml doxycycline was added on day 3 for 24h to induce TLR9 expression. Cells were stimulated with 10µM CpG ODN 2006 (**B) only**) and lysed on day 9. **B, C)** mRNA levels of Rab11a and Rab39a were measured by RT-qPCR and normalized to TBP. Results shown represent fold change relative to Allstar-treated cells. The experiment was done once. Error bars in **B, C)** represent standard deviation between two technical replicates.

no siRNA – mock treated samples only with Lipofectamine 3000

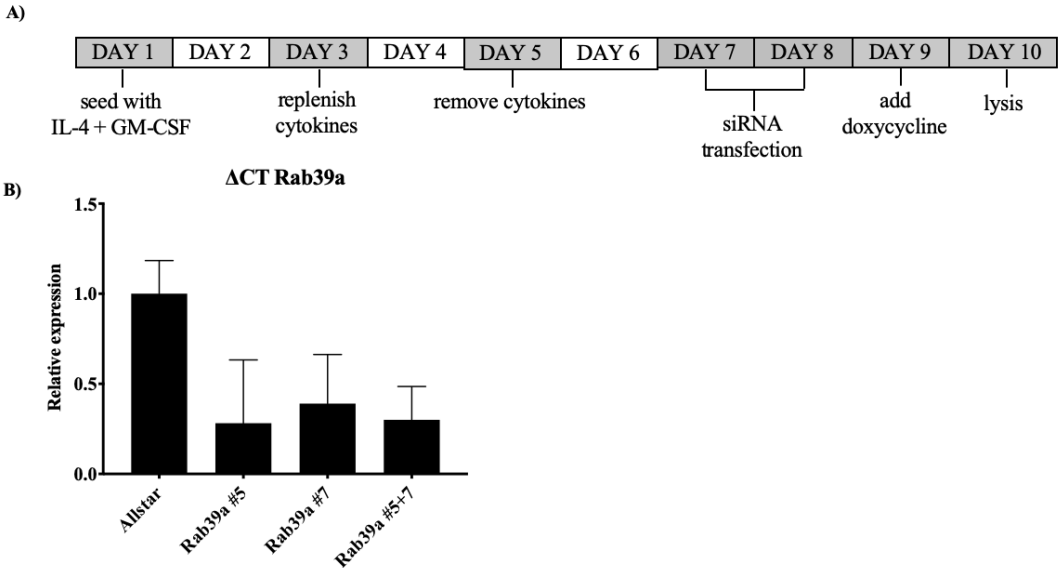

Supplementary Figure 20: **Forward siRNA transfections with Lipofectamine 3000 on days 7 and 8 in IL-4-, GM-CSF-differentiated have weak silencing effect on Rab39a**. **A)** THP-1 TLR9 mCherry cells (400 000 cells/well) were differentiated with rhIL-4 (200ng/ml) and rhGM-CSF (100ng/ml) in antibiotic-free medium. Cytokines were replenished on day 3 and removed on day 5. Cells were transfected with Lipofectamine 3000 on day 7 for 24h, and then again on day 8. Medium was changed on day 9 before addition of 1µg/ml doxycycline. Cells were lysed 24h after doxycycline was added. **B)** mRNA levels of Rab39a were measured by RT-qPCR and normalized to TBP. Results shown represent fold change relative to Allstar-treated cells. The experiment was done once. Error bars in **B)** represent standard deviation between two technical replicates.

no siRNA – mock treated samples with Lipofectamine 3000 only

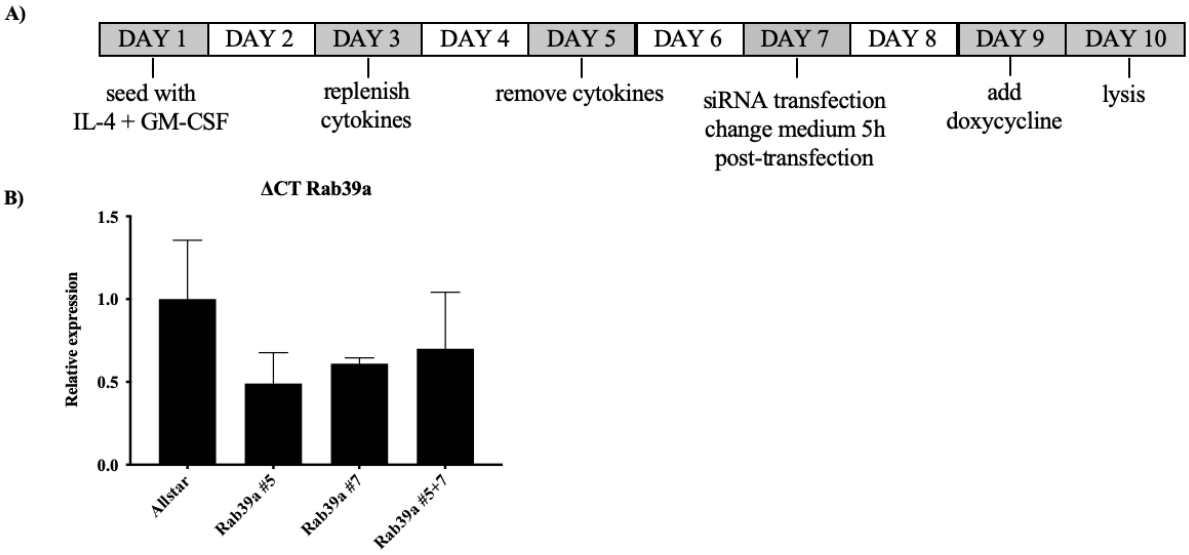

Supplementary Figure 21: Forward siRNA transfections with DOTAP in IL-4-, GM-CSF-differentiated cells results in ≈45% knockdown of Rab39a but reduces cell viability. A) THP-1 TLR9 mCherry cells were differentiated with rhIL-4 (200ng/ml) and rhGM-CSF (100ng/ml) in antibiotic-free. Cytokines were replenished on day 3 and removed on day 5. Cells were transfected with DOTAP on day 7, and medium was changed after 5h of transfection. Final siRNA concentration was 160nM. 1µg/ml doxycycline was added on day 9 for 24h, and cells were subsequently lysed and assayed for **B)** Rab39a mRNA by RT-qPCR and normalized to TBP. Results shown represent fold change relative to Allstar-treated cells. The experiment was done once. Error bars in **B)** represent standard deviation between two technical replicates.

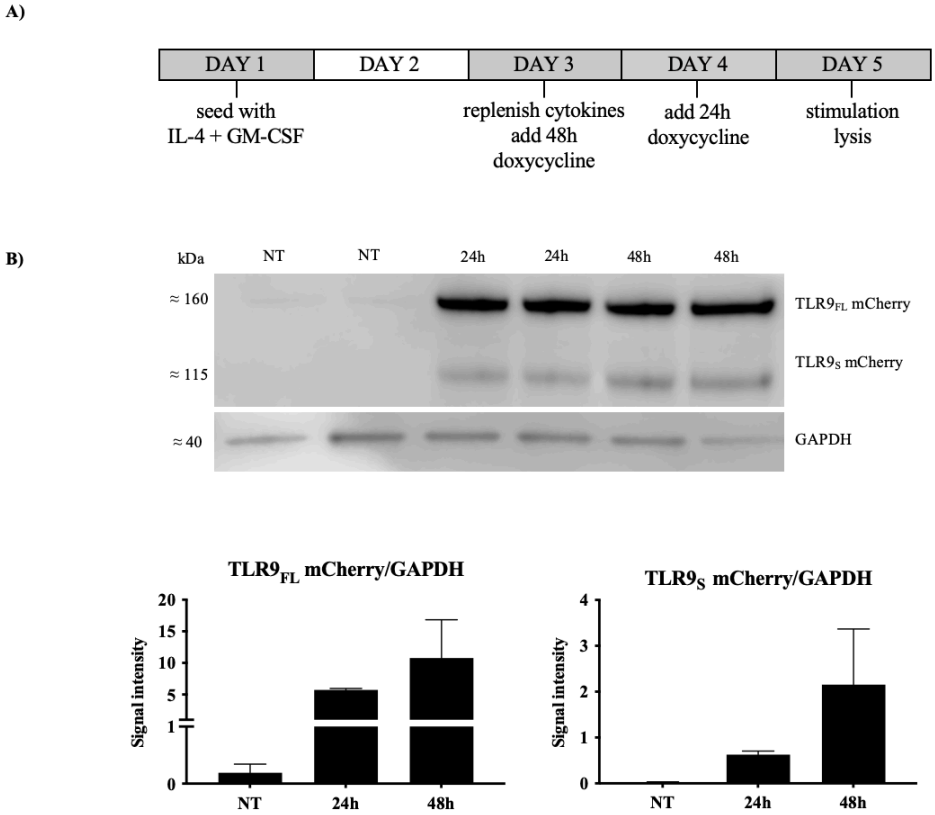

Supplementary Figure 22: **1µg/ml doxycycline for 24h is enough to induce expression of TLR9$_{FL}$ mCherry and TLR9$_{S}$ mCherry in IL-4, GM-CSF-differentiated cells**. **A)** Cells were seeded at a density of 400 000 cells/well in THP-1 medium with 0.25µg/ml puromycin, rhIL-4 (200ng/ml), rhGM-CSF (100ng/ml). Cytokines were replenished on day 3. 1µg/ml doxycycline was added on day 3 for 48h, and on day 4 for 24h. Cell lysis was done on day 5. **B)** Western blot was run on whole cell lysates to determine protein levels of TLR9. Signal intensity was normalized to GAPDH. Western blot is a representative of two independent experiments run on the same membrane. Error bars in **B)** represent standard deviation between two biological replicates.

TLR9FL mCherry – full length TLR9 mCherry, TLR9S mCherry.- short TLR9 mCherry

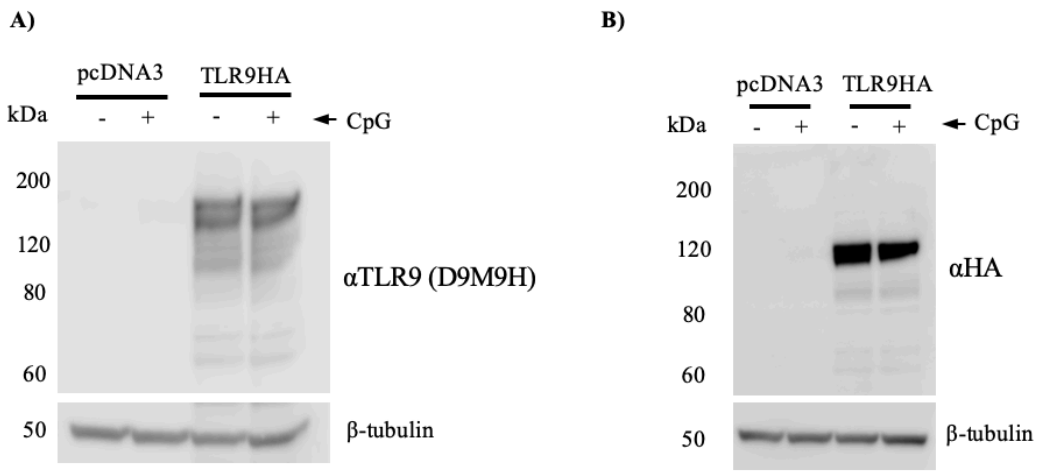

Supplementary Figure 23: Hek293 cells transfected with TLR9HA plasmid express TLR9. pcDNA3 plasmid was used as a negative control. Cells were stimulated with CpG ODN 2006 overnight for 16h. Membranes were blotted with **A)** anti-TLR9 (D9M9H) or **B)** anti-HA antibodies.